2023-10-01

Functional Characterization Of The Human And Murine Schlafen Family Group Iii

Carlos A. Valenzuela
University of Texas at El Paso

FUNCTIONAL CHARACTERIZATION OF THE HUMAN AND MURINE SCHLAFEN FAMILY GROUP III

CARLOS A. VALENZUELA

Doctoral Program in Biological Sciences

APPROVED:

Manuel Llano, M.D., Ph.D., Chair

Douglas Watts, Ph.D.

Kathryn Hanley, Ph.D.

Siddhartha Das, Ph.D.

Giulio Francia, Ph.D.

Stephen L. Crites, Jr., Ph.D.
Dean of the Graduate School

Dedication

I dedicate this work to my family for their unwavering love and support throughout my graduate career. Especially, to my wife, whose love and encouragement have been essential during my journey. She has not only been my partner in life, and soulmate but also the driving force behind my achievements. Thank you for sharing your life with me; I love you with all that I am.

To my precious daughters, Mona and Lisa, your presence and boundless love have filled my life with joy and purpose. Thinking of you always brings a smile to my face, and I am immensely proud to be your father.

I am also grateful to my mother and father for their enduring support and for instilling in me the belief that I could achieve my dreams. Their unwavering faith in my abilities has been a constant source of motivation.

This work is dedicated to my family, who have been my pillars of strength, my inspiration, and my greatest source of love and happiness.

CHARACTERIZATION OF THE HUMAN AND MURINE SCHLAFEN FAMILY GROUP III

by

CARLOS A. VALENZUELA, B.S.

DISSERTATION

Presented to the Faculty of the Graduate School of

The University of Texas at El Paso

in Partial Fulfillment

of the Requirements

for the Degree of

DOCTOR OF PHILOSOPHY

Department of Biological Sciences

THE UNIVERSITY OF TEXAS AT EL PASO

December 2023

Acknowledgements

To my wife and daughters, their love gave me courage to face all obstacles in my journey, and the strength to overcome them. I would not be here without them, this accomplishment and all the others to come will be because of your love, patience, support, kindness, and affection. Your presence gives me inspiration to dream and the motivation to achieve those dreams.

I owe a debt of gratitude to my mentor, Dr. Manuel F. Llano, whose unwavering support and guidance have laid a strong foundation for my growth as a scientist. Thank you for your invaluable mentorship.

I am deeply appreciative of the financial support provided by my father and mother throughout my career. Without their assistance, I would not have been able to make it this far.

To my dedicated lab mates, your assistance with experiments and the provision of essential materials have been instrumental in my research journey. Your collaboration has been invaluable.

I extend my thanks to Dr. Kristine Garza, who played a significant role in my Ph.D. career as a member of my dissertation committee. Your time and insightful feedback have been instrumental in shaping my research.

I am grateful to my entire dissertation committee—Dr. Douglas Watts, Dr. Kathryn Hanley, Dr. Das Siddhartha, and Dr. Guilio Francia. Your invaluable feedback and support have played a pivotal role in the success of my academic endeavors.

Abstract

The Schlafen (SLFN) family of proteins are known for being encoded by interferon stimulated genes. The family is divided into three groups (I, II, III), for which the largest in size belong to the subgroup III. In humans, group III has the most members (SLFN5, SLFN11, SLFN13 and SLFN14); there is no member of group I and only one member of group II (SLFN12). All human SLFNs belonging to group III have been reported to impair viral protein expression or infection across a variety of viruses. The antiviral function is mediated in SLFN11 and SLFN13 by their tRNase activity, and in the catalytically inactive SLFN5 by its DNA binding properties. The mechanism of SLFN14 to impair the expression of viral proteins is unknown. In contrast to human SLFNs, the antiviral activity of murine SLFN group III, including SLFN5, SLFN8, SLFN9 and SLFN14, has not been reported.

In my thesis work I have advanced our knowledge of this family. I studied the antiviral activity of SLFNs using as models West Nile virus (WNV) and HIV-1. I identified a major role of SLFN14 in regulating at the translational level the expression of HIV-1 viral proteins encoded by codon-biased mRNAs. In addition, I discovered that SLFN11 and SLFN13, and their mouse orthologs SLFN9 and SLFN8, inhibit HIV-1 protein expression by a codon-biased mechanism, whereas SLFN11 and SLFN9, but not SLFN8, impairs WNV replication. Furthermore, I identified the nuclear localization signals that drive nuclear localization of SLFN11, and the role of proteolysis in the regulation of levels of SLFN13 and SLFN14.

Table of Contents

List of Tables

List of Figures

Chapter 1: Introduction

1.1 Overarching Hypothesis

Our laboratory focuses on the study of the antiviral innate immune response. In particular, we study the SLFN family of proteins. These proteins are upregulated by type I IFN and impair transcription or protein translation, inhibiting viral replication. Generally, viruses have evolved mechanisms to counteract restriction mechanisms; however, the anti-SLFN viral mechanisms are unknown. Therefore, a deep understanding of the interplay of the antiviral innate immune mechanisms and the viral immune evasion mechanisms will allow the development of therapeutic strategies to block viral infection. For example, the viral immune evasion mechanism could serve as target for antiviral drug development. Similarly, the proteins mediating the innate immune mechanism could be biomarkers of disease susceptibility. Thus, characterizing the antiviral properties of the SLFN family will potentially identify targets for antiviral drug development or biomarkers of disease. This is particularly important in the case of WNV, because of the lack of specific treatments or biomarkers of disease severity for this infection. Furthermore, because the SLFNs affect a variety of different viruses, new therapeutics targeting members of this family could be of a broad spectrum.

1.2 Flaviviruses and Lentiviruses as Models

Similarly, to the cell, most of viruses express their proteins by transcribing their DNA or RNA genomes into mRNAs, generating multiple copies. This amplification step is not followed by positive-sense single-stranded RNA (+ssRNA) viruses. The genome of these viruses is not copied to mRNA but is directly translated at the ribosomes. The lack of the amplification step makes these viruses more vulnerable than the host and other viruses to protein translation inefficiencies. In this research, we focused on flaviviruses, medically relevant +ssRNA viruses. Flaviviruses are important human pathogens with a global distribution. Moreover, the range of many flaviviruses are expected to expand, because of ease of transportation and adaptation of arthropods to new environments[1]. Flavivirus disease severity is difficult to predict, and there is no treatment available. This make discovery and characterization of host restriction factors

against flaviviruses of major importance, since this can lead to the development of biomarkers that will be predictive of disease severity in case of infection or development of new therapies.

Another group of +ssRNA viruses, the lentiviruses are also more susceptible than the host and other viruses to protein translation impairments. Although the cDNA viral genome is transcribed to multiple copies of mRNA, lentiviral transcripts are enriched in rarely used codons that are decoded by low abundance tRNAs, making their translation less efficient than the translation of host mRNAs. Therefore, in addition to flaviviruses we focused on HIV-1, also a major human pathogen.

1.3 The Innate Immune Response Against Viruses

Viruses are recognized by the innate immune system through pattern recognition receptors (PRRs) that trigger the production of antiviral cytokines, of which type I IFNs are some of the most important. Type I IFNs induce the expression of a set of more than 100 genes collectively called interferon-stimulated genes (ISGs) that mediate the antiviral functions of these cytokines. SLFNs are among the ISGs that affect viral protein synthesis.

The most important PRRs in the detection of WNV infection are RIG-I-like receptors, such as RIG-I and MDA5, that are cytosolic sensors belonging to the family of DExD/H box RNA helicase and can detect viral RNA in the cytosol[2]. RIG-I can detect dsRNA structure within the WNV genome, such as 5' and 3' UTRs[2]. MDA5 receptor detects high molecular weight RNA[3]. Activation of any of these two receptors leads to the expression of type-I IFN[2,3]. Toll-like receptors (TLRs) are membrane-bound receptors that also participate in viral recognition and immune signaling, each of these receptors can be divided into three domains. A transmembrane domain and a TIR domain initiates downstream signaling by binding and activating different adaptor proteins such as MYD88 or TRIF60. TLR3, TLR7, and TLR8 can identify foreign nucleic acid inside endosomes[4]. TLR3 can bind dsRNA and trigger TRIF. TLR7 and TLR8 detect ssRNA and trigger MYD88. Both types of receptors can trigger type I IFN[4]. The NOD-like receptors are cytosolic sensors able to recognize damage-associated molecular patterns and trigger inflammation and promote immune response trafficking[5].

Identification of PRRs responsible for HIV-1 detection had been difficult to find since HIV-1 is a retrovirus which integrates to the cell genome and viral mRNAs are indistinguishable from the host's own. Some of the PRRs that have been identified are TLR7, and cyclophilin A, which are important in dendritic cells[6,7]. As mentioned before TLR7 detects ssRNA within endosomes, while cyclophilin a detects the HIV-1 capsid[7]. TRIM-5α also recognized the capsid, but of incoming HIV-1 before RT and tag it with ubiquitin, which ultimately culminates in IFN activation[6]. There are unknown but important cellular sensors that detect DNA, and it is believed to be the major innate immune pathway in CD4+ T cells[8].

As mentioned above, type I IFN plays a significant role in the inhibition of the replication of a wide spectrum of viruses including flaviviruses and lentiviruses[9–12]. Pre- or co-treatment of type I IFN during WNV or dengue virus infection impairs viral replication in vitro[13,14]. Mice lacking IFN-α/β have higher viral titers and higher mortality upon WNV infection compared to WT mice[11]. Also, pre- and post-treatment oc mice with IFN-β reduces the lethality of WNV infection[11].

Type I IFN is secreted by the infected cell and acts in an autocrine and paracrine fashion by binding to the IFN-α/β receptor (IFNAR) and signaling through the JAK-STAT signaling pathway, which ultimately leads to the transcription of ISGs. Type I IFN receptor binding triggers phosphorylation of JAK1 and TYK2. Once JAK has been phosphorylated, it can phosphorylate the IFN receptor chain, which leads to the binding and phosphorylation of STAT1 and STAT2 which form heterodimers with one another. STAT1/STAT2 heterodimer can recruit IFN-regulatory factor 9 (IRF9), this complex is known as the IFN-stimulated gene factor 3 (ISGF3). ISGF3 is translocated to the nucleus to promote the expression of ISGs[15]. These enhance viral sensing by increasing expression of PRRs, and inhibit viral replication by expression of restriction factors[15].

1.4 General Characteristics of the SLFN Family

The SLFN family of proteins are among the hundreds of ISGs triggered by type I IFN. They were first described in 1998 as proteins that suppress cell growth in NIH-3T6 cells and thymocytes.

Since expression of these proteins arrested cells in G1 to S phase, the protein was named schlafen, which in German means “to sleep”. Further investigation have implicated members of this family in different processes such as cancer[16–21], programmed cell death[22], cell differentiation[23–26] and anti-viral efficacy against different viruses[27–30].

Originally it was thought that the SLFN family was exclusive to mammals. However, SLFN genes have also been found in Chondrichthyes and Amphibia[31]. The SLFN family has been characterized in mouse (m) and human (h) cells and is organized into three groups (I, II, and III). Importantly, some of the members are only expressed in mouse or human cells. Group I include the shortest SLFN proteins (37 - 42 kDa), which localize to the cytoplasm[32]. This group is formed by mSLFN1, mSLFNL1 and mSLFN2. Proteins in group II are also cytoplasmic and include mSLFN3, mSLFN4, and hSLFN12. The size of these proteins ranges from 58 kDa to 63 kDa[24]. Group III is the largest, including most of the human SLFNs and its members are the longest proteins (~100 kDa) in the family. This group is composed of mSLFN5, mSLFN8, mSLFN9, mSLFN14, hSLFN5, hSLFN11, hSLFN13, and hSLFN14[32,33], and the pseudogene mSLFN10. Group III SLFNs are localized in the nucleus; except hSLFN13 and mouse and human SLFN14 which are found in the cytoplasm[24,30].

There is a significant protein and nucleotide identity among the SLFN group III members (Tables 1 and 2). Importantly, mSLFN8 and mSLFN9 arose by gene duplication and they are proposed to be the mouse orthologs of hSLFN11 and/or hSLFN13, these two human SLFNs also exhibited a high degree of identity at the protein level.

Table 1. Percent identity matrix between the subgroup III murine and human SLFN proteins. In red and blue are marked the most likely to be orthologs to human SLFN11 and SLFN13 respectively.

	Protein Identity Matrix								
	hSlfn5	mSlfn5	mSlfn8	mSlfn9	mSlfn10ps	hSlfn11	hSlfn13	hSlfn14	mSlfn14
hSlfn5	100	59.48	48.9	49.36	48.76	53.23	52.43	42.4	40.44
mSlfn5	59.48	100	41.79	41.91	42.86	44.25	44.29	39.43	37.88
mSlfn8	48.9	41.79	100	85.82	85.71	60.59	63.08	42.58	40.21
mSlfn9	49.36	41.91	85.82	100	87.25	61.82	63.41	42.92	40.9
mSlfn10ps	48.76	42.86	85.71	87.25	100	62.18	63.16	43.86	41.6
hSlfn11	53.23	44.25	60.59	61.82	62.18	100	77.75	44.63	43.92
hSlfn13	52.43	44.29	63.08	63.41	63.16	77.75	100	44.61	43.42
hSlfn14	42.4	39.43	42.58	42.92	43.86	44.63	44.61	100	70.68
mSlfn14	40.44	37.88	40.21	40.9	41.6	43.92	43.42	70.68	100

Table 2. Percent identity matrix between the subgroup III murine and human SLFN CDS. In red and blue are marked the most likely to be orthologs to human SLFN11 and SLFN13 respectively.

	Nucleotide of CDS Identity Matrix								
	hSlfn5	mSlfn5	mSlfn8	mSlfn9	mSlfn10ps	hSlfn11	hSlfn13	hSlfn14	mSlfn14
hSlfn5	100	72.71	59.92	60.03	60.46	63.62	63.61	55.57	53.9
mSlfn5	72.71	100	57.12	56.81	57.24	58.14	57.88	53.19	52.02
mSlfn8	59.92	57.12	100	92.72	93.03	69.99	71.74	54.75	53.77
mSlfn9	60.03	56.81	92.72	100	94.02	70.32	72.19	55.2	54.38
mSlfn10ps	60.46	57.24	93.03	94.02	100	70.74	72.05	55.24	54.42
hSlfn11	63.62	58.14	69.99	70.32	70.74	100	85.4	56.3	55.07
hSlfn13	63.61	57.88	71.74	72.19	72.05	85.4	100	57.1	55.38
hSlfn14	55.57	53.19	54.75	55.2	55.24	56.3	57.1	100	78.32
mSlfn14	53.9	52.02	53.77	54.38	54.42	55.07	55.38	78.32	100

1.5 SLFN Protein Domain Organization

Domains of the SLFN proteins remain largely uncharacterized and are only software-predicted based on sequence homology analyses. Most of the predicted domains are conserved among family members, regardless of the species[23] (Fig. 1).

The N-terminal portion of SLFN proteins contains a Schlafen-like protein domain with significant sequence identity to a protein (vSLFN) found in Vaccinia, Variola and Cowpox viruses, which function is unknown[34]. The crystal structure of N-terminal SLFN13 indicates a region essential for tRNA/rRNA binding and degradation located within the Schlafen-like domain[30]. Within the Schlafen-like protein domain, an Alba_2 domain is predicted, sometimes referred to as AAA_4 domain (pfam04326), and it has been proposed to bind and hydrolyze ATP[31,35,36]. Inside the Alba_2 domain, there is a COG2868 domain which is found in transcriptional regulators and

helicases[23]. Adjacent to the Schlafen-like domain is the SWADL sequence conserved in the entire family and whose function is unknown.

The C-terminal domain harbors a sequence motif belonging to the superfamily I of RNA helicases such as the GDxxQ motif which is characteristic of this family[23,32,37,38]. Within the RNA helicase region an AAA_22 domain is found which is a ATP binding domain with homology to RNA helicases from ssRNA viruses[23]. The helicase domain contains a section with sequence homology to UvrD helicases[23].The UvrD helicases in *E. coli* have been observed to participate in DNA repair, suppress illegitimate recombination, and assist DNA replication[37]. However, structural analysis has been shown that SLFN11 does not bind nor hydrolyze ATP and the helicase is in an autoinhibited state[39].

In addition to the predicted domains discussed above, functional residues have been determined in rat (r) SLFN13 and hSLFN11 by structural and mutagenesis analyses, respectively. Structural characterization of rSLFN13 revealed important residues implicated in the tRNase activity of this protein[30]. Two positively charged patches (K38, R39, K42 and R217, K224, K276) in the protein mediate tRNA binding and a catalytic site (E205, E210, and D248) cleaves the tRNA at the acceptor stem[30]. All these functional residues are located in the N-terminus of SLFN which is necessary and sufficient for the tRNase and anti-viral activities[30,40]. These functional residues are mostly conserved in mSLFN8, SLFN11, and SLFN14 and RNase activity has been demonstrated in mSLFN8, hSLFN11, hSLFN13 and hSLFN14[30,41,42]. hSLFN5 and mSLFN5 are missing two of the residues in the first positively charged patch and one in the second patch. Interestingly, the canonical catalytic site is present; however an evolutionarily conserved D247 adjacent to the catalytic triad is substituted by a histidine. Experimentally, it has been demonstrated that SLFN5 lacks nuclease activity[30,43].

SLFN11 is regulated by the phosphorylation and dephosphorylation of specific residues (S219, T230, S753)[44]. Protein phosphatase 1 catalytic subunit γ dephosphorylates these residues activating the hSLFN11 tRNase function. The kinase responsible for phosphorylation of these residues and inactivation of hSLFN11 has not been identified yet. Importantly, residues S219,

T230, and S753 appear to be poorly conserved in murine SLFN proteins, with mSLFN9 missing all of them.

Structural analysis of SLFN11 indicates that SLFN11 forms homodimers and that this dimerization is important for SLFN11 cellular function[39]. Functionally relevant homodimerization has been proposed also for SLFN14.

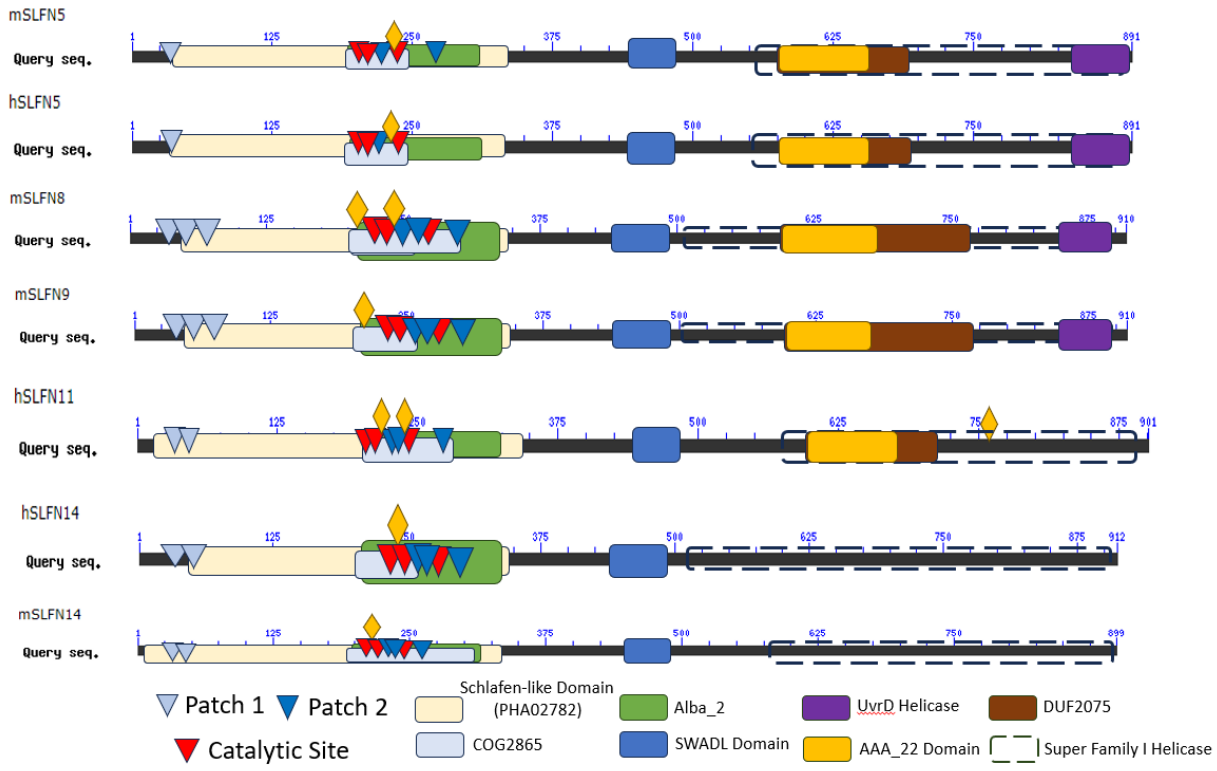

Figure 1. Domain organization of group III SLFN proteins. Note that domains indicated in mSLFN proteins in the diagram are only those conserved in hSLFN11. Domain prediction was done with the NCBI conserved domain database software.

1.6 Cellular Function of the SLFN Family of Proteins

The physiological role of the SLFN proteins is unknown. Several human and mouse Schlafen proteins belonging to group III are known to impair viral protein expression or infection of several family of viruses, including flavivirus, lentivirus, influenza, and Varicella zoster virus [45–47]. The mechanism implicated is poorly characterized. In addition, viruses such as Camelpox

virus have appropriated host SLFNs (vSLFN) and their expression in heterologous viruses such as Vaccina virus attenuates infection of mice by an unknown mechanism[48]. In general, these proteins degrade nucleic acid or impair transcription.

1.6.1 SLFN5 Function

SLFN5 lacks the residues necessary for nuclease function, however it still acts as a restriction factor against HSV-1 and HIV-1[49,50]. This activity depends on the ability of SLFN5 to bind viral (v) DNA and suppress transcription, by preventing recruitment of RNA polymerase II to the viral promoter[49,50]. SLFN5 binding to vDNA appears to be sequence-independent since it is found ubiquitously distributed through the vDNA[50]. Furthermore, SLFN5 strongly interacts with histone H3 and PRC2 complex. The PRC2 complex is known for epigenetic silencing through the regulation of structural components such as histone H3 methylation (poly comb complex). Silencing of some of the components of the PRC2 complex such as EZH1 or G9a results in the loss of activity of SLFN5[49]. Like other members of the SLFN family the activity resides on the N-terminal domain, and require the nuclear localization signal[49].

Besides SLFN5 role as a viral restriction factor, SLFN5 also plays a role in oncogenesis. Expression of SLFN5 in glioblastoma cells promotes a malignant phenotype by repressing STAT1-mediated gene transcription, in renal cell carcinoma and malignant melanoma reduced cell mobility[17,20], and in breast cancer and lung adenocarcinoma cells drives apoptosis[51–53]. However, the mechanism and *in vivo* relevance of these functions is unknown.

1.6.2 SLFN11 Function

Two functions of SLFN11 have been characterized in some detail so far. SLFN11 promotes cancer chemosensitization to DNA damaging agents[19,54] and displays antiviral activity. In both cases the role of this protein in regulating the tRNA pool seems to be relevant. Nevertheless, recruitment of SLFN11 to the stalled replication fork in response to replication stress has been proposed to mediate its role in cancer chemosensitization [16].

Viruses are completely dependent on the host to produce viral proteins. Some viruses such as herpes, retroviruses, polyoma, papilloma, adenovirus, and parvovirus tend to have an unusual, skewed codon usage compared to the host. This allows regulation of the expression of structural and late viral genes[55]. For example, in HIV-1 early genes (tat, rev and nef) have similar codon usage to the host, however late genes (gag, pol, vif, and env) use rare codons[56]. It has been demonstrated that SLFN11 impairs HIV-1 infection exploiting the differences in codon usage between the virus and the cells. Human cells lacking SLFN11 expression show a global increase in the levels of tRNA when infected with HIV-1, thus increasing viral protein synthesis. SLFN11 opposes HIV-1-induced changes in the host tRNA repertoire, affecting synthesis of HIV-1. Similarly, equine SLFN11 impairs the lentivirus equine infectious anemia virus (EIAV) infection in a codon usage-dependent manner[57]. Furthermore, SLFN11 expression has been found higher in HIV-1 elite controllers than in progressors[58,59].

In addition to HIV-1 proteins, SLFN11 regulates the expression of cellular proteins encoded by transcripts with strong codon bias[27,28]. This phenomenon may be because tRNAs need to pass a certain threshold to be efficiently used for protein synthesis, below certain threshold synthesis of proteins using these tRNAs become impaired. In contrast to SLFN5, SLFN11 localization does not play a role in its antiviral activity[16,28,57]. Both, the full-length and the N-terminus SLFN11 have antiviral activity although the full-length is nuclear while the N-terminal region which is fully cytoplasmic[27,28]. These data suggest that SLFN11 could exert its antiviral activity by targeting tRNAs either in the cytoplasm or in the nucleus.

Human SLFN11 has been also demonstrated to play an important role during viral replication of +ssRNA viruses such as flavivirus (WNV, dengue virus, Zika virus) but not of -ssRNA viruses such as vesicular stomatitis virus and Rift Valley fever virus[28]. This selectivity could reside in the replication strategy that these viruses follow, as indicated above. The genome of +ssRNA viruses have to be translated immediately after entry to initiate viral replication, instead, the genome of -ssRNA viruses is amplified upon entry by the RNA-dependent RNA polymerase packed within the virion generating multiple +ssRNA copies that are subsequently translated. Therefore, small

variations in the efficiency of translation are expected to affect +ssRNA viruses more than other viruses and the host.

Nevertheless, the mechanism implicated in flavivirus restriction is not very well understood yet. Analysis of tRNA abundance in infected cells indicates that in the absence of SLFN11 a subset of tRNAs decreases, suggesting that SLFN11 could have a sentinel role preserving physiological levels of tRNAs in response to viral infections. Importantly, the tRNAs reduced are frequently used in the translation of structural proteins in WNV. Codons read by less abundant cognate tRNAs will decrease the rate of translational elongation, facilitating co-translational polypeptide folding[28,60], thus increasing the amount of infectious viral particles generated. Indeed, WNV produced in cells lacking SLFN11 are more infectious than those produced in control cells. Similarly, reduction of translational elongation rate through rare tRNA usage has been linked to an enhanced function of RNA replicase and 3C protease of foot-and-mouth disease virus and *Neurospora crassa* circadian clock protein[28,61,62]. Furthermore, studies done on the capsid proteins of poliovirus and hepatitis A, demonstrated that replacement of native rare codons for synonymous more abundant codons decrease viral fitness[63,64].

Even though both mechanisms employed by flaviviruses, and lentiviruses seem opposite, they are both affecting translational kinetics that could affect production of both viral and host proteins. These observations suggest a physiological role for hSLFN11 in preserving the abundance of the tRNA pool.

Finally, at least for the case of hSLFN11, its anti-WNV activity appears to be cell specific. In cells such as HeLa and HEK293T that do not express endogenous hSLFN11, stable exogenously expressed SLFN11 lacks the antiviral activity[28], suggesting that other host factors may regulate the activity of this protein.

1.6.3 SLFN13 Function

Schlafen 13 was the first family member which crystal structure was resolved (PBD: 5YD0). Expression of hSLFN13 impairs HIV-1 production in HEK293T by inhibiting viral protein

synthesis[30]. In addition to tRNAs degradation, SLFN13 is able to degrade 5s, 18s and 28s ribosomal subunits[30].

The crystal structure of the N-terminus of rSLFN13 gave a molecular insight into the mechanism employed for the cleavage of tRNAs. rSLFN13-N is described as a U-pillow shaped protein made of an N and C terminal lobes bound together by a bridging domain[30]. In each lobe there is a positively charged patch (Patch 1: K38, R39, K42 and Patch 2: R217, K224, K276) with a distance suitable for tRNA docking, and catalytic triad composed of negatively charge residues (E205, E210 and D248) with a structure similar to other endoribonucleases (RNase E and RNaseIII)[30,65,66]. Mutation in any of the aforementioned sites identify reduces SLFN13 nucleolytic activity with the most drastic effect observed with at least two amino acids of the catalytic triad (E205A and E210A) which renders the protein RNase activity completely inactive[30].

1.6.4 SLFN14 Function

SLFN14 was first isolated from rabbit reticulocytes. This study observed a short form of SLFN14 to be strongly associated to the ribosomes, with a higher affinity for the 40s ribosomal subunit. The SLFN14 was reported to have RNase activity and target rRNAs and rRNA-associated mRNAs[40].

SLFN14 has also been observed to impair the translation of influenza and Varicella zoster virus suggesting that SLFN14 could has a broad-spectrum antiviral activity[29]. SLFN14 regulation is ill-defined. SLFN14 is upregulated by type I and III IFN in some cell types[29].

Human SLFN14 mutations (K218E, K219N, V220D, and K223W) have been linked to thrombocytopenia [42]. Patients carrying one of these mutations in only one of the SLFN14 alleles are born with defects on megakaryocyte maturation and platelet dysfunction a condition known as inherited thrombocytopenia[42,67,68]. This dominant negative mutant effect is not due to loss of ribosomal binding or RNase activity, but likely due to miss folding of SLFN14 which lead to the degradation of WT and mutant proteins through dimerization[42]. Lastly, this phenotype can be recapitulated in mice carrying the mutation K208N, which is analogous to human SLFN14 K219N

mutation[69]. Mice homozygotic for this mutation in SLFN14 do not survive to weaning age due to severe anemia[69]. These findings indicate that SLFN14 play an important role in hematopoiesis, conserved across species. SLFN14 may also have an important function in the protection of the genome against transposon-induced mutations, as it has been observed that expression of SLFN14 to drastically inhibit LINE-1 retrotransposition[70].

1.7 Significance and Hypothesis

Despite the emerging role of SLFN proteins in viral infection, cancer, and hematopoiesis, these proteins remain largely uncharacterized. My research fills some of these gaps in knowledge, contributing to a better understanding of the physiological and pathogenic mechanism of these proteins. Potentially, my findings could help to identify SLFN proteins as therapeutic targets or disease susceptibility biomarkers.

Due to the conservation of key residues implicated in SLFN13 in the tRNase activity, I hypothesize that SLFN11, SLFN8 and SLFN9 will degrade tRNAs, affecting through a codon-biased mechanism, HIV-1 infection. Identification of SLFN11 murine orthologs will facilitate studying the roles of these antiviral mechanisms *in vivo*, using mouse models. Furthermore, because mRNAs enriched in rare codons could cause ribosomal stalling during translation, I postulate that SLFN14 could oppose the translation of these messengers. Because of the evolutionary conservation of SLFN8, SLFN9, and SLFN11, I predict that these proteins could share their anti-WNV activity. The broad nuclease activity of these proteins suggests that a tight control in their expression is required to maintain cell integrity. In my thesis work I will investigate these aspects of the molecular biology of the SLFN proteins.

Chapter 2: Evaluation of the Antiviral Activity of SLFN14

This chapter has been submitted into bioRxiv.

Valenzuela, C., Saucedo, S. & Llano, M. Schlafen14 Regulates Gene Expression Depending on Codon Usage. bioRxiv (2023). doi:10.1101/2023.03.19.533350

2.1 Introduction

Codon usage is one of the factors influencing the amount of polypeptide produced per mRNA in bacterial and eukaryotic cells, and tRNA abundance seems to be a major factor in this process[71–79]. The relative deficiency of charged tRNAs, associated with the translation of transcripts rich in rare codons, causes ribosome pausing reducing the translation elongation rate and leading to ribosome stalling[75,80–83]. This event decreases global protein synthesis by premature termination and degradation of the truncated protein through the ribosome-associated protein quality control[84,85], triggering degradation of the associated mRNAs through the No-go decay mechanism[86–89], rRNA degradation through the nonfunctional 18S rRNA decay pathway, or by inhibit translation initiation via the Integrated Stress Response[90].

The tRNA repertoire is modified during stress[91–98] including viral infection[27,28,56,99,100]. The innate immune system has evolved mechanisms to regulate protein expression based on rare codon usage bias through the effect of the type I IFN-induced protein SLFN11. By tRNA degradation, SLFN11 negatively regulates expression of proteins encoded by transcripts with bias towards rare codons[27,28,41,101]. SLFN13 also degrades tRNAs[30], whereas SLFN5 and SLFN2 bind to tRNA without degrading them, and through this interaction SLFN2 protects stress-induced, angiogenin-mediated tRNA degradation[43,95].

Another member of the SLFN family, SLFN14, was discovered as a stalled ribosome-associated endoribonuclease, and the purified protein was shown to degrade mRNA, tRNA, and ribosomes in vitro[40,42,69], and to degrade LINE-1 mRNA[70] in cells. SLFN14 was also reported to impair the expression of two varicella zoster virus proteins, immediately early and glycoprotein E[29,70], and the nucleoprotein from influenza virus[29]. Intriguingly, all these viral proteins are encoded by transcripts enriched in rare codons that exhibit low codon adaptation indexes (CAI),

a measurement of the synonymous codon usage bias[102]. For example, varicella zoster virus proteins, immediately early 62 and glycoprotein E have a CAI of 0.72 and 0.70, respectively, and the nucleoprotein from influenza virus has a CAI of 0.75. Proteins with CAIs <0.8 are considered to have codon usage bias. Therefore, we postulated that SLFN14 could inhibit translation of transcripts with bias toward rare codons in response to constraints that these transcripts likely encounter during translation elongation, i.e. ribosome stalling. To evaluate our hypothesis, we selected as a model HIV-1, since this viral genome is rich in adenine nucleotides determining a strong codon usage bias that differs from that of the host[103,104].

Our data indicate for the first time that SLFN14 potently inhibits expression of transcripts rich in rare codons, i.e., HIV-1 Gag and firefly luciferase; but not of those poor in rare codons, i.e., codon optimized HIV-1 Gag, HIV-1 Tat, cyan, monomeric (m) cherry, and green fluorescent proteins, and human CD4. As a consequence, HIV-1 replication is inhibited by SLFN14. The anti-HIV-1 effect was observed in primary monocytes and CD4+ T lymphocyte, and in cancer (SUP-T1) and transformed (HEK293T) cell lines. This activity is type I IFN-independent but requires the endoribonuclease function of SLFN14. Expression of SLFN14 was associated with ribosome degradation in cells co-expressing wild type but not codon optimized HIV-1 Gag mRNA. In sum, our results indicate a novel function of SLFN14 in restricting expression of transcripts rich in rare codons.

2.2 Materials and Methods

2.2.1 Cell lines

SUP-T1, CEM and MOLT-3 cells and primary immune cells were grown in RPMI 1640 medium supplemented with 20% heat-inactivated fetal calf serum, 2 mM L-glutamine, and 1% penicillin-streptomycin, while HEK293T cells were grown in Dulbecco's modified Eagle's

medium (DMEM) supplemented with 10% heat-inactivated fetal calf serum, 2 mM L-glutamine, and 1% penicillin-streptomycin. All the cell lines used were previously obtained from ATCC.

2.2.2 Expression plasmids

pHluc was derived from pNL4-3luc-R- E- as described in[105]. This single-round infection HIV-1 expresses LTR-driven firefly luciferase from the nef slot, lacks VPR expression, and has a 426 nt deletion in the env gene. FLAG-tagged human and mouse SLFN14 (Origene, RC226257 and MR225976) were expressed from pCMV6-Entry. Empty plasmid was derived from the human SLFN14 expression plasmid by deleting the entire open reading frame (2.8 kb) by digestion Sal I / Xho I and religation of the backbone (4.8 kbs). FLAG-tagged human SLFN14 D249A was generated by site directed mutagenesis with the QuickChange Lightning Site-Directed Mutagenesis Kit (Agilent) using reverse primer SS1 (5'-atccaccccaatgaggacatatcc-3') and forward primer SS2 (5'-gCtaagagcaaagaagtggttggatg-3'), the point mutation is indicated in upper case in the primer sequence. The entire sequence of the SLFN14 D249A cDNA was verified by overlapping DNA sequencing. Wild type Gag was expressed from pCMVΔR8.91 (a gift of D. Trono) and codon optimized Gag from pARP-8675 (NIH AIDS Reagent Program). This construct expresses a codon-optimized HIV-1 clone 96ZM651.8 Gag pre-protein[106]. Cyan fluorescent protein expression plasmid was pECFP-C1 (Clontech). Plasmids pCAGGS-CD4-Myc (Addgene, 58537), and pRP-mCherry/Puro-CAG>hCXCR4 (VectorBuilder, VB900125-2200scz) were used to express CD4 and CXCR4 respectively. The CXCR4 expression plasmid contains an independent mCherry expression cassette (bicistronic plasmid). pCI Luc contains firefly luciferase cDNA cloned MluI / Xba I in pCI (Promega). pNLENG1-ES-IRES (a gift of D.N. Levy, NYU) encodes a single-round infection HIV-1 (HIVeGFP) that lacks Env and

expresses LTR-driven eGFP from the nef slot[107]. pNL4-2 encodes a wild type HIV-1 (strain NY5/BRU, LAV-1).

2.2.3 Generation of viruses

Procedures previously described[108,109] were used for production of Hluc, HIVeGFP, and NL4-3. Briefly, HEK293T cells by calcium-phosphate co-transfection of 15 ug of pHluc or pNLENG1-ES-IRES and 5 ug of pMD.G, a vesicular stomatitis virus glycoprotein G (VSV-G) expression plasmid, or 15 ug of pNL4-3. Seventy-two hours after transfection, the viral supernatants were harvested and in the case of Hluc and HIVeGFP concentrated using Lenti-X concentrator (Clontech 631231) following the manufacturer instructions. VSV reporter viruses expressing eGFP[110] were produced by infecting HEK293T at MOI 0.01 and collecting the cell supernatant 18 hrs later.

2.2.4 Immunoblotting

HEK293T cells (~$3x10^6$) were lysed in 100 ul of Laemmli sample buffer (12 mM Tris-Cl, pH 6.8, 0.4% SDS, 2% glycerol, 1% β-mercaptoethanol, 0.002% bromophenol blue). SUP-T1, CEM and MOLT-3 cells, PBMCs, CD4+ T lymphocytes, and monocytes were lysed for 15 min on ice in 100 µl of CSK I buffer[111] (10 mM PIPES [piperazine-N,N′-bis(2-ethanesulfonic acid)] (pH 6.8), 100 mM NaCl, 1 mM EDTA, 300 mM sucrose, 1 mM MgCl2, 1 mM dithiothreitol (DTT), 0.5% Triton X-100) containing protease inhibitors (final concentrations of 2 µg/ml leupeptin, 5 µg/ml aprotinin, 1 mM phenylmethylsulfonyl fluoride [PMSF], and 1 µg/ml pepstatin A). Cell lysates were centrifuged at 22,000 × g for 3 min at 4°C, and the supernatant mixed with Laemmli sample buffer, boiled for 10 mins, and saved at -80ºC for further analysis. Cell lysates (15 ul) was resolved by SDS-PAGE and transferred overnight to polyvinylidene difluoride (PVDF) membranes at 100 mA at 4°C. Membranes were blocked with Tris-buffered

saline (TBS) containing 10% milk for 1 h and then incubated with the corresponding primary antibody diluted in TBS-5% milk-0.05% Tween 20 (antibody dilution buffer). FLAG-tagged mouse and human SLFN14 was detected with anti-FLAG MAb (1/500) (M2; Sigma), non-tagged human SLFN14 was detected with antibodies anti-SLFN14 PAb (Abcam, ab254806) (1/500) and anti-SLFN14 PAb (Invitrogen, PA520868) (1/500), that recognize epitopes in the N-terminal and C-terminal regions, respectively. As a loading control, anti-α-tubulin MAb (clone B-5-1-2; Sigma) was used at a 1/4,000 dilution. Membranes were incubated overnight at 4°C with anti-FLAG and -SLFN14 antibodies, whereas anti-α-tubulin MAb was incubated for 30 mins at 25°C. Primary antibody-bound membranes were washed in TBS-0.1% Tween 20, and bound antibodies were detected with goat anti-mouse Ig-horseradish peroxidase (HRP) (Sigma, 1/2,000) or mouse anti-rabbit IgG-HRP (Santa Cruz Biotech, 1/4,000) diluted in antibody dilution buffer. These antibodies were incubated for 1 hr at 25°C. Unbound secondary antibodies were washed as described above and bound antibodies detected by chemiluminescence.

2.2.5 Analysis of SLFN14 activity

HEK293T cells were plated at 0.45×10^6 cells/well in a six-well plate, or at 10^6 cells in a T25 flask and transfected by calcium-phosphate with corresponding plasmids, and transfection medium was replaced with fresh culture medium 18 hrs later. In experiments evaluating the effect of SLFN14 on protein expression, cells were transfected in six-well plates. Each well was transfected with 1 ug of empty plasmid or 1ug of mouse or human SLFN14 and 1ug of the target plasmid (pHLuc, pCILuc, pCMVΔR8.9, or pARP-8675), and cells were analyzed 72 hrs after transfection. In experiments evaluating the effect of SLFN14 on the viral infection, cells were plated in T25 flasks and transfected with 5 ug of empty plasmid or mouse or human SLFN14. Cells were infected 48 (HIV-1) or 72 (VSV) hrs after transfection. Cells infected with VSV were

challenged with this replication competent virus at MOI 0.03 to reduce the cytopathic effect. Infection was carried out for 1 hr or 6 hrs that the input virus was removed by washing infected cells and then cells were cultured in the presence of a neutralizing anti-VSV-G antibody until analysis. Infected cells were analyzed by FACS 24 hrs after infection. Cells infected for 1 hr allowed analysis of the effect of SLFN14 on the first round of infection and cells infected for 6 hrs informed on the activity of SLFN14 on viral spreading. In experiments evaluating the activity of SLFN14 on HIV-1 wild type (NL4-3) or HIVeGFP, 48 hrs after transfection cells were detached mechanically and infected with HIV-1 by spin-inoculation. For this, cells (~$2x10^6$) were resuspended in 500 ul of 37ºC-warmed culture medium in a 15 ml tube and centrifuged at 1,200g for 2 hrs at room temperature. Input HIV-1 wild type was removed the next day by extensive washing in culture medium and viral replication was determined by p24 ELISA at days 3 and 5 post-infection. HIVeGFP infection was measured by flow cytometry 72 hrs post-infection.

2.2.6 Purification of Primary Cells

Blood samples were obtained from two deidentified healthy individuals in concordance with approved protocol (IRB #1741809) from the Institutional Biosafety Committee of the University of Texas at El Paso and after informed consent was obtained from all subjects. All experiments were performed in accordance with relevant guidelines and regulations of our institution. Blood (60 mls) was centrifuged at 600 xg for 10 mins and plasma removed. Blood cells were mixed with 6 mls of PBS and 25 mls of this cell suspension was layered on 18 mls of Ficoll-Paque (Fisher Scientific, 17144003) and spun down for 35 mins at 400 x g at room temperature. The PBMC fraction was harvested, diluted three-fold in PBS, and collected by centrifugation at 600 xg for 10 mins. Uncultured fresh PBMCs (10^6) were lysed in 50ul of CSKI, as described above, an analyzed by immunoblot. PBMCs ($0.33X10^6$) were plated in round bottom wells in 96 wells-plates in 100ul of culture medium and treated with different stimuli for 72 hrs. In addition,

PBMCs ($4X10^6$) were subjected to isolation of naïve CD4+ T cells (MiltenyiBiotec 130-094-131) or monocytes (MiltenyiBiotec 130-096-537) following the manufacturer instructions, and isolated cells were plated in round-bottom wells in 96 wells plates in 100ul of culture medium and treated with different stimuli for 72 hrs. Treatments were culture medium (control), IL2 (30 U/ml) plus PHA (5 ug/ml), PMA (100 ng/ml), and IFN-α1 (10,000 U/ml). PBMCs and CD4+ T cells were also treated with Anti-Biotin MACSiBead (MiltenyiBiotec 130-091-441) loaded with anti-CD3 and anti-CD28 antibodies (anti-CD3/CD28 immunobeads) using one bead per two cells, and monocytes with GM-CSF (50 ng/ml) plus IL4 (50 ng/ml). Cells from one well of the 96-wells tissue culture plate were lysed in 50ul of CSKI, as described above, an 15ul of the cell lysate analyzed by immunoblot.

2.2.7 Electroporation of immune cells

SUP-T1 cells and primary CD4+ T lymphocytes and monocytes were electroporated using Amaxa Cell Line Nucleofector Kit V (VCA-1003), and programs O-017 (T cells) or V-001 (Monocytes) with 1ug pNL4-3 and 1ug empty plasmid or human SLFN14 expression plasmid. Seventy-two hrs after electroporation cell viability was determined by measuring ATP levels (Promega G9241) and 30 ul of cell supernatant was transferred to fresh SUP-T1 cells (10^5 cells in 500 ul). HIV-1 p24 was determined by ELISA in the SUP-T1 cell culture supernatant at different times post-transfer.

2.2.8 RNA polymerase III (RNA Pol III) and Janus kinase (JAK) inhibitors

HEK293T cells were transfected as described above with empty or human SLFN14 expression plasmids and a plasmid encoding Hluc in the presence of RNA Pol III inhibitor (Sigma ML-60218, 40 and 20 uM) or tofacitinib (Sigma PZ0017, 200 and 100 nM). Transfection

medium was replaced with fresh culture medium 18 hrs later and inhibitors were added again. Cells were analyzed 72 hrs after transfection.

2.2.9 HIV-1 p24 ELISA

HIV-1 p24 levels were determined by a sandwich ELISA according to the manufacturer's instructions (ZeptoMetrix, 22157319). Briefly, cell culture supernatants were diluted appropriately and incubated on the ELISA antibody pre-coated wells overnight at 37°C. Unbound proteins were removed by washing the wells 6 times with 200 µl of washing buffer, and bound HIV-1 p24 was detected by incubating each well with 100 µl of the anti-HIV-1 p24-HRP secondary antibody for 1 h. Unbound antibodies were removed by washing as described above, and bound antibodies were detected by incubating each well with 100 µl of substrate buffer for 30 min at room temperature until the reaction was stopped by adding 100 µl of stop solution into each well. The absorbance of each well was determined at 450 nm using a microplate reader (Versa max microplate reader; Molecular Devices).

2.2.10 Luciferase assay

Cells in suspension (100 ul, ~3X105) were mixed with 75ul of 0.1% Triton X100 PBS and 25 µl of substrate (Bright-Glow™ Luciferase Assay System, Promega), and 50ul aliquots were distributed in triplicate wells of a 96-wells white plate and analyzed in a microplate luminometer.

2.2.11 CD4 and CXCR4 Expression by Flow Cytometry analysis

CD4 and CXCR4 expression was detected in HEK293T cells (10^6) transfected with 5 ug of empty plasmid or plasmids expressing human or mouse SLFN14 together 5 ug of plasmids expressing human CD4 and CXCR4. Transfected cells were harvested by mechanical

dissociation and 10^5 cells re-suspended in 100 uL of 1x PBS containing 1 uL of Alexa 488-labeled anti-human CD4 (eBioscience™, 53-0048-42) and incubated on ice for 5 min. CXCR4 and mCherry are expressed from the same bicistronic plasmid and therefore mCherry was used as a proxy of CXCR4 transfection efficiency. Cells were analyzed with a Gallios flow cytometer (Beckman Coulter). Fluorescence minus one control were used to set up the flow cytometer. Data was analyzed with Kaluza Analysis software version 1.3.

2.2.12 Quantitative RT-PCR and PCR, and rRNA integrity analyses

Total RNA was isolated from cells or sucrose density gradient fractions using TRIzol LS reagent (Invitrogen 10296010) according to the manufacturer's instructions. All RNA samples had ratios of absorbance at 260/280 nm of 1.8 to 2.0, indicating that samples were contaminant-free. Purified RNA samples were stored at -80°C until use. Different mRNAs were detected by RT-PCR (BioRad, 1725151) using 1 ng of total RNA. HIV-1 Gag wild type mRNA was detected with primers DR22 (5'-agcaggaactactagtaccc-3') and DR23 (5'-ttgtcttatgtccagaatgc-3'), while primers CV35 (5'-cgccggcaccacaagcaccc-3') and CV36 (5'-ctgcttgatgtccaggatgc-3') were used to detect Gag codon optimized, and primers EL9 (5'-acccctggccaaggtcatcc-3') and EL10 (gacggcaggtcaggtccacc) were used for GAPDH. Human SLFN14 was detected by RT-PCR using primers CV43 (5'-atggatgttttcagccttccactaaggatttgc-3') and SS1 (5'-atccaccccaatgaggacatatcc-3') that bind to exon 3 which encodes the N-terminal region of the protein. DNA was extracted from cells transfected with pCMVΔR8.91 using TRIzol LS reagent and PCR amplified with primers DR22 and DR23 using IQ SYBR Green Supermix (BioRad, 1708882). Total RNA from $0.33x10^6$ cells was used for electrophoretic analysis of rRNA integrity with an Agilent Technologies 4200 TapeStation. As previously reported[112], RNA degradation bands where considered those that migrate between the 18S rRNA and small RNAs bands in the region of

1500 base pairs (bp) to 200 bp. RNA degradation bands were quantified with the Agilent TapeStation Controller Software 4.1.

2.2.13 Sucrose Density Gradient

HEK293T cells ($3X10^6$) were plated in a T25 and calcium-phosphate transfected with 4 ug of empty plasmid or human SLFN14 expression plasmid and 4 ug of pCMVΔR8.91 or pARP-8675. The next day the transfection medium was replaced with fresh culture medium and 48 hrs later cells were mechanically harvested and used for the sucrose density gradient as previously described[40,42]. Briefly, cells were lysed by incubation in ice in Buffer A (20 mM Tris-HCl, pH 7.5, 100 mM KCl, 2.5 mM MgCl 2 , 1 mM DTT, 0.25 mM spermidine) supplemented with 0.5% Triton x100 and protease inhibitors (final concentrations of 2 μg/ml leupeptin, 5 μg/ml aprotinin, 1 mM phenylmethylsulfonyl fluoride [PMSF], and 1 μg/ml pepstatin A). Cell lysates were centrifuged at 2000 g for 10 mins at 4ºC and the supernatant loaded on top of a 15 ml 10-30% sucrose density gradient (SDG) prepared in buffer A supplemented with 0.1 mg/ml cycloheximide and protease inhibitors. Cycloheximide was used to prevent polysome runoff[40] SDG was centrifuged at 117,100xg for 3.5 hrs at 4ºC in a Sorvall WX 80+ Ultracentrifuge in a Surespin 630 rotor in 17 ml tubes (Thermo, 79386). Fractions (500 ul) were collected from top to bottom of the gradient (30 fractions). SLFN14 was detected by immunoblotting with an anti-FLAG antibody in each fraction, loading per lane 12 ul; whereas RNA was extracted from 400 ul of the fraction with TRIzol LS reagent, as described above**.**

2.2.14 Statistical Analysis

GraphPad Prism version 9.4.1 was used for statistical analysis. One-way ANOVA was used to test the impact of human and mouse SLFN14 on the expression of the proteins of interest, and

the Dunnett's post hoc test was used to identify significant differences between cells expressing empty plasmid (control group) and cells expressing SLFN14 proteins (experimental groups). Two-tailed t test was used to evaluate the statistically significant of experiments with only two groups (control and experimental). Experiments where the comparison was between a specific control and a specific experimental group one-way ANOVA and Bonferroni post hoc test was utilized. p-values were indicated as follow: no significant (ns) > 0.05, * ≤ 0.05, ** ≤ 0.01, *** ≤ 0.001, **** ≤ 0.0001.

2.2.15 Accession Number: The sequence of the 5' end of the SLFN14 exon 3 that we detected in MOLT-3 cells is deposited under OP548624 and OP548623.

2.2.16 In silico analysis

Codon adaptation index (CAI) was determined with the CAIcal program [http://genomes.urv.cat/CAIcal[113]], as described in[114] using as reference the human codon usage table (http://genomes.urv.cat/CAIcal/CU_human_nature). SLFN14 molecular weight was predicted using Expasy.

2.3 Results

2.3.1 Human and Mouse SLFN14 Preferentially Impairs the Expression of Proteins Enriched in Rare Codons

To evaluate the effect of SLFN14 on the expression of genes enriched in rare codons we used HIV-1 as a model. Advantageously, HIV-1 gene expression can be studied with plasmids encoding this virus or its individual proteins or using the copy of the viral genome integrated into the host chromosome, whose expression is regulated as any cellular gene is. Furthermore, HIV-1 has open reading frames with different codon usage that are included in a common transcript produced from the viral promoter. Moreover, different reporter genes can be efficiently inserted into the HIV-1 genome. We have used the methodology described before to determine the anti-

HIV-1 activity of SLFN11[27,28], SLFN13[30], and N4BP1[115]. This method has been also extensively used to evaluate the production phase of the HIV-1 life cycle. In this experimental strategy, HEK293T cells are co-transfected with plasmids expressing the proteins being evaluated and a plasmid encoding HIV-1. Because HEK293T cells lack detectable expression of SLFN14 mRNA[42] and proteins (see figure 2A below), these cells are suitable to study SLFN14.

The HIV-1 reporter[116] that we used to analyze the activity of SLFN14 expresses from the viral promoter a transcript that contains open reading frames with synonymous codon-usage that greatly differ from the host, such as Gag (CAI of 0.56). A fraction of this transcript experiences splicing, generating other transcripts containing open reading frames whose synonymous codon-usage resemble the host preferences, as for example Tat (CAI of 0.761), and a reporter gene (eGFP) that is codon optimized for human cells (CAI of 0.962). Transcription of this precursor mRNA is Tat-dependent. Therefore, this reporter offers the possibility to evaluate the effect of SLFN14 on the expression of transcripts with three different CAIs.

BLAST analysis[117] indicated that the primary structure of human and mouse SLFN14 proteins is 70% identical, representing the highest evolutionary conservation between human SLFNs and their mouse orthologs in the SLFN group III[33]. Therefore, we hypothesized that mouse and human SLFN14 will share relevant biological functions and tested this prediction in our experiments.

HEK293T cells were co-transfected with the plasmid expressing this HIV-1 reporter[116] and a plasmid expressing cyan fluorescence protein (CFP), together with either a plasmid empty (control) or plasmids expressing mouse or human SLFN14. Seventy-two hours later the expression of CFP and eGFP, and HIV-1 p24 (a limited proteolysis product of Gag) was analyzed by flow cytometry and ELISA, respectively. HIV-1 p24 values were normalized to the % of CFP+ cells to account for transfection efficiency. In addition, levels of SLFN14 in these cells was determined by immunoblot analysis. Data in Fig. 2.1A-I showed that cells expressing either mouse or human SLFN14 produced ~86% less HIV-1 p24 than control cells. Despite this severe reduction in HIV-1 p24, the eGFP Mean Fluorescence Intensity (MFI), an estimate of the number eGFP molecules

per cell, was similar in cells expressing or no SLFN14 proteins (Fig. 2.1A-II). SLFN14 levels were verified in these cells by immunoblot (Fig. 2.1A-III). Because the transcript encoding eGFP derives from the messenger encoding Gag, preservation of eGFP expression indicated that SLFN14 impaired Gag production at a post-transcriptional step. Furthermore, since expression of both Gag and eGFP are dependent of on Tat expression, we can conclude that since eGFP levels are not affected neither is Tat expression affected by SLFN14. Therefore, SLFN14 proteins selectively impaired the expression of Gag due to lower CAI.

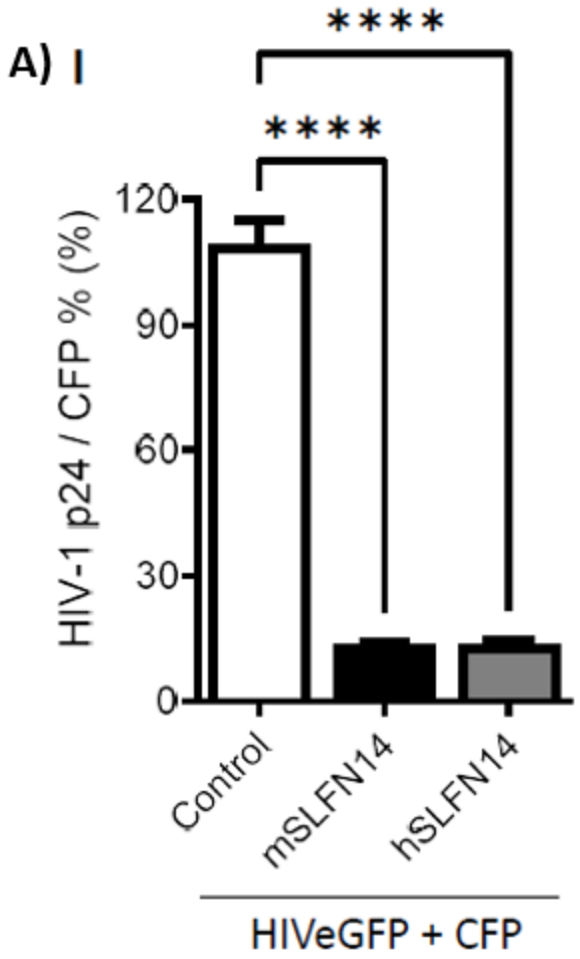

A) II

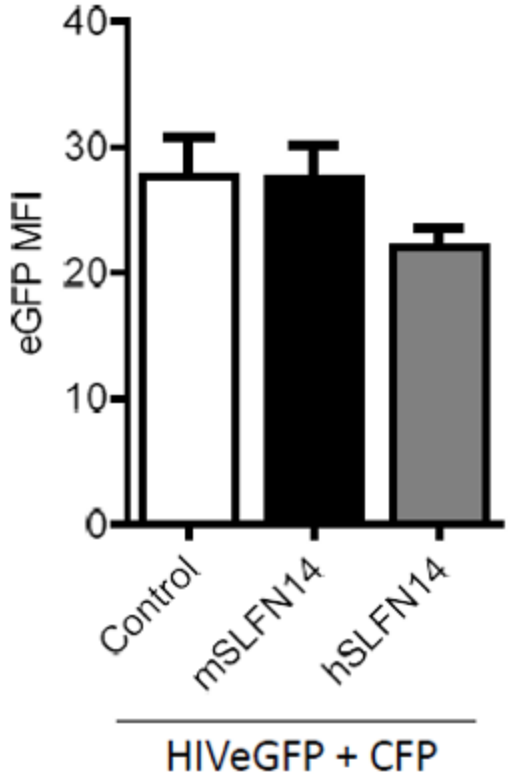
40
30
20
10
0
eGFP MFI
Control
mSLFN14
hSLFN14
HIVeGFP + CFP

A) III

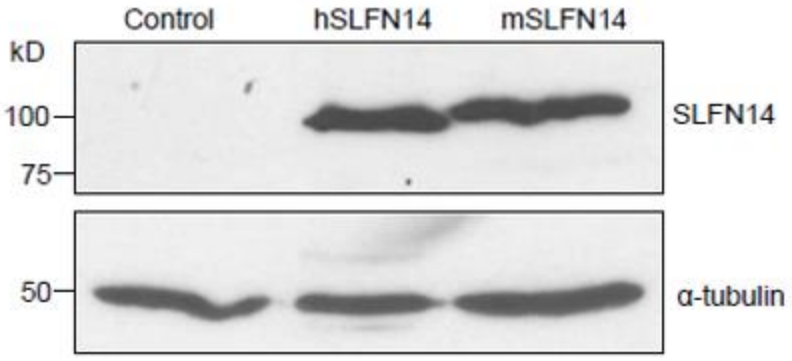
Control
hSLFN14
mSLFN14
kD
100
75
SLFN14
50
α-tubulin

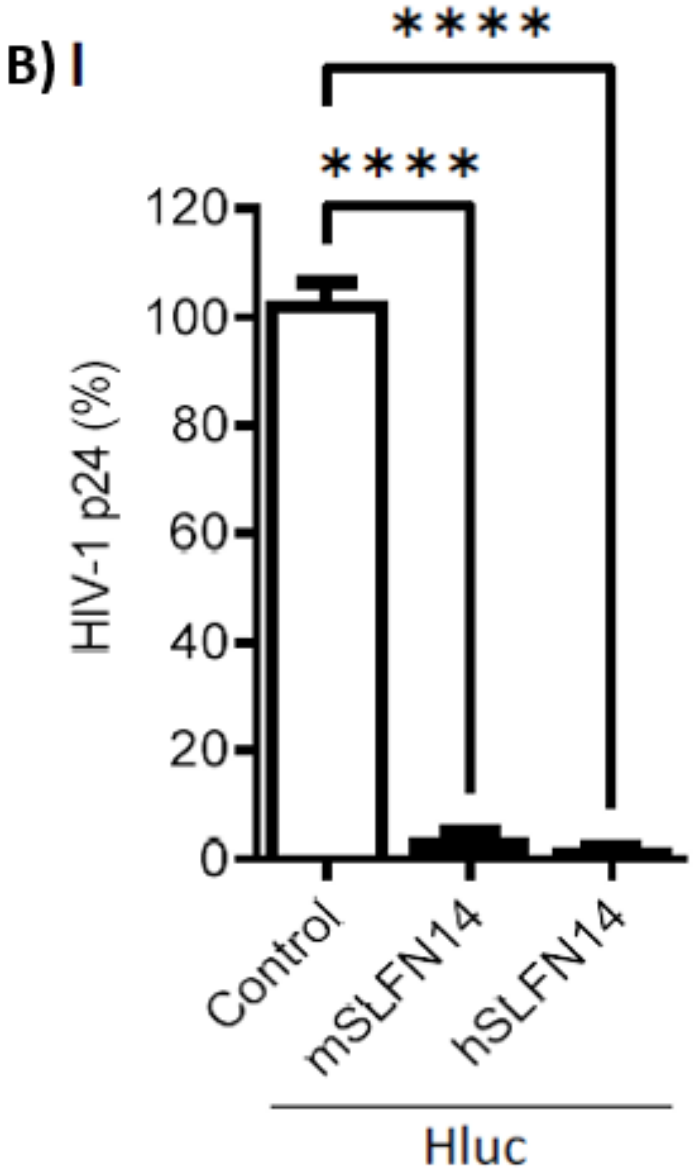
B) I
****
****
120
100
80
60
40
20
0
HIV-1 p24 (%)
Control
mSLFN14
hSLFN14
Hluc

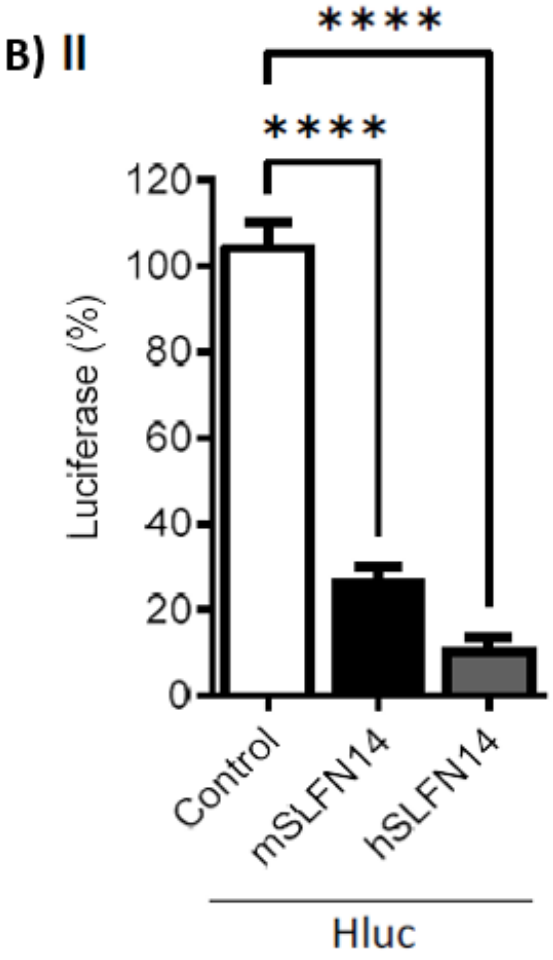
B) II
****
****
120
100
80
60
40
20
0
Luciferase (%)
Control
mSLFN14
hSLFN14
Hluc

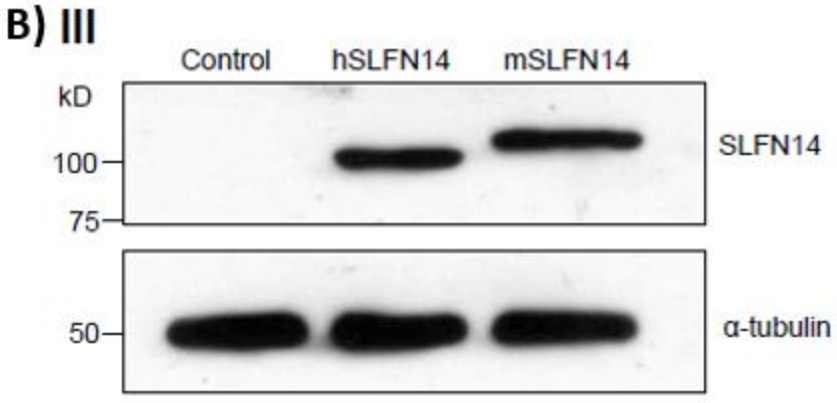
B) III
Control
hSLFN14
mSLFN14
kD
100
75
50
SLFN14
α-tubulin

Fig. 2.1 Effect of SLFN14 on HIV-1-driven protein expression. (A) HEK293T cells that were co-transfected with a plasmid encoding an HIV-1 virus expressing eGFP and a plasmid expressing CFP together and either an empty plasmid (control cells) or a plasmid expressing human (h) or mouse (m) SLFN14. (I) HIV-1 p24 levels were normalized for transfection efficiency (% of CFP+ cells) and expressed as % of control cells. (II) eGFP MFI levels and (III) SLFN14 protein expression in cells represented in panel (I). In the immunoblot (III) an anti-FLAG antibody was used to detect SLFN14 and α-tubulin levels were determined as a loading control. Data corresponds to a triplicate experiment and are representative of five independent experiments. (B) HIV-1 p24 (I) and luciferase levels (II) expressed as % of control cells in HEK293T cells that were co-transfected with a plasmid encoding an HIV-1 virus expressing firefly luciferase (Hluc) and either an empty plasmid (control cells) or a plasmid expressing human (h) or mouse (m) SLFN14. (III) Expression of SLFN14 in these cells was detected by immunoblot as described in Fig. 1A-III. Data correspond to a triplicate experiment and are representative of more than twenty independent experiments performed over several months. Statistical significance in (A) and (B) was calculated with one-way ANOVA and Dunnett post hoc tests. **** $P \leq 0.0001$. Data showing not statistically significant differences (NS $P > 0.05$) were not indicated in any of the figures of this work.

Next, we used a different HIV-1 reporter[105] that expresses Tat-dependent, viral promoter driven firefly luciferase (CAI of 0.71), instead of eGFP. As before, HEK293T cells were co-transfected with an empty plasmid (control) or plasmids expressing human or mouse SLFN14, and a plasmid encoding the luciferase HIV-1 reporter and analyzed seventy-two hrs later. Again, cells expressing mouse and human SLFN14 produced ~97% less HIV-1 p24 than the control cells (Fig. 2.1B-I); whereas luciferase expression was reduced by ~73% and ~89% by mouse and human

SLFN14, respectively (Fig. 2.1B-II). SLFN14 levels were verified in these cells by immunoblot (Fig. 1A-III). These findings further demonstrated that SLFN14 impairs the expression of viral and non-viral proteins with low CAIs.

We also determined the effect of SLFN14 proteins on luciferase levels using a simpler expression system. HEK293T cells were co-transfected with the empty plasmid or plasmids expressing SLFN14 proteins, and a plasmid expressing firefly luciferase from a CMV enhancer/promoter (pCI Luc), and luciferase activity was measured three days after transfection. In these experiments, SLFN14-transfected cells produced ~79 % (mouse) and ~53% (human) less luciferase than the control cells (Fig. 2.2A-I), indicating an HIV-1-independent effect of SLFN14 proteins on the expression of luciferase. SLFN14 levels were verified in these cells by immunoblot (Fig. 2.2A-II).

The effect of SLFN14 on the expression of a codon optimized messenger in a simpler expression system was also evaluated. HEK293T cells were co-transfected with a plasmid expressing CFP (CAI of 0.96) and plasmids expressing mouse or human SLFN14 or not (empty, control). Transfected cells were evaluated by flow cytometry three days later. As data in Fig. 2.2B indicate, expression of mouse or human SLFN14 did not reduce CFP MFI, in comparison to the control cells, indicating again that SLFN14 does not affect expression of codon optimized messengers.

To further evaluate a potential function of SLFN14 in codon usage-based control of gene expression, we determined the effect of SLFN14 on the expression of HIV-1 Gag wild type and codon optimized (CAI of 0.99). These Gag open reading frames are under the transcriptional control of the CMV enhancer/promoter. HEK293T cells were co-transfected with plasmids expressing CFP and either empty plasmid or SLFN14 expression plasmid together with plasmids expressing wild type or codon optimized Gag. HIV-1 p24 and CFP levels were measured 72 hrs after transfection by ELISA and flow cytometry, respectively, and HIV-1 p24 levels were normalized to the transfection efficiency (% of CFP+ cells). In these experiments, despite that similar levels of SLFN14 were achieved in cells expressing wild type and codon optimized Gag

(Fig. 2C-I), SLFN14 impaired by ~10 folds the expression of wild type Gag and by only ~1.8 folds the expression of codon optimized Gag (Fig. 2C-II), indicating that SLFN14 preferentially impairs expression of transcripts enriched in rare codons.

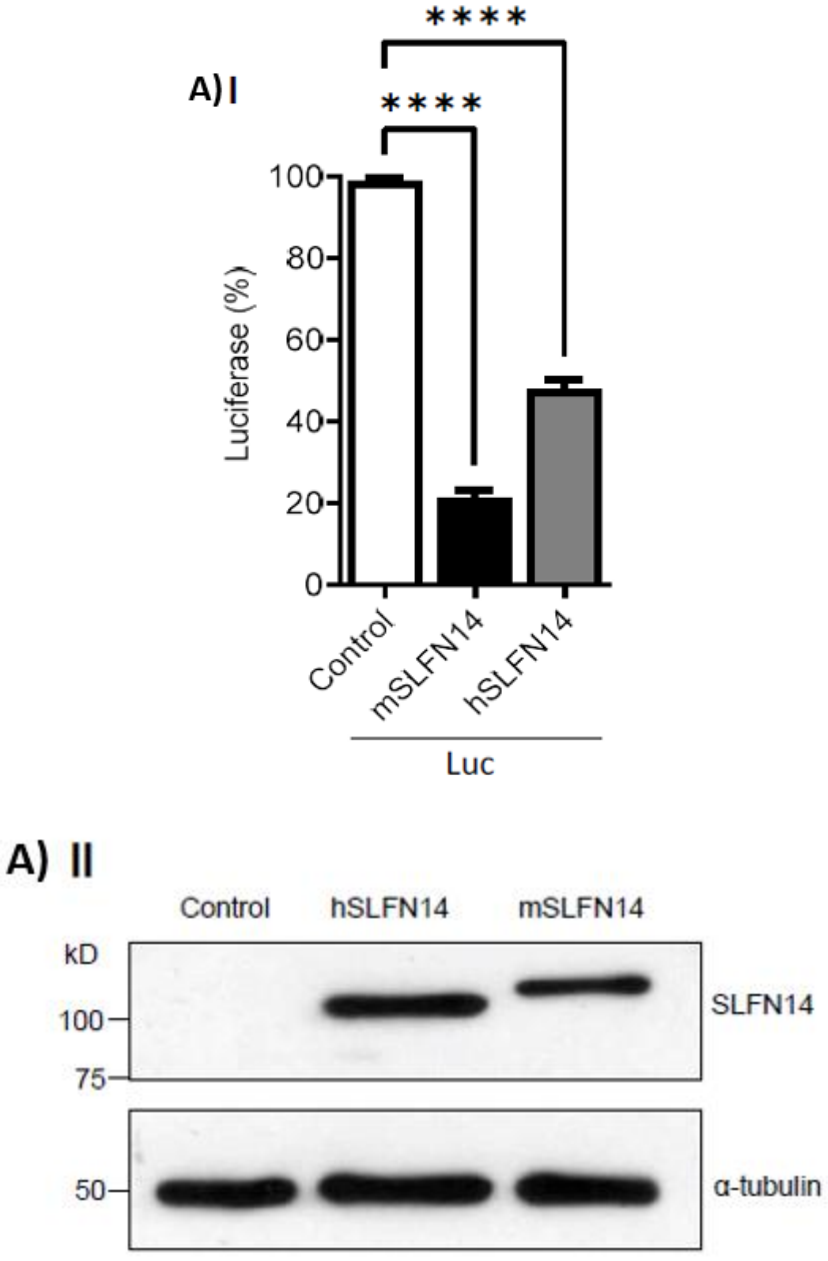

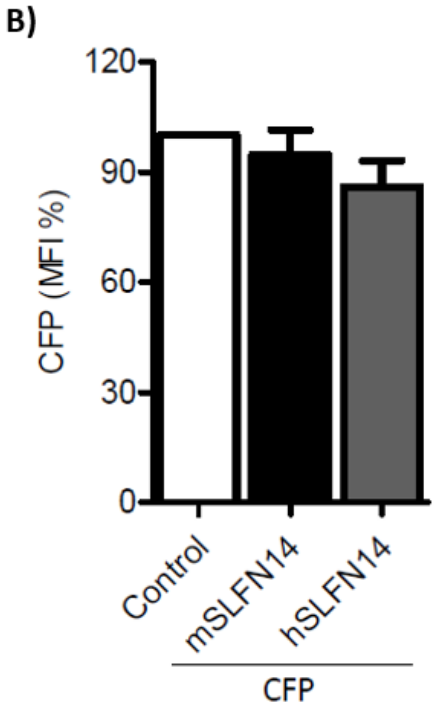
B)
120
90
60
30
0
CFP (MFI %)
Control
mSLFN14
hSLFN14
CFP

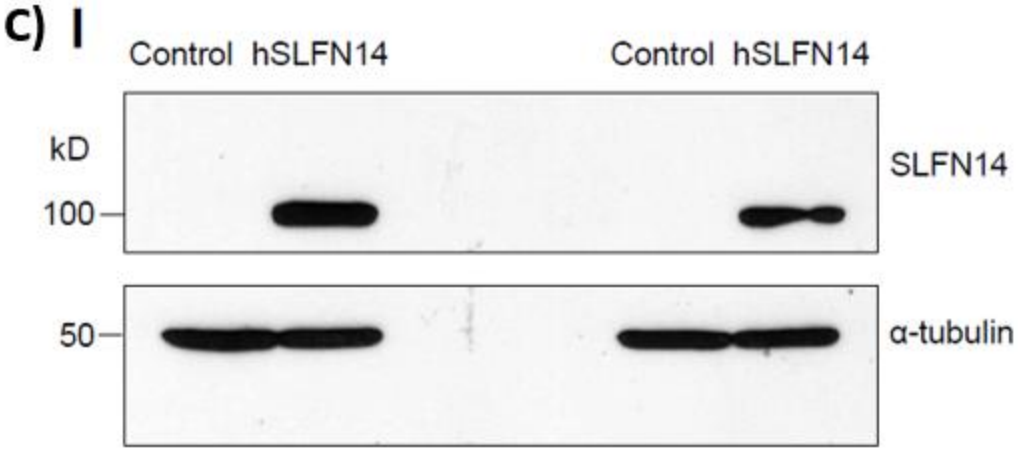
C) I
Control hSLFN14
Control hSLFN14
kD
100
50
SLFN14
α-tubulin

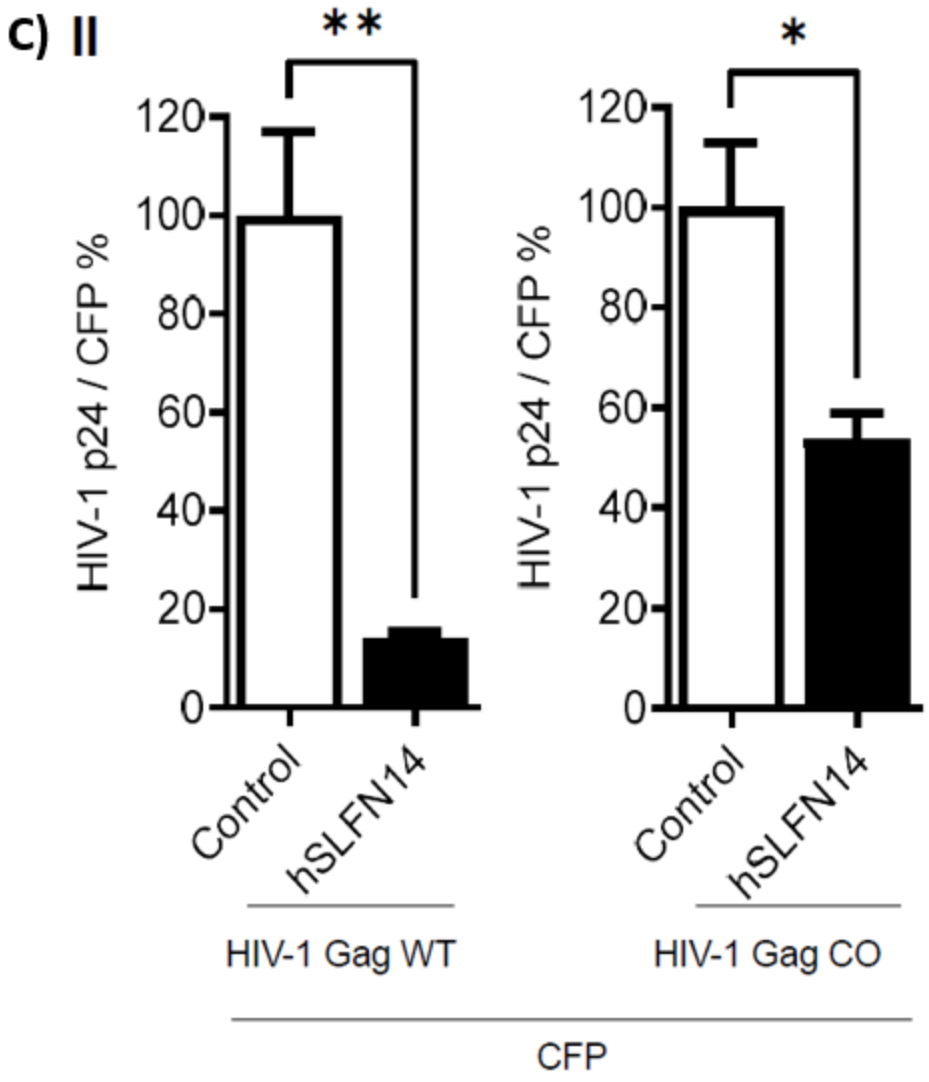

Fig. 2.2 Effect of SLFN14 on the expression of transcripts with different codon usage. HEK293T cells were co-transfected with a plasmid expressing firefly luciferase or CFP and either an empty plasmid (control cells) or a plasmid expressing human (h) or mouse (m) SLFN14. Luciferase activity **(A-I)** and CFP MIF **(B)** were expressed as % of control cells. **(A-III).** Expression of SLFN14 in these cells was detected as described in Fig. 1A-III. Statistical

significance was determined by one-way ANOVA and Dunnett *post hoc* tests. **** $P \leq$ 0.0001. Data corresponds to a triplicate experiment and are representative of five **(A-I)** or six **(B)** independent experiments. **(C)** Effect of SLFN14 on HIV-1 Gag wild type (WT) and codon optimized (CO) expression. HEK293T cells were co-transfected with a plasmid expressing CFP and plasmids expressing either HIV-1 Gag WT or CO together with either an empty plasmid or a SLFN14 expression plasmid. **(I)** Expression of SLFN14 in these cells was detected as described in Fig. 1A-III. **(II)** HIV-1 p24 was normalized for transfection efficiency (% of CFP+ cells) and expressed as % of control cells. Statistically significant differences were calculated using two-tailed, two sample t test. ** $P \leq 0.01$ and * $P \leq 0.05$. Data correspond to a triplicate experiment and are representative of eight independent experiments.

2.3.2 Expression of SLFN14 in Cells of the Immune System

Since SLFN14 potently impairs HIV-1 Gag expression, we predicted that this protein should not be very abundant in cells naturally permissive to HIV-1. Therefore, we characterized the expression of endogenous SLFN14 in cells of the immune system by immunoblot. In this analysis we used the only two anti-SLFN14 antibodies commercially available. These antibodies recognize the N-terminal (residues 100 - 250) and the C-terminal (amino acids 730 - 780) regions of SLFN14. As control, we analyzed HEK293T since SLFN14 mRNA was reported undetectable in these cells[42]. HEK293T cells were transfected with an empty plasmid or a plasmid expressing human SLFN14 and seventy-two hrs later analyzed by immunoblot. As expected, no endogenous SLFN14 was detected in these cells with any of the anti-SLFN14 antibodies evaluated although both recognized the exogenous SLFN14 (Fig. 2.3A).

In addition, SUP-T1 cells (lymphoblastic lymphoma-derived CD4+T cell line), and the acute lymphoblastic leukemia-derived CD4+T cell lines CEM and MOLT-3 were evaluated by immunoblot with these antibodies. Data in Fig. 2.3A indicate that the anti-C-terminal SLFN14

antibody (I), but not the antibody directed against the N-terminus (II), reacted with a band that migrated slightly above 50 kD in the three cell lines, suggesting the expression of an N-terminal truncated form of the protein.

We also analyzed the expression of SLFN14 in primary immune cells. PBMCs were isolated by sedimentation on Ficoll-Paque, lysed, and proteins analyzed by immunoblot with anti-SLFN14 antibodies recognizing the C- and the N-terminus. No SLFN14 protein was detected in freshly isolated, uncultured PBMCs (Fig. 2.3B-I lane 1). Furthermore, we explored the effect of different stimuli on the expression of SLFN14 in primary cells. Equal number of PBMCs (Fig. 2.3B-I), CD4+ T cells (Fig. 3B-II), or monocytes (Fig. 3B-III) were treated with culture medium alone (Control, Figs. 2.3B-I lane 2 and 2.3B-II and -III lane 1) or supplemented with phorbol myristate acetate (PMA, Figs. 2.3B-I lane 4 and 2.3B-II lane 2), interferon α1 (IFN-α1, Figs. 2.3B-I lane 4, 2.3B-II lane 3, and 2.3B-III lane 2), phytohemagglutinin and interleukin-2 (PHA/IL2 Figs. 2.3B-I lane 5, 2.3B-II lane 4, and 2.3B-III lane 3), anti-CD3/-CD28 antibody-coated beads (αCD3/CD28, Figs. 2.3B-I lane 6 and 2.3B-II lane 5), or interleukin-4 and granulocyte-macrophage colony-stimulating factor (IL4/GMCSF, Fig. 2.3B-III lane 4).

After three days of treatment all the cells in the culture were lysed in the same volume and equal volumes of the cell lysates were evaluated by immunoblot. Notice that rather than equal protein amounts, the same number of initial cells in the culture were loaded per electrophoresis lane in these immunoblots. This strategy, combined with the detection of α-tubulin by immunoblot, additionally allowed verifying the effect of the treatments on cellular proliferation. As positive controls in these immunoblots were analyzed HEK293T cells transfected with SLFN14 (Fig. 2.3B-I lane 7) and SUP-T1 cells (Fig. 2.3B-II lane 6).

In contrast to fresh PBMCs (Fig. 2.3B-I lane 1), after three days of in vitro culture, a band of similar size that the one detected in CD4+ T cell lines (Fig. 2.3A and Fig. 2.3B-II lane 6) was observed in PBMCs (Fig. 3B-I lane 2) as well as in CD4+ lymphocytes (Fig. 2.3B-II lane 1) and monocytes (Fig. 2.3B-III lane 1). This band was detected only with the anti-C terminal SLFN14

antibody whereas the anti-N-terminal failed to recognize any protein in any of the primary cell lysates (Data not shown).

PMA, PHA/IL-2, and anti-CD3/-CD28 immunobeads induced robust cellular proliferation in PBMCs (Fig. 2.3B-I) and CD4+ T cells (Fig. 3B-II), as indicated by the α-tubulin levels detected in these cells, compared to the untreated cells (control). Similarly, PHA/IL-2, and IL-4/GMCSF induced cellular proliferation in monocytes (Fig. 2.3B-III). Considering α-tubulin levels as a proxy of the number of cells analyzed, stimuli that induced cell proliferation also decreased the expression of the truncated SLFN14 per cell (Fig. 2.3B). In contrast, IFN-α1 increased the levels of low molecular band reactive with the anti-SLFN14 antibody 199 in CD4+ T cells (Fig. 2.3B-II) but not in PBMCs or monocytes (Fig. 2.3B-I and III).

To analyze a potential mechanism implicated in the lack of expression of full-length SLFN14 in MOLT-3 cells, we determined whether these cells express an SLFN14 mRNAs carrying nucleotides 386 - 788 of exon 3 that encode amino acids 115 - 248. This protein region contains the epitope recognized by the anti-N-terminal SLFN14 antibody that seems to be missing in the shorter protein recognized only by the anti-C-terminal SLFN14 antibody in immune cells. RT-PCR analysis (Fig. 2.3C-I) indicated robust expression of mRNAs harboring this region of exon 3, and as expected, no amplification was observed in the minus RT control, excluding inadvertent detection of genomic DNA. The identity of the RT-PCR product was determined by overlapping DNA sequencing (GenBank accession numbers OP548624 and OP548623), and by restriction digestion with NsiI (Fig. 2.3C-II). This enzyme is predicted to split the 402 bp RT-PCR product in 215 and 187 bp bands. In this experiment, partial digestion was obtained as indicated by the presence of the 402 bp RT-PCR product and a thick ~200 bp band that we interpreted as the 215 and 187 bp bands closely migrating. Similar results were obtained with another set of primers targeting nucleotides 302 - 788 that encode amino acids 86 - 248 in SLFN14 (Data not shown). These findings agree with the reported exon/intron organization of SLFN14 (NM_001129820.2), excluding alternative splicing as a mechanism in the generation of the N217 terminal deleted form

of SLFN14 detected in immune cells. Therefore, a post-splicing event seems to determine the absence of SLFN14 full-length in these cells.

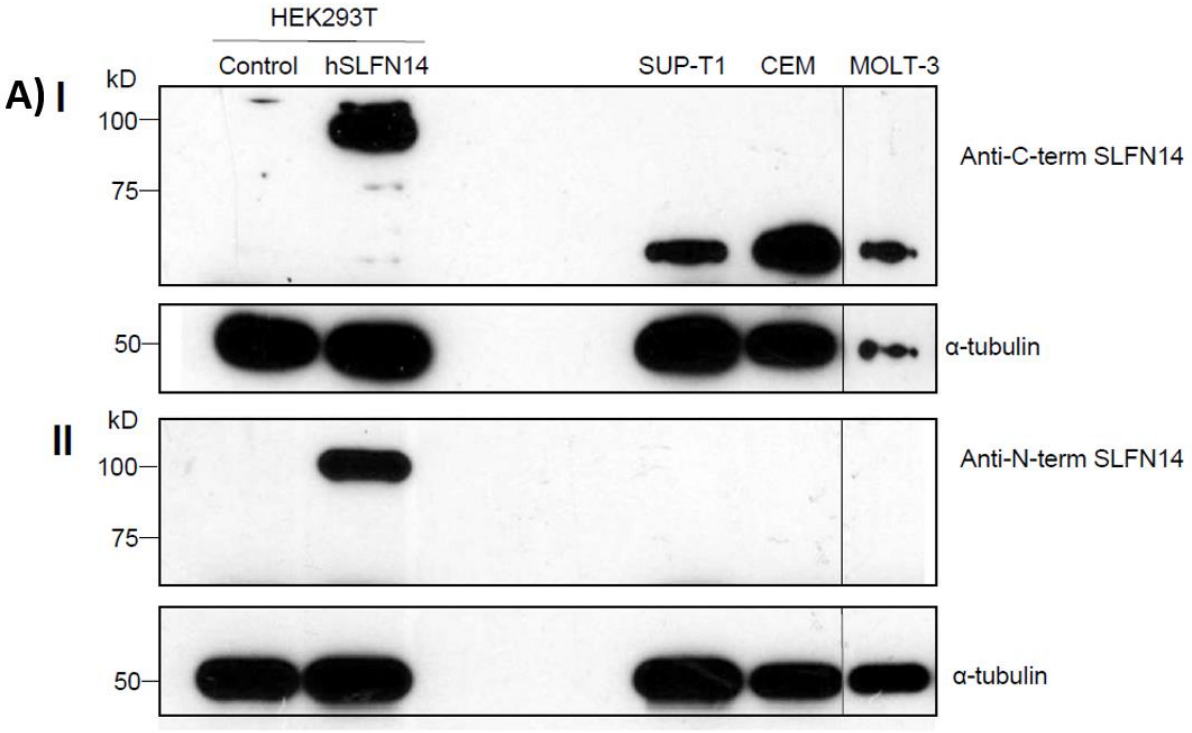

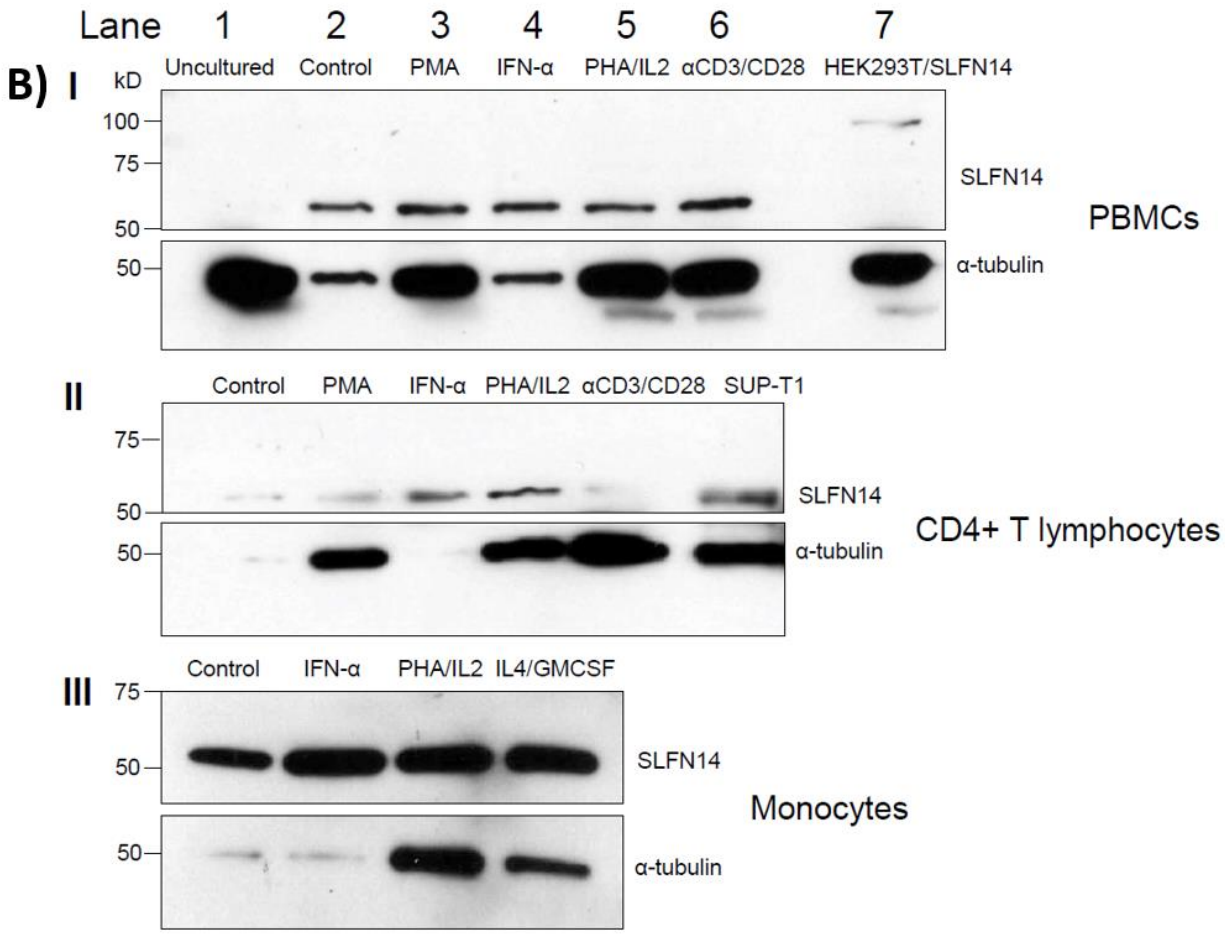
Lane 1 2 3 4 5 6 7
B) I
kD
Uncultured
Control
PMA
IFN-α
PHA/IL2
αCD3/CD28
HEK293T/SLFN14
100
75
50
50
SLFN14
α-tubulin
PBMCs
II
Control
PMA
IFN-α
PHA/IL2
αCD3/CD28
SUP-T1
75
50
50
SLFN14
α-tubulin
CD4+ T lymphocytes
III
Control
IFN-α
PHA/IL2
IL4/GMCSF
75
50
50
SLFN14
α-tubulin
Monocytes

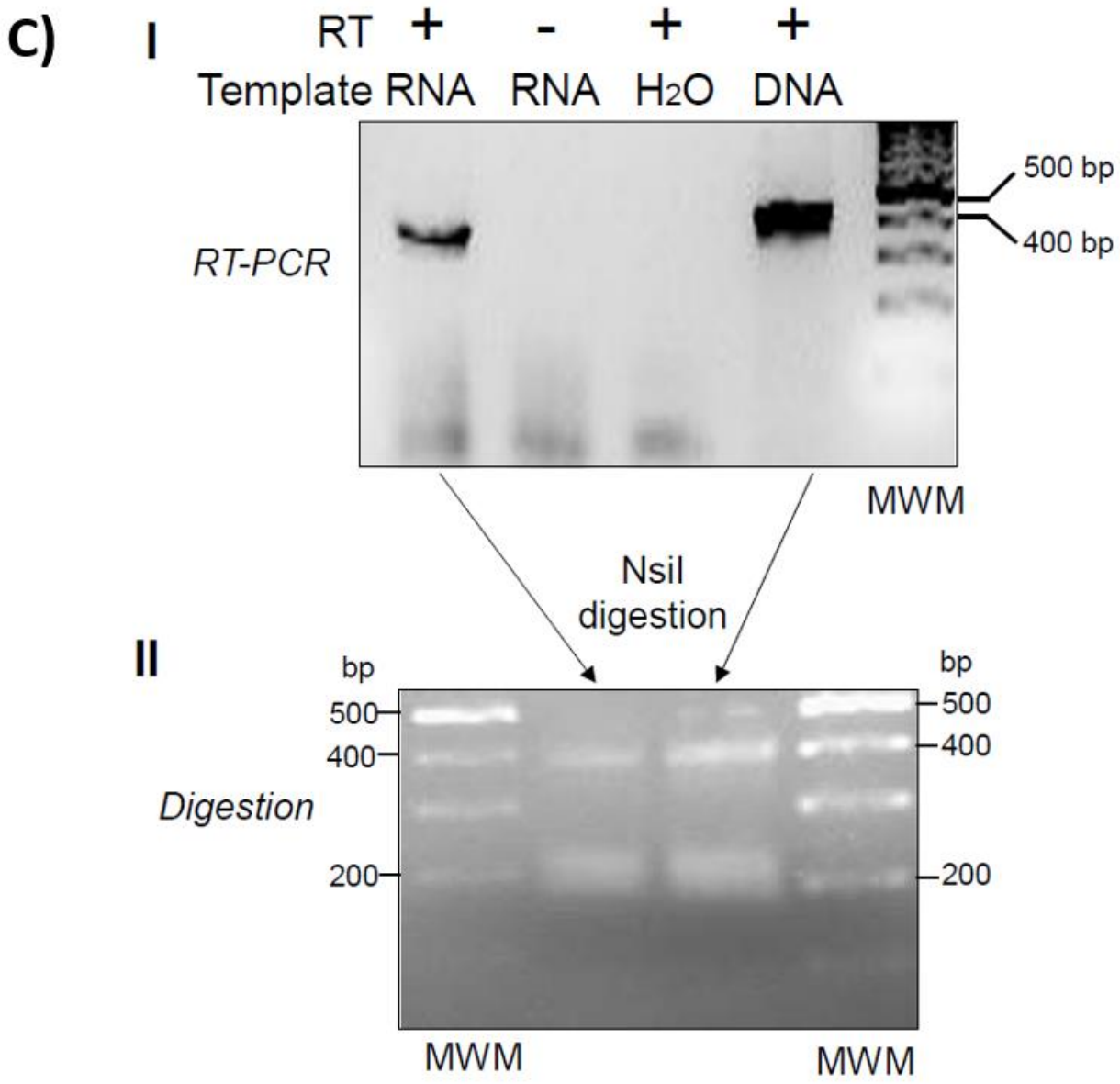
C)
I
RT + - + +
Template RNA RNA H2O DNA
RT-PCR
500 bp
400 bp
MWM
NsiI
digestion
II
bp
500
400
200
Digestion
bp
500
400
200
MWM
MWM

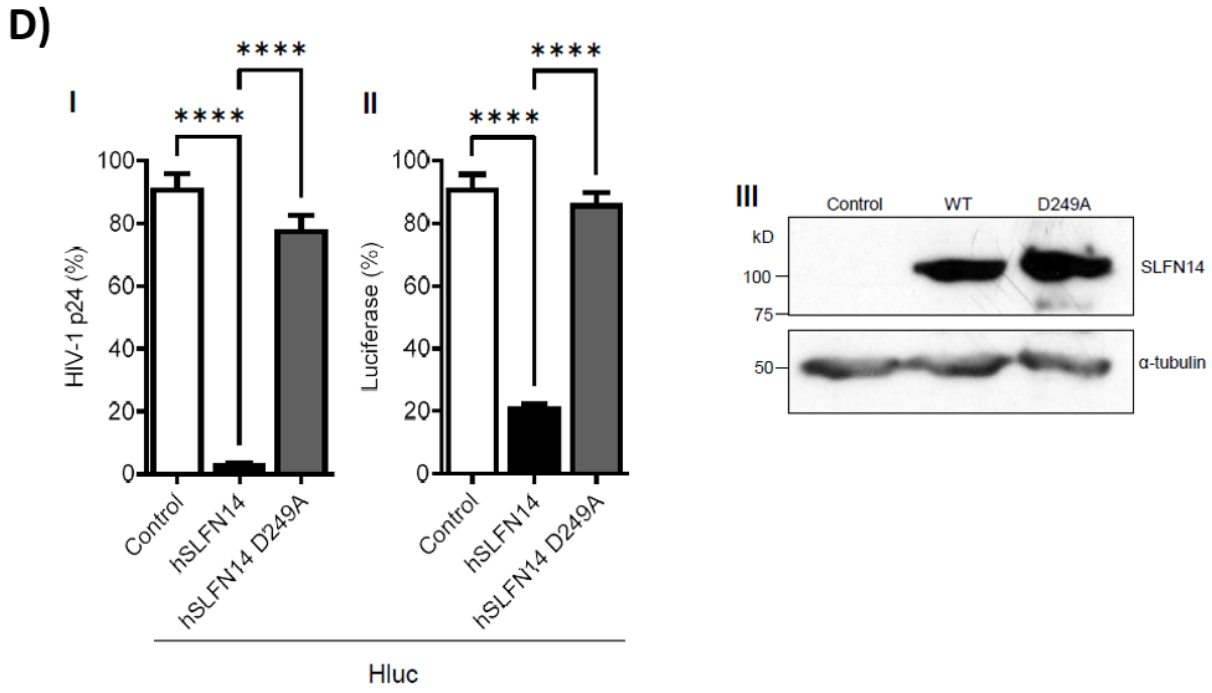

Figure 2.3. Expression of SLFN14 in Immune Cells. **(A).** Immunoblot analysis of SLFN14 expression in HEK293T co-transfected with an empty plasmid (Control) or a plasmid expressing human SLFN14, and in non-transfected SUP-T1, CEM, and MOLT-3 cells. The MOLT-3 cell lysate was in the same immunoblot membrane as the other samples but separated by irrelevant samples that were removed from the image presented. Anti-SLFN14 antibodies recognizing the N- or the C-terminus of the protein were used as indicated, and α-tubulin levels were determined as a loading control with a specific antibody. (B) Immunoblot analysis of SLFN14 expression in PBMCs, and PBMC-derived CD4+ T lymphocytes and monocytes with an anti-C-terminal SLFN14 antibody. α-tubulin was determined as a loading control. Cells were subjected to the stimuli indicated. Positive controls were HEK293T cells co-transfected with human SLFN14 (HEK393T/SLFN14) and SUP-T1 cells. (C) Analysis of SLFN14 mRNA in MOLT-3 cells. (I). Agarose gel electrophoresis analysis of the reverse transcription (RT)-PCR evaluating SLFN14 expression in MOLT-3 cells with primers SS1 and CV43. Samples were loaded in the gel in the following order: RT-PCR with RNA, No RT control (PCR with RNA), No template control (RT-PCR with no RNA), Positive control (RT-

PCR with SLFN14 expression plasmid), and DNA Molecular Weight Marker (Thermo Fisher, FERSM1331). (II). Agarose gel electrophoresis analysis of the digestion with NsiI of the RT-PCR products obtained with primers CV43 and SS1 using as template the SLFN14 expression plasmid and RNA extracted from MOLT-3 cells. DNA molecular weight markers are indicated. (D) Effect of D249A mutation on the activity of human (h) SLFN14 on transgene expression. HEK293T cells that were co-transfected with a plasmid encoding an HIV-1 virus expressing firefly luciferase and either an empty plasmid (control cells) or a plasmid expressing human SLFN14 WT or D249A mutant. HIV-1 p24 levels (I) and luciferase activity (II) were expressed as % of control cells. (III) SLFN14 expression was validated by immunoblot as described in Fig. 1A-III. Statistically significant differences were calculated with two-way ANOVA Dunnett post hoc tests. **** $P \leq 0.0001$. Data correspond to a triplicate experiment and are representative of three independent experiments.

2.3.3 SLFN14 Requires the Endoribonuclease Activity to Impair HIV-1 Expression

Protein molecular weight prediction (Expasy) indicated that SLFN14 full-length protein is 104 kD, as evidenced by our immunoblots (for example Fig. 2.3A-I). A SLFN14 protein lacking the first 330 or 420 amino acids is estimated to be 69 or 56 kD, respectively, being in the molecular weight range of the N-terminal truncated form of SLFN14 detected in immune cells (Fig. 2.3A and 3B). These predicted N-terminal truncated SLFN14 proteins will lack the epitope recognized by the anti-N-terminal antibody (residues 100 - 250), including residue 249 which is essential for the endoribonuclease activity[40].

Since cells expressing the N-terminal truncated form of SLFN14 are susceptible to HIV-1, we predicted that SLFN14 requires the endoribonuclease activity to repress expression of HIV-1 Gag. Therefore, we determined the anti-HIV-1 activity of an SLFN14 endoribonuclease-dead mutant (D249A)[40]. HEK293T cells were co-transfected with a plasmid expressing an HIV-1 reporter that expresses LTR-driven luciferase[105] and either the empty plasmid or plasmids

expressing human SLFN14 wild 232 type or the D249A mutant. In concordance with our previous observations, SLFN14 wild type decreases HIV-1 p24 (Fig. 2.3D-I) and luciferase (Fig. 2.3D-II) levels by approximately 98% and 80%, respectively. However, this inhibitory activity was drastically reduced by the D249A mutation, despite the wild type and mutant proteins being expressed at similar levels (Fig. 2.3D-III). Therefore, the endoribonuclease activity of SLFN14 is required for the role of this protein in gene expression regulation, and likely the N-truncated form of the protein expressed in HIV-1-permissive immune cells is inactive.

2.3.4 SLFN14 Impairs HIV-1 Protein Expression in CD4+ T Cells and Monocytes

To evaluate the effect of SLFN14 on HIV-1 protein expression in HIV-1-permissive immune cells, SUP-T1 cells and primary CD4+ lymphocytes and monocytes were electroporated with an empty plasmid (control) or a human SLFN14 expression plasmid, and a plasmid encoding wild type HIV-1 (pNL4-3). Three independent cultures of SUP-T1 cells and one culture of CD4+ lymphocytes per donor (two donors) were electroporated. Because of their low yield, monocytes from the two donors were mixed right before electroporation and electroporated as one culture. Seventy-two hours after electroporation, ATP levels were measured in triplicate in each of the cultures, and cell supernatant was transferred in triplicate to fresh, non-electroporated, SUP-T1 cells. Viral replication in the target SUP-T1 cells was evaluated by measuring HIV-1 p24 in the cell supernatant at different days post-transfer.

We found similar ATP levels of SUP-T1 and monocytes cells electroporated with the empty or the SLFN14 expression plasmids (Fig. 2.4A), in contrast to ATP levels of CD4+ cells which were statistically significantly different. However, in one donor viability is greater on SLFN14 electroporated cells, while in donor 2 the opposite effect was observed (Fig 2.4A). These results suggest that differences in viability did not account for the difference in HIV-1 p24 later observed (Fig. 2.4B). In contrast, viral production as severely impaired by SLFN14 in all the cells electroporated, as demonstrated by the differences in the HIV-1 replication curves observed in the SUP-T1 cells infected with the produced viruses (Fig. 2.4B). At the earliest collection time after

viral transfer, SUP-T1 cells infected with virus produced in SUP-T1 cells co-electroporated with the control plasmid showed approximately 30-fold more virus than the cells infected with the virus from SUP-T1 cells co-electroporated with SLFN14 plasmid (Fig. 2.4B-I). These differences were around 3- and 22-fold in CD4 cells from donor 1 and in the monocytes, respectively (Fig. 2.4B-II and IV). However, we did not see differences in HIV-1 levels in SUP-T1 cells infected with the virus produced by the CD4 cells from the second donor at this early time point (Fig. 2.4B-III). Nevertheless, at the second collection time point SUP-T1 cells infected with the virus from CD4 cells from donor 2 co-electroporated with the control plasmid showed approximately 500-fold more virus than SUP-T1 cells infected with virus from the SLFN14 co-electroporated CD4 cells (Fig. 2.4B-III). Similarly, all the cells studied showed important differences at the second collection indicating that SLFN14 impaired viral production in the electroporated cells (Fig. 2.4B). At the third collection time no differences were observed in SUP-T1 cells infected with the virus produced in electroporated SUP-T1 or CD4 cells from donor 1 (Fig. 2.4B-I and II) and viral cytopathic effect were marked, correlating with the high levels of HIV-1 p24 (1000 - 500 ng/ml) of these cultures.

In contrast, differences in viral replication persisted very markedly in SUP-T1 cells infected with virus produced in CD4 cells from donor 2 (~104-folds, Fig. 4B-III) and in monocytes (~103-folds, Fig. 2.4B-IV). These SUP-T1 cells exhibited less viral cytopathic effect and their HIV-1 p24 levels were between 80 to 1 ng/ml. Therefore, SUP-T1 cultures showing no differences at the last collection time likely were exhausted by viral replication. In sum, findings in Fig. 2.4 demonstrated that SLFN14 can also inhibit HIV-1 expression in cell types that are relevant in vivo to this virus.

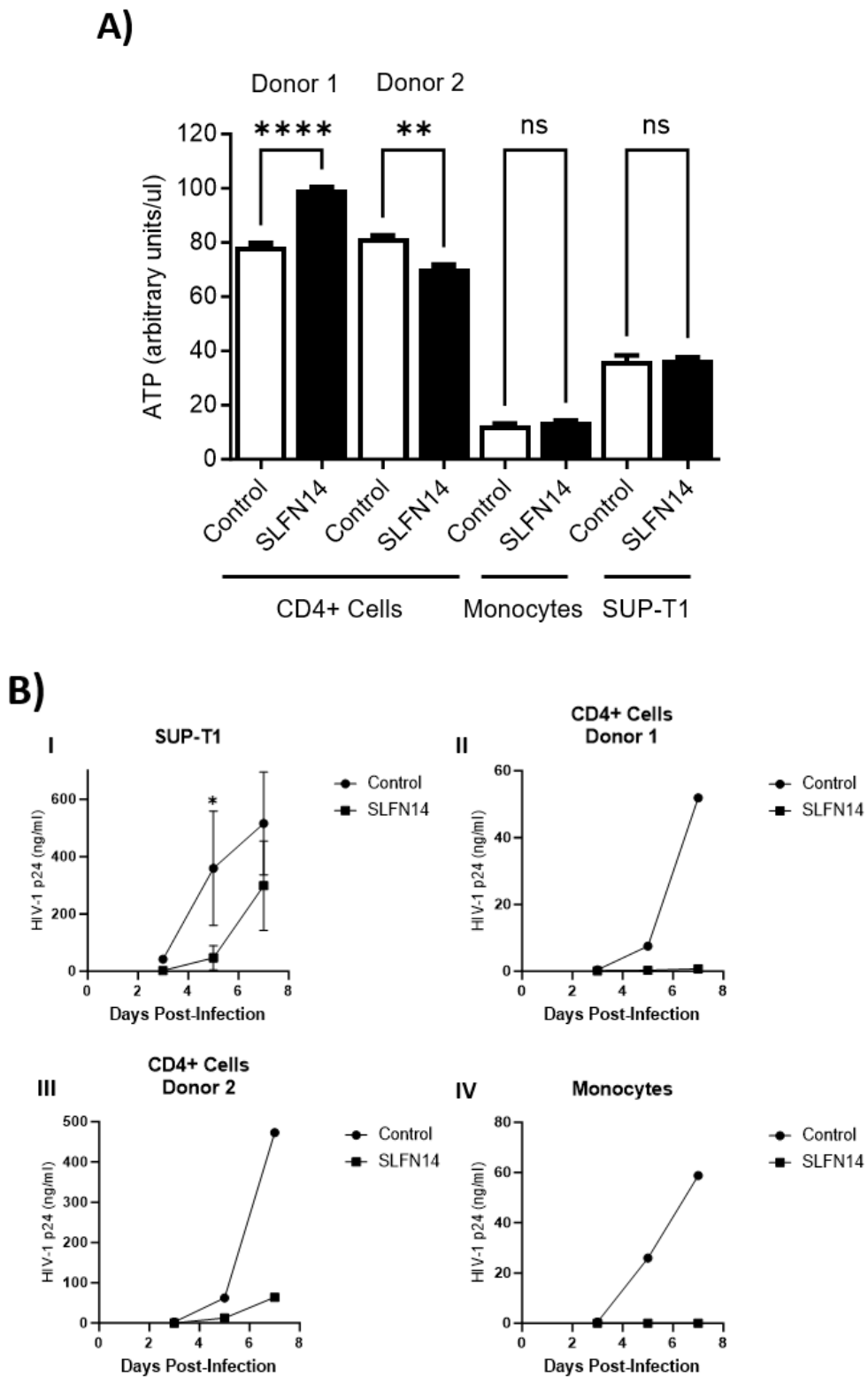

Fig. 2.4. Effect of SLFN14 on HIV-1-driven Protein Expression in Immune Cells.

Primary CD4+ T lymphocytes and monocytes, and SUP-T1 cells were electroporated with a

plasmid expressing HIV-1 wild type and either an empty plasmid (control) or a plasmid expressing human SLFN14. Supernatant from the electroporated cells was transferred to fresh SUP-T1 cells and HIV-1 replication was followed by measuring HIV-1 p24 levels in the cell supernatant. **(A)** ATP levels in electroporated primary CD4+ T lymphocytes and monocytes, and SUP-T1 cells. **(B).** Fold differences in HIV-1 p24 levels in SUP-T1 cells infected with the virus produced in electroporated SUP-T1 cells **(I),** CD4+ lymphocytes from donor 1 **(II)** or donor 2 **(III),** and donors 1 and 2 pooled monocytes **(IV).** Data corresponds to a triplicate experiment. Statistical analysis was conducted in by one-way ANOVA follow by Sidak's post hoc test **(A).** Statistical analysis of **(B-I)** was done using two-way repeated measurements ANOVA follow by Sindak's post hoc test.

2.3.5 Effect of SLFN14 on Viral Infection.

Experiments reported above shown that SLFN14 impairs expression of rare codons-enriched transcripts expressed from transfected plasmids. Since SLFN14 preferentially affects the expression of wild type (AT-rich) rather than codon optimized (AT-poor) Gag, the RNA Pol-III-RIG-I pathway could be implicated. RNA Pol III transcribes AT-rich DNA templates producing short AU-rich RNA fragments that induce type I IFN via RIG-I[118], and this innate immune pathway is active in HEK293T cells[119]. Furthermore, transfection of HEK293T cells with in vitro transcribed HIV-1 wild type-encoded RNAs has been reported to trigger type I IFN, and this effect was inhibited by codon optimization of the viral sequences to resemble the human codon usage[120].

We investigated the role of type I IFN signaling in the inhibitory effect of exogenous expressed SLFN14 on gene expression. We wanted to study if the inhibitory effect of SLFN14 was aided by interferon signaling. We also investigate the role of polymerase III, since play an important role in detecting foreign DNA in the cytoplasm of the cell and transcribing AT-rich DNA regions that trigger the I IFN response[121]. Since experiments were conducted by transfection of plasmids that were replicated in bacteria it is very likely that they would trigger type I IFN.

HEK293T cells were co-transfected with a plasmid encoding an HIV-1 reporter that expresses LTR-driven luciferase[105] and either, an empty plasmid or a plasmid expressing SLFN14. Transfected cells were treated with RNA polymerase III or pan-Janus kinase inhibitors during the entire duration of the experiment, and luciferase activity was measured in cell lysates 72 hrs after transfection. As expected, SLFN14 reduced by 80% the expression of luciferase found in control cells (Fig. 2.5A). This effect was not modified by RNA polymerase III or pan-Janus kinase inhibitors, indicating that the RNA Pol-III-RIG-I-IFN pathway is not involved in the ability of SLFN14 to impair gene expression. Interestingly the statistically significant changes observed in inhibition of HIV-1 p24 production in the presence of Pol-III or IFN I inhibitors, favor SLFN14 inhibition of p24, rather than being detrimental to SLFN14 activity. These results were somewhat expected for RNA Pol III inhibitors since this will affect production of new ribosomes and tRNA, which will affect translation downstream. A clear conclusion on the effect of RNA Pol III inhibition on aiding SLFN14 activity is difficult to reach since the experiment design lacks a proper control (control + RNA Pol III Inh) to test if the effect is independent of SLFN14 expression. The positive effect of IFN I inhibition on SLFN14 activity is not clear since the changes are of ~2% values, if the experiment is done additional times these differences are likely to disappear.

To evaluate the effect of SLFN14 on codon biased transcripts expressed independently of plasmid transfection, and since the inhibitory activity of SLFN14 is type I IFN-independent, we evaluated the effect of SLFN14 on the expression of rare codon-enriched transcripts expressed by viral infection. Then, we took advantage of HIV-1 again. Upon infection, HIV-1 inserts a cDNA copy of the viral genome in the host chromosome, and genes in this cDNA are expressed as any other gene in the cell. To maximize the frequency of HIV-1 infected cells containing the control or SLFN14 plasmids, we co-transfected HEK293T cells with plasmids expressing the HIV-1 receptor (CD4) and co-receptor (CXCR4) with either plasmids empty or encoding SLFN14. Ectopic expression of HIV-1 receptor has been successfully used to study different aspects of HIV-1 biology [for example[122,123]]. In addition, we used this cellular model because of the high

transfection efficiency of HEK293T cells and their lack of endogenous CD4 and SLFN14 expression.

Forty-eight hrs after transfection, cells were infected with HIV-1 wild type (NL4-3 strain). Input virus was removed by extensive washing 24 hrs after infection, and cell supernatant collected at 0 (after wash), 3 and 5 days after infection to measure HIV-1 p24 by ELISA. Surface CD4 expression was measured at the time of infection by immunostaining with a specific antibody, and since CXCR4 was expressed from a bicistronic plasmid together with mCherry, levels of the fluorescence protein served as a surrogated of CXCR4 expression. HIV-1 p24 levels were normalized to the % of CD4+/mCherry CXCR4+ cells to account for transfection efficiency.

The MFI of CD4 and mCherry was similar in cells transfected with control and SLFN14 expression plasmids (Fig. 2.5B-I), indicating that SLFN14 did not affect the expression levels of CD4 or mCherry that exhibit CAIs of 0.82 and 0.976, respectively. However, cells expressing SLFN14 produced approximately ~73% and ~83% less HIV-1 p24 than control cells at days 3 and 5 post-infection, respectively (Fig. 2.5B-II). HIV-1 p24 at day zero was undetectable. These findings demonstrated that SLFN14 can impair expression of Gag from an integrated provirus.

A)

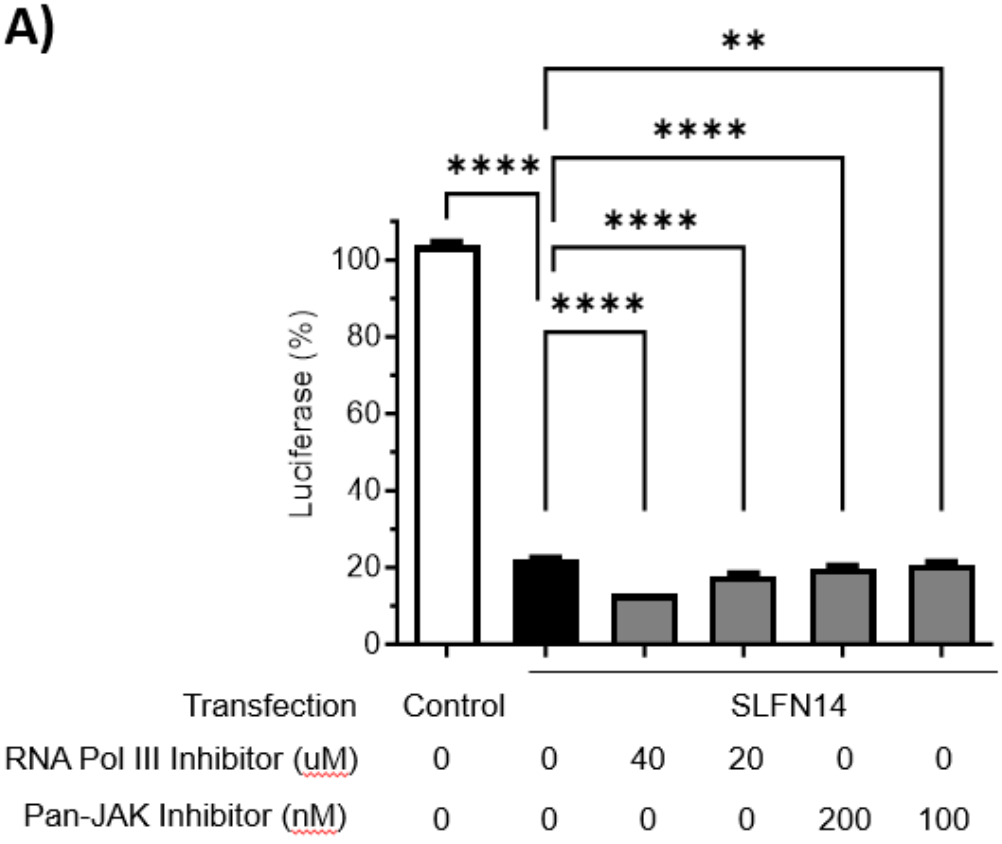
**
****
****
****
****
Luciferase (%)
0
20
40
60
80
100
Transfection
Control
SLFN14
RNA Pol III Inhibitor (uM)
0
0
40
20
0
0
Pan-JAK Inhibitor (nM)
0
0
0
0
200
100

B)

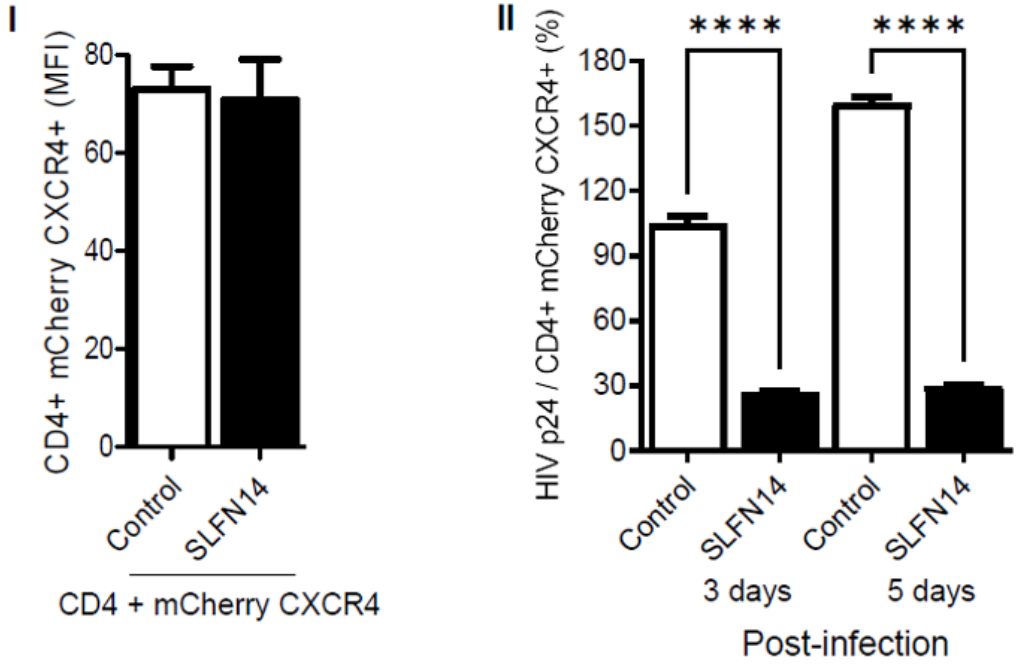
I
CD4+ mCherry CXCR4+ (MFI)
0
20
40
60
80
Control
SLFN14
CD4 + mCherry CXCR4
II
HIV p24 / CD4+ mCherry CXCR4+ (%)
0
30
60
90
120
150
180
****
****
Control
SLFN14
Control
SLFN14
3 days
5 days
Post-infection

Figure 2.5. Effect of SLFN14 on viral replication. (A) Role of the RNA Polymerase III-RIG-I-IFN signaling pathway in the SLFN14 activity. HEK293T cells co-transfected with HIVluc expression plasmid and an empty plasmid (control cells) or a plasmid expressing human SLFN14 that were treated or not with inhibitors indicated. Luciferase activity was expressed as % of control cells. Data corresponds to a triplicate experiment and are representative of three independent experiments. Although not indicated, statistically significant differences were found between the control and each of the other groups as calculated with two-way ANOVA Dunnett post-hoc test **** $P \leq 0.0001$. **(B)** Effect of SLFN14 on HIV-1 replication. **(I)** HEK293T cells were co-transfected with plasmids expressing CD4 and a bicistronic plasmid encoding CXCR4 and mCherry, together with either an empty (control cells) or a human SLFN14 expression plasmid. MFI values of CD4 and mCherry (CXCR4). **(II)** These cells were infected with HIV-1 wild type and viral replication followed by measuring HIV-1 p24 in the cell supernatant. Data pertain to a triplicate experiment, and they are representative of two independent experiments. Statistically significant differences were calculated with one-way ANOVA Bonferroni post-hoc test **** $P \leq 0.0001$.

2.3.6 SLFN14 Caused Ribosomal RNA Degradation in Cells Co-Expressing Gag Wild Type

SLFN14 is a ribosome-associated endoribonuclease[40,42]. Purified SLFN14 was reported to degrade purified ribosomal, tRNA, and mRNA in vitro[40]. In addition, our results here indicate that SLFN14 restricts the expression of transcripts rich in rare codons at a post-transcriptional step and requires the endoribonuclease activity. Therefore, we sought to evaluate the effect of SLFN14 on rRNA and mRNA levels. In these studies, we used as a model wild type and codon optimized Gag, expecting to identify a SLFN14-dependent mechanism that operates preferentially in the cells expressing wild type Gag.

HEK293T cells were co-transfected with plasmids expressing HIV-1 Gag wild type or codon optimized together with a plasmid expressing firefly luciferase (pCI Luc), and either empty plasmid or plasmids expressing human or mouse SLFN14. Seventy-two hours after transfection, supernatant from these cells was used to measure HIV-1 p24, and cell lysates were evaluated for luciferase activity and the levels of SLFN14 proteins (immunoblot). Total RNA and DNA were also extracted from these cells to measure ribosomal RNA integrity by gel electrophoresis, Gag mRNA levels by quantitative reverse transcription PCR, and Gag DNA by quantitative PCR.

Similar amounts of mouse and human SLFN14 were detected by immunoblot in cells expressing wild type or codon optimized Gag (Fig. 2.6A). In contrast, SLFN14 proteins decreased wild type Gag expression by over 500 folds as compared to control cells, whereas codon optimized Gag expression was diminished only ~2 folds (Fig. 2.6B). Luciferase levels were also diminished by SLFN14 proteins. In cells co-expressing Gag wild type, luciferase dropped by 17 folds and in cells co-expressing Gag codon optimized, luciferase was diminished by ~2 folds (Fig. 2.6B). The fact that the expression of the same luciferase transcript was ~8 folds more affected in cells expressing non-optimized (wild type) than optimized Gag is intriguing. This could be due to differences in transfection efficiency, although this possibility seems to be unlikely because equal levels of SLFN14 were observed in cells expressing Gag wild type and codon optimized (Fig. 2.6A). Nevertheless, after normalization for the effect of SLFN14 proteins on luciferase, still SLFN14s impaired expression of Gag wild type by ~36 folds but Gag codon optimized expression was not affected (0.9 folds). After reverification of the differential effect of SLFN14 on the expression of wild type and codon optimized Gag, we proceeded to evaluate the effect of SLFN14 on the stability of nucleic acids obtained from these cells. Importantly, purified total RNA exhibited similar RNA Integrity Numbers equivalent (RINe) (Fig. 2.6C-I) indicating a comparable high quality. This total RNA was used to calculate ribosomal RNA degradation with the Agilent TapeStation Controller Software 4.1 following criteria previously reported[40,112]. As compared to the corresponding control cells, cells transfected with SLFN14 showed a 1.7- or 1.1-fold increase in ribosome degradation when co-expressed with wild type or codon optimized Gag, respectively

(Fig. 2.6C-II). These findings suggest that ribosome degradation could mediate the differential effects of SLFN14 on the expression of wild type and codon optimized Gag.

We also measured in these total RNA samples the levels of Gag mRNA using a set of primers that bind to the same region in Gag wild type and codon optimized, and values were normalized to GAPDH mRNA levels in the same samples. SLFN14 diminished by 2- and 3-fold the Mrna levels in cells co-expressing Gag wild type and codon optimized, respectively (Fig. 2.6C-III). Similar degradation of Gag mRNA in these cells cannot explain the differential effect of SLFN14 on the expression of Gag wild type and codon optimized but suggest an additional mechanism for the inhibitory effect of SLFN14 on the expression of wild type and codon optimized HIV-1 p24 expression.

Because SLFN14 impaired the expression of genes located in plasmids or in the HIV-1 genome integrated in the host chromosome, it is unlikely that DNA degradation is implicated in the SLFN14 inhibitory activity. Nonetheless, levels of Gag wild type expression plasmid were determined in cells studied in Fig. 6 by quantitative PCR. Gag DNA cycle threshold (Ct) were 11.1 +/- 0.1 in control cells and 11.6 +/- 0.2 in SLFN14 cells (Fig. 2.6C-IV), indicating that the differences in HIV-1 p24 observed in these cells (Fig. 2.6B) were not due to different amounts of the Gag plasmid, excluding DNA degradation as a mechanism for these differences.

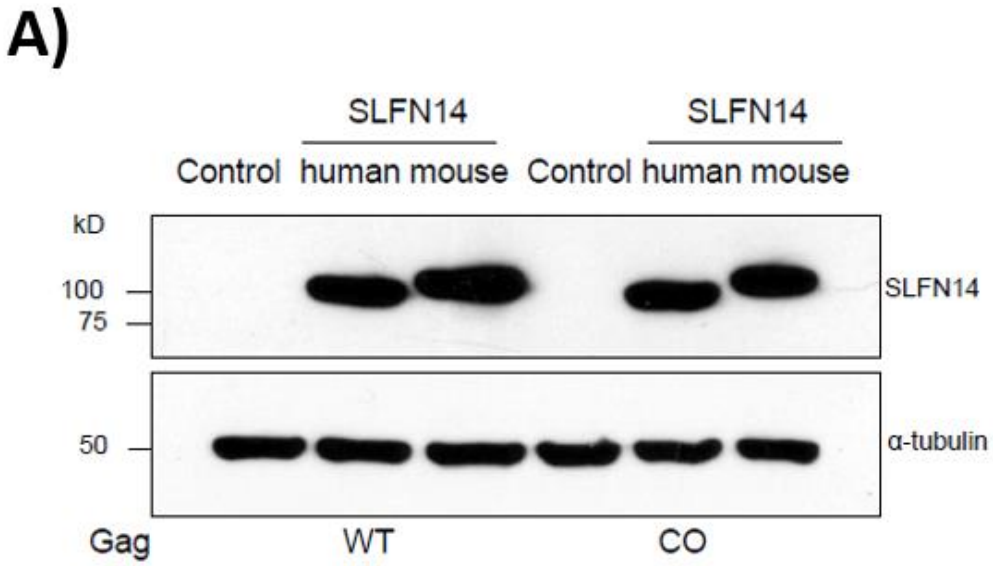

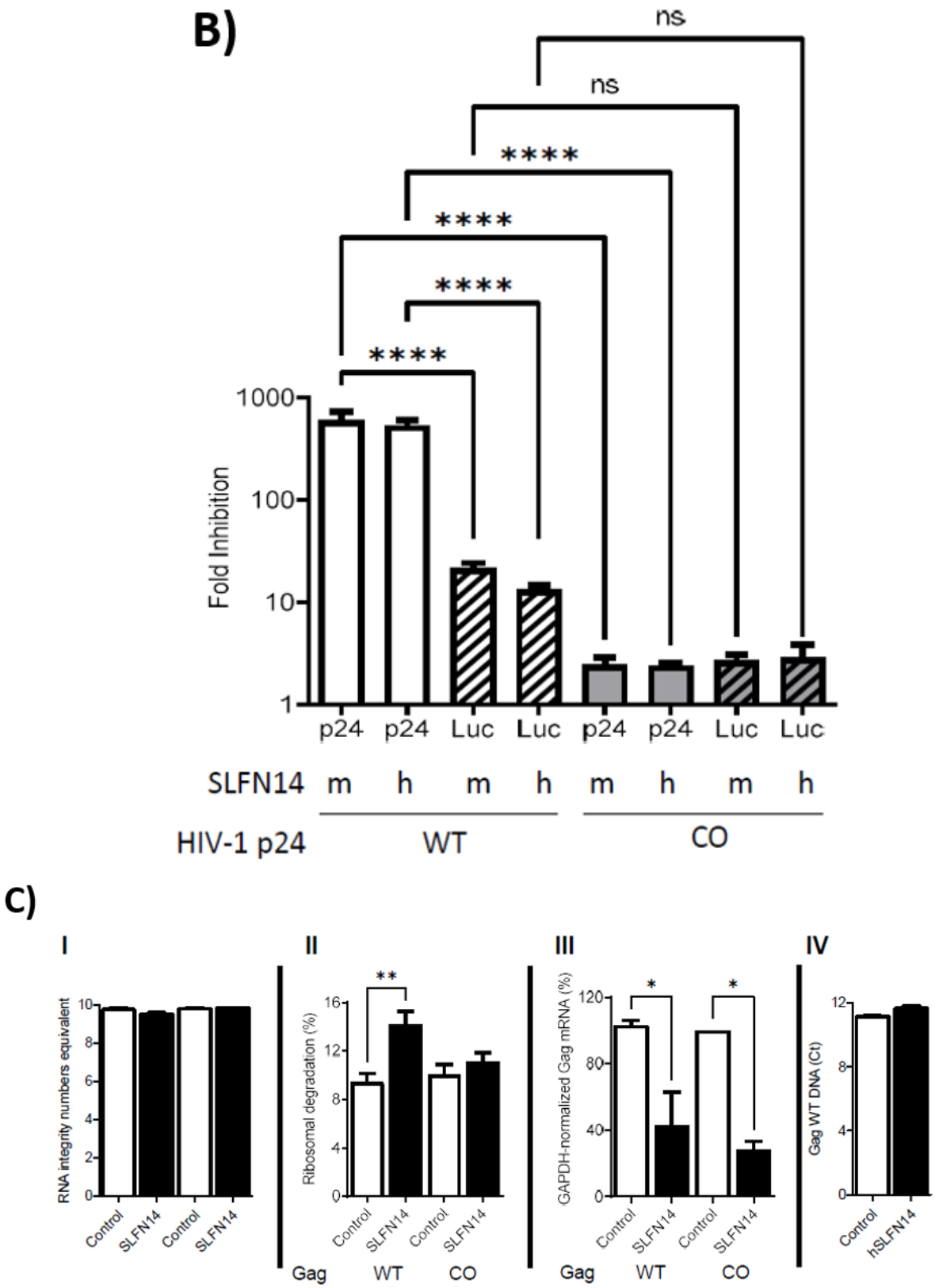
B)
ns
ns
****
****
****
****
1000
100
10
1
Fold Inhibition
p24 p24 Luc Luc p24 p24 Luc Luc
SLFN14 m h m h m h m h
HIV-1 p24 WT CO
C)
I
II
III
IV
RNA integrity numbers equivalent
Control SLFN14 Control SLFN14
Ribosomal degradation (%)
**
Control SLFN14 Control SLFN14
Gag WT CO
GAPDH-normalized Gag mRNA (%)
*
*
Control SLFN14 Control SLFN14
Gag WT CO
Gag WT DNA (Ct)
Control hSLFN14

Figure 2.6. Effect of SLFN14 on Nucleic Acid Integrity. HEK293T were co-transfected with a plasmid encoding Gag wild type (WT) or codon optimized (CO), and plasmids expressing luciferase (Luc) and either an empty plasmid (control cells) or a plasmid encoding SLFN14, human or mouse. **(A)** SLFN14 expression was verified by immunoblot as described in Fig. **2.1AIII. (B)** HIV-1 p24 levels and luciferase activity determined in these cells were expressed as fold inhibition relative to control cells. Note that the Y axes of the graphic is in log10 scale. Data corresponds to a triplicate experiment that is representative of five independent experiments. Statistically significant differences were calculated using one-Way ANOVA and a Tukey pos hoc test. **(C)** Effect of SLFN14 on nucleic acids. RNA quality **(I),** ribosomal RNA degradation **(II),** GAPDH mRNA-normalized Gag mRNA levels **(III),** and Gag WT cDNA levels **(IV)** were expressed relative to values found in control cells. Data corresponds to a triplicate experiment and is representative of two independent experiments. Statistically significant differences were calculated with one-way ANOVA and Dunnett post hoc tests. **** $P \leq 0.0001$, *** $P \leq 0.001$, ** $P \leq 0.01$, * $P \leq 0.05$, and NS $P > 0.05$.

2.3.7 Subcellular distribution of SLFN14

Since SLFN14 affect the expression of rare codon biased mRNAs at a post-transcriptional step and this is associated to ribosomal degradation, we also determined the subcellular distribution of human and mouse SLFN14 by immunostaining and confocal microscopy analysis. HEK293T cells were transfected with plasmids expressing mouse or human SLFN14 or an empty cassette, and a plasmid encoding a single-round infection HIV-1 expressing eGFP (HIVeGFP)[116]. Transfected cells were stained with an anti-FLAG antibody. As expected, SLFN14 proteins were distributed exclusively to the cell cytoplasm (Fig. 2.7A), and their localization did not change in cells co-expressing HIV-1 proteins (eGFP+ cells).

Furthermore, we verified the association of SLFN14 with ribosomes by sedimentation analysis in a sucrose density gradient, as previously described[40,42]. HEK293T cells were co-

transfected with plasmids expressing human SLFN14 or an empty plasmid and a plasmid expressing HIV-1 wild type Gag. The cells were lysed, and the cytoplasmic fraction was resolved in a sucrose density gradient. All the fractions obtained were analyzed for the presence of SLFN14 by immunoblotting with an anti-FLAG antibody, but this protein was visible only in the middle region of the top quarter of the gradient (Fig. 2.7B-I). Gel electrophoresis analysis of RNA isolated from the SLFN14-containing fractions and the corresponding flanking fractions lacking the protein indicated the presence of SLFN14 in ribosomal RNA-enriched fractions (Fig. 2.7B). Therefore, SLFN14 co-sedimented with ribosomal fractions, in concordance with previous reports[40,42]

A)

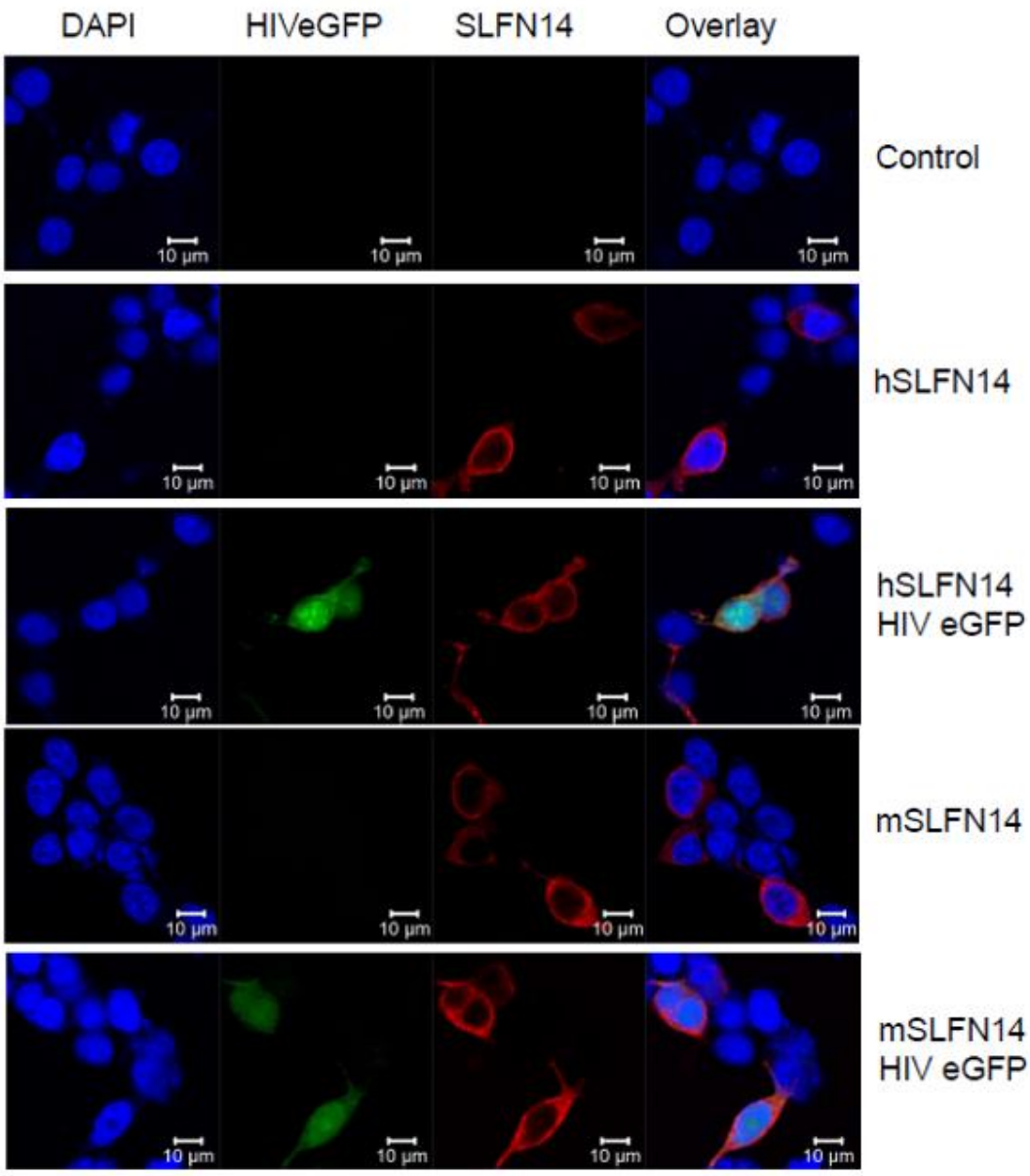
DAPI
HIVeGFP
SLFN14
Overlay
Control
hSLFN14
hSLFN14
HIV eGFP
mSLFN14
mSLFN14
HIV eGFP
10 µm

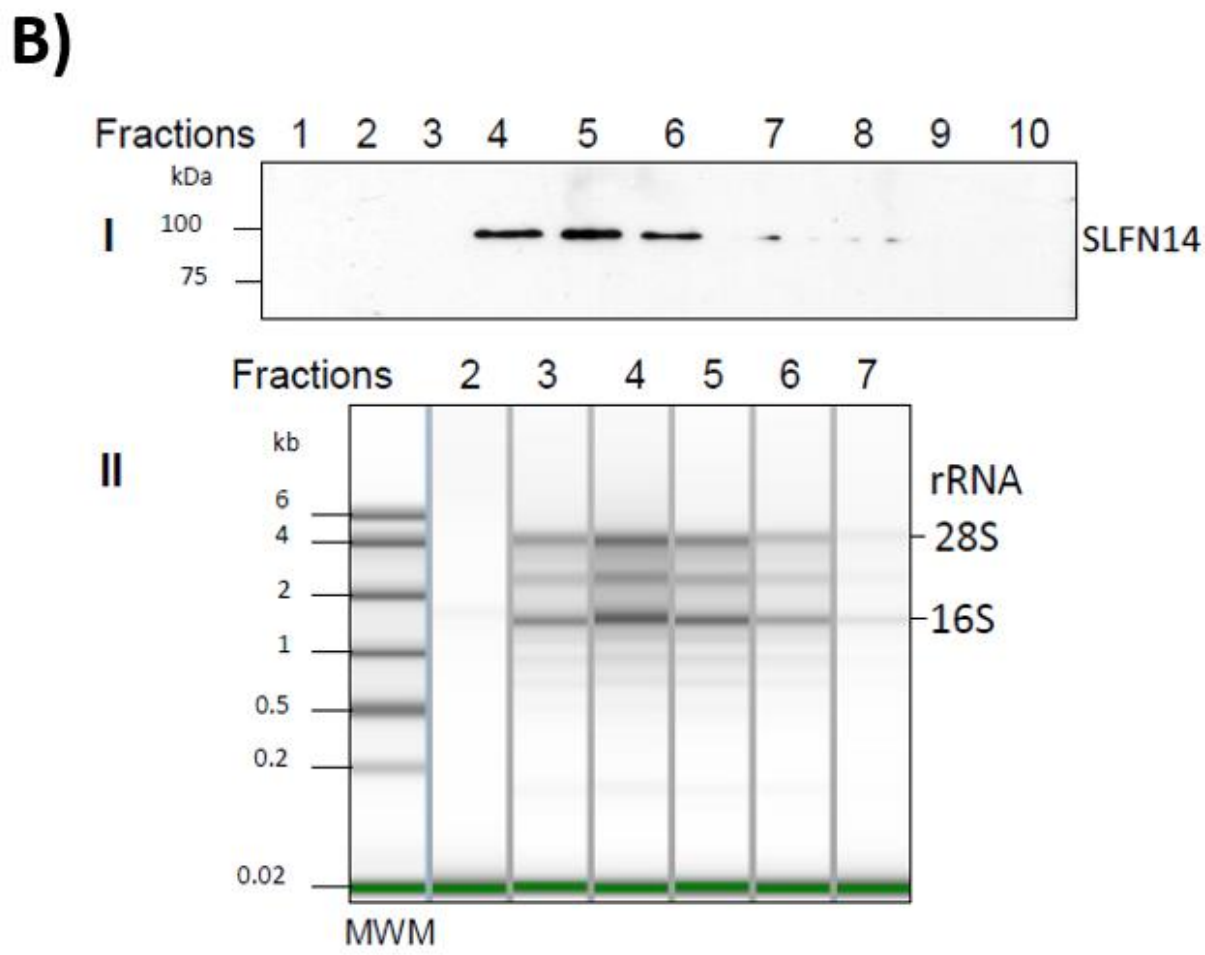

Fig. 2.7. Ribosome Association of SLFN14. **(A)** Subcellular distribution of SLFN14. SLFN14 was detected with an anti-FLAG antibody (red fluorescence) in HEK293T co-transfected with plasmids expressing mouse (m) and human (h) SLFN14 or 915 an empty plasmid (control cells), and HIVeGFP expression plasmid or not. Nuclei were stained with DAPI. Data in the figure corresponds to more than 100 cells in different fields of one experiment and are representative of three independent experiments. **(B)** Co-sedimentation of SLFN14 with ribosomes. **(I)** Immunoblotting detection of SLFN14 with an anti-FLAG antibody in sucrose gradient fractions obtained from HEK293T co-transfected with plasmids expressing human SLFN14 and HIV-1 Gag wild type. **(II)** The presence of ribosomes in selected fractions was determined by RNA gel electrophoresis. Data in the figure correspond to one experiment and are representative of five independent experiments

Chapter 3: Characterization of the Antiviral Activity of SLFN8 and SLFN9

3.1 Introduction

An important limitation to the characterization of SLFN11 antiviral activity *in vivo* is that this protein is absent in the mouse, a useful model organism in the study of the pathogenesis of many viruses including flaviviruses[124]. DNA and protein sequence analysis (Table. 1 and 2) indicate that murine SLFN8 and SLFN9 are the orthologs of SLFN11 and/or SLFN13. Indeed, these mouse SLFNs are around ~61% conserved compared to SLFN11. It has been proposed that these mouse genes have arouse by gene duplication, a genetic event that often leads to functional specialization of the genes. Therefore, despite of their homology, they could have unique and shared functions. Then, it is important to determine the antiviral properties of SLFN8 and SLFN9 in an attempt to determine which of these genes is the functional ortholog of SLFN11. This knowledge will pave the characterization *in vivo* of SLFN11 orthologs in mouse models.

3.2 Materials and Methods

3.2.1 Cell Lines

HEK293T, A172 and NIH/3T3 cells were grown in Dulbecco's modified Eagle's medium (DMEM) supplemented with 10% heat-inactivated fetal calf serum (FBS), 2 mM L-glutamine, and 1% penicillin. LL-MK2 cells in Eagle's Minimum Essential Medium (E-MEM) supplemented with 10% FBS, 1% penicillin, streptomycin, 1% non-essential amino acids (NEAA), and 1% sodium pyruvate. Maintenance media used to perform plaque assays consisted in E-MEM supplemented with 2% FBS, 1% NEAA, 1% penicillin/streptomycin, and 1% sodium pyruvate. Maintenance media used during viral infection consisted in DMEM in 2% FBS, and 1% penicillin/streptomycin.

A172-derived cell line SLFN11-knockdown (KD), its backcomplemented line (A172-BC), and a control cell line (A172-SCR) were previously derived[28] by lentiviral transduction of shRNAs or SLFN11.

3.2.1.1 Generation of A172-derived Cell Lines.

A172-SLFN11 knockdown (KD) were transduced with lentiviral vectors expressing a chimeric protein containing N-terminal SLFN9 (amino acids 1-447) fused to C-terminal SLFN11 (amino acids 442-912), and SLFN8 variant 2 (V2, amino acids 1-407). Transduced cells were selected in puromycin. Lentiviruses were produced as previously described[108]. Briefly, HEK293T cells were CaPO4-transfected with the corresponding transfer plasmids derived from pTRIP (15 ug), the packing plasmid pCMVΔR8.91 (15 ug), and VSV-G envelope expression plasmid pMD.G (5 ug). The viral supernatants were harvested 72 hr post-transfection and concentrated using Lenti-X^{TM} Concentrator protocol (Takara, 631232) following the manufacturer instructions.

3.2.2 West Nile Virus Production and Characterization

The WNV strain TVP-7767 (Passage: Vero, #3) was obtained from the World Reference Center for Emerging Viruses and Arboviruses, University of Texas Medical Branch. Viral stocks were produced by infecting Vero cells at 0.1 multiplicity of infection (MOI).

3.2.2.1 Virus Replication Dynamics

A172-derived cells were plated in T25 ($0.5x10^6$ cell/flask) in 5 mL of complete media and infected the next day with 0.1 MOI with WNV. Infection was carried out for 1 hr at 37ºC and then cells were washed three times with complete media to remove input virus and cultured in maintenance media at 37ºC. Cell culture supernatant were collected every 8 hrs for 48 hrs and stored at -80ºC until plaque assay was performed.

3.2.2.2 Plaque Assay

Cell supernatants containing WNV were subjected to ten-fold serial dilutions, and 12-well plates containing monolayers of LLC-MK2 cells were inoculated with 100uL of the ten-fold serial dilution and incubated at 37ºC for 1 hr with gentle rocking every 15 min. The cells were then overlaid with 1 mL of 0.5% agarose in E-MEM maintenance medium. Three days later the agarose layer was removed, and cells were then stained with Naphthol Blue Black (1g/L of Naphthol Blue

Black, 13.6g/L of Sodium Acetate anhydrous, 60ml/L glacial acetic acid) to visualize plaques. Plaque formation of each cell line was quantified, and viral titers were expressed as plaque-forming units per mL (PFU/mL).

3.2.3 Mouse Tissue

Mouse tissue was obtained from C57BL/6 mice. Organ tissue was collected and lysed using TRIzol LS reagent (Invitrogen 10296010) according to the manufacturer's instructions. All RNA samples had ratios of absorbance at 260/280 nm of 1.8 to 2.0, indicating that samples were contaminant-free. Purified RNA samples were used to detect SLFN8, SLFN9, and GAPDH by RT-PCR using specific primers (table 5).

3.2.4 Expression Plasmids

FLAG-tagged mouse SLFN8 V1 (Genescript OMu17465D), SLFN8 V2 (Origene MR214985), and SLFN9 (Genescript, OMu04073D) were subcloned into the pTrip IRESp backbone for expression. This plasmid was used also to express the chimeric protein SLFN9/11 that was generated by swapping amino acids 1-441 of SLFN11 by amino acids 1-447 of SLFN9 using NEBuilder® HiFi DNA Assembly Master Mix (New England BioLabs, E2621S) with primers CV3 and CV4 (table 3).

Table 3. Primers used for generation of SLFN9/11 chimera.

Mutant	Primer	Sequence	Extension Time	Annealing Temp
SLFN9/11	CV3	5'-CCGACTCTAGCTAGAGGATCCACTAGTATGGAGACATATCTCTCCTTAG-3'	30'	65°C
	CV4	5'-CCACAGCCCAACTTCTAGAGAGGATCAGCAAACCACAGG-3'		

HIV-1 Gag wild type (WT) and codon optimized (CO) were expressed from pCMVΔR8.91 (a gift of D. Trono) and pARP-8675 (NIH AIDS Reagent Program), respectively.

Gag was codon optimized from HIV-1 clone 96ZM651.8[106]. pECFP-C1 (Clontech 6076-1) was used to express cyan fluorescent protein (CFP). FLAG-tagged hSLFN14 was purchased from Origene (RC226257).

3.2.5 Immunoblotting

HEK293T cells (~$3x10^6$) were lysed in 100 ul of Laemmli sample buffer (12 mM Tris-Cl, pH 6.8, 0.4% SDS, 2% glycerol, 1% β-mercaptoethanol, 0.002% bromophenol blue). Cell lysates were centrifuged at 22,000 × g for 3 min at 4°C, and the supernatant mixed with Laemmli sample buffer, boiled for 10 mins, and saved at -80ºC for further analysis. Cell lysates (15 ul) was resolved by SDS-PAGE and transferred overnight to polyvinylidene difluoride (PVDF) membranes at 100 mA at 4°C. Membranes were blocked with Tris-buffered saline (TBS) containing 10% milk for 1 h and then incubated with the corresponding primary antibody diluted in TBS-5% milk-0.05% Tween 20 (antibody dilution buffer). FLAG-tagged mouse SLFN8 V1, V2, and SLFN9, were detected with anti-FLAG MAb (1/500) (M2; Sigma), non-tagged human SLFN11 and chimeric SLFN9/11 were detected with antibodies directed to the C-terminus anti-SLFN11 mAb E-4 (Santa Cruz Biotechnology, sc-374339) (1/500). As a loading control, anti-α-tubulin MAb (clone B-5-1-2; Sigma) was used at a 1/4,000 dilution. Membranes were incubated overnight at 4°C with anti-FLAG and -SLFN14 antibodies, whereas anti-α-tubulin MAb was incubated for 30 mins at 25°C. Primary antibody-bound membranes were washed in TBS-0.1% Tween 20, and bound antibodies were detected with goat anti-mouse Ig-horseradish peroxidase (HRP) (Sigma, 1/2,000) or mouse anti-rabbit IgG-HRP (Santa Cruz Biotech, 1/4,000) diluted in antibody dilution buffer. These antibodies were incubated for 1 hr at 25°C. Unbound secondary

antibodies were washed as described above and bound antibodies detected by chemiluminescence.

3.2.6 Analysis of Mouse SLFNs Activity

HEK293T cells (0.45×10^6 cells/well) plated in a six-well plate were transfected by calcium-phosphate with corresponding plasmids, and transfection medium was replaced with fresh culture medium 18 hrs later. In experiments evaluating the effect of mouse SLFNs on protein expression, cells were transfected with 2 ug of empty plasmid or mouse SLFNs, together with 2 ug of the target plasmid (pCMVΔR8.9 or pARP-8675 or pHΔELuc), and 0.5 ug of CFP. 72 hrs post-transfection CFP expression was measured by flow cytometry, supernatant was used for HIV-1 p24 quantification by ELISA, and cell lysates were analyzed for the transfected proteins by immunoblot.

3.2.7 Fluorescence Microscopy Analysis

A172-derived cells stably expressing different SLFNs plated ($0.08x10^6$ cells) in Lab-Tek® II Chamber Slide™ system (VWR, 15461) were fixed and permeabilized with Cytofix/Cytoperm buffer (BD Bioscience, Cat# 554714). FLAG-tagged mouse SLFNs were detected with anti-FLAG MAb (1/500) (M2; Sigma) in 1x Cytoperm buffer for 2 hrs at room temperature. After washing twice with 500 uL of 1x Cytoperm buffer, cells were incubated with goat anti-mouse IgG-FITC (1/200) (Santa Cruz Biotech, sc-2010) for 1 hr at room temperature in the dark. The secondary Ab was washed twice with 500 uL of 1x Cytoperm buffer, and cells were stained with 300uL of DAPI at 1ug/mL for 10 min at room temperature in the dark. DAPI was washed once with 1x PBS, Dakocytomation Fluorescent Mounting Medium added (Agilent, S3023), and a 1oz cover slide placed.

3.2.8 HIV-1 p24 ELISA

HIV-1 p24 levels were determined by a sandwich ELISA according to the manufacturer's instructions (ZeptoMetrix, 22157319). Briefly, cell culture supernatants were diluted appropriately and incubated on the ELISA antibody pre-coated wells overnight at 37°C. Unbound proteins were removed by washing the wells 6 times with 200 µl of washing buffer, and bound HIV-1 p24 was detected by incubating each well with 100 µl of the anti-HIV-1 p24-HRP secondary antibody for 1 h. Unbound antibodies were removed by washing as described above, and bound antibodies were detected by incubating each well with 100 µl of substrate buffer for 30 min at room temperature until the reaction was stopped by adding 100 µl of stop solution into each well. The absorbance of each well was determined at 450 nm using a microplate reader (Versa max microplate reader; Molecular Devices).

3.2.9 Quantitative RT-PCR and PCR

Total RNA and DNA were isolated from SLFN8 V1- and SLFN8 V2-transfected HEK293T cells or mouse tissues using TRIzol LS reagent (Invitrogen 10296010) according to the manufacturer's instructions. SLFN8, and SLFN9 and β-actin mRNA were detected with specific primers (table) using iTaq Universal SYBR® Green One-Step Kit (Biorad, 1725151) and IQ SYBR Green Supermix (BioRad, 1708882), respectively.

Table 4.

Purpose	Primer	Sequence	Anneling	Extention Time
β-actin	CV48	5'-TGGAATCCTGTGGCATCCATGAAC-3'	62°C	10 sec
	CV49	5'-TAAAACGCAGCTCAGTAACAGTCCG-3'		
SLFN9	CV46	5'-GGCATATATCAAATGCAGTCCG-3'	58°C	15 sec
	CV51	5'-CTCTGCTTTGATCACACCACCTCC-3'		
SLFN8	CV44	5'-AGGCATGTATCAAATACAGGCCT-3'	62°C	1 min 20 sec
	CV45	5'-ACTGAGCCCCCATTGGTCTCAA-3'		

Table 4. List of primers used for quantitative RT-PCR and PCR.

3.2.10 Statistical Analysis

GraphPad Prism version 9.4.1 was used for statistical analysis. One-way ANOVA was used to test the impact of human or mouse SLFNs on the expression of the proteins of interest, and the Dunnett's post hoc test was used to identify significant differences between cells expressing empty plasmid (control group) and cells expressing SLFNs proteins (experimental groups). Two-tailed t test was used to evaluate the statistically significant of experiments with only two groups (control and experimental). Experiments where the comparison was between a specific control and a specific experimental group two-way ANOVA and Dunnett post hoc test was utilized. p-values were indicated as follow: no significant (ns) > 0.05, * ≤ 0.05, ** ≤ 0.01, *** ≤ 0.001, **** ≤ 0.0001.

3.3 Results

3.3.1 SLFN8 and SLFN9 Codon Usage-Based Inhibition of HIV-1 Protein Expression

Data in Fig. 3.1 C show that cells co-transfected with either SLFN8 V1, SLFN8 V2 or SLFN9 and HIV-1 Gag WT showed a ~80% to ~60% reduction in p24 production compared to the control, once normalized for transfection efficiency (% of CFP+ cells). This reduction of p24 seems to be specific since CFP expression (Mean Fluorescence Intensity, MFI) was not affected by these SLFN proteins (Fig. 3.1 D).

Despite equivalent transfection efficiencies (Fig 3.1 B) and a similar inhibitory effect on HIV-1 Gag WT expression, SLFN8 V1 showed a poorer expression than SLFN8 V2 and SLFN9 (Fig, 3.1 A).

SLFN11 has been proposed to affect expression of mRNAs rich in codons rarely used. Codon usage is dictated by tRNA abundance; therefore, the amount of tRNAs to decode rare codons is less than those engaged in translation of commonly used codons. For this reason, SLFN11-mediated global tRNA degradation will preferentially affect mRNAs enriched in rare codons, these mRNAs are called non-codon optimized and have a lower value in the codon adaptation index (CAI). In order to evaluate the role of mouse SLFNs on codon usage-based expression, we determined their effect on HIV-1 Gag WT (non-codon optimized, CAI of 0.56) and HIV-1 Gag CO (codon optimized, CAI of 0.99) expression, using plasmids that have the same promoter (CMV enhancer/promoter).

CFP %-normalized HIV-1 p24 values of HEK293T cells co-expressing Gag WT and either SLFN8 V1, SLFN8 V2, SLFN9 or hSLFN14 were lower than cell expressing no SLFN proteins (Fig. 3.1 B). More importantly any of these SLFN proteins affected the expression of Gag CO (Fig. 3.1 B) or CFP MFI (Fig. 3.1 C), used as transfection control in all these experiments. In multiple experiments we noticed that the expression of SLFN8 V1 was lower than other SLFNs. It is particularly striking in the experiment represented in Fig. 3.1 A, in cells expressing Gag CO. This makes it difficult to conclude that this protein does not affect Gag CO expression. However, because SLFN8 V2 shares the active region of SLFN8 V1 is likely that they both act through the same codon usage-based inhibition of protein expression.

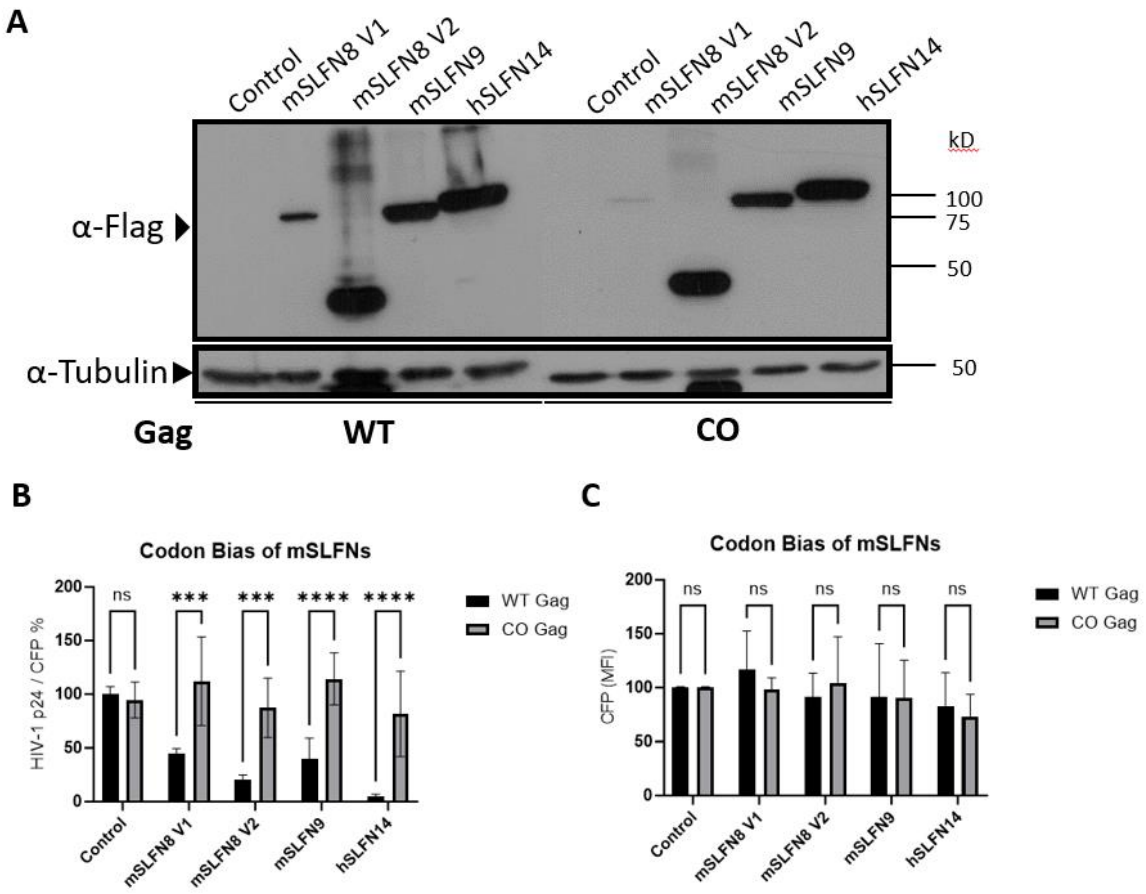

Fig. 3.1. SLFN8 and SLFN9 Codon Based Inhibition of HIV-1. HEK293T cell co-transfected with a plasmid expressing CFP and either an empty plasmid (control cells) or a plasmid expressing human (h) SLFN14 or mouse (m) SLFN8 or SLFN9. Immunoblot **(A)** of HEK293T co-transfected with a plasmid expressing CFP or plasmids expressing either Gag WT or CO together with empty (control) or SLFNs tested. Normalized p24/CFP% **(B)** of Gag WT and CO. Mean fluorescence intensity (MFI) **(C)** of HEK293T co-transfected cells as recorded by flow-cytometry. Statistically significant differences were calculated with repeated measures using two-way ANOVA Dunnett pos hoc test. ** $P \leq 0.01$ and * $P \leq 0.05$. Data correspond to a triplicate experiment and are representative of eight independent experiments.

3.3.2 Anti-WNV Activity of SLFN8 and SLFN9

Since both SLFN8 and SLFN9 are active against HIV-1, we cannot conclude if only one of them is the functional ortholog of SLFN11; therefore, we evaluated their anti-WNV activity. In these experiments, WNV replicated with a similar kinetics in SLFN11-KD cells expressing SLFN9 or a chimeric protein containing the N-terminal region of SLFN9 (aa 1-447) fused to the C-terminus of SLFN11 (aa 442- 901) than in SLFN11-KD cells expressing SLFN11 (A172-BC). These data indicate that, similarly to SLFN11, the N-terminal region of SLFN9 mediates its anti-WNV activity (Fig. B-II and B-III). Next the anti-WNV activity of SLFN8 was evaluated with its variant 2 since this protein contains the N-terminal region of SLFN8 V1 and is expressed better (Fig. B-IV). Importantly, SLFN8 V2 did not affect WNV replication in spite of its protein identity with SLFN9 N-terminus (82.8%).

However, in these experiments we encountered technical difficulties. The differences in WNV replication between the SLFN11-KD and SLFN11-BC cell lines were significantly smaller than previously observed[28], making it difficult to arrive to solid conclusions regarding the anti-WNV activity of SLFN8 and SLFN9. In addition, standard deviations in these experiments were too large to reach statistical conclusions. We think that the reason for the smaller differences of WNV replication in cells expressing or not SLFN11 is due to the re-expression of SLFN11 in the KD cell line. This is a common phenomenon in stable cell lines generated without antibiotic selection. SLFN11-KD cell line was selected by eGFP-based cell sorting. Currently, we are developing SLFN11 knockout cell lines to have a more reliable system to evaluate the anti-WNV activity of SLFN8 and SLFN9. Nevertheless, my preliminary conclusions are that SLFN9 but not

SLFN8 has anti-WNV activity, suggesting SLFN9 to be the SLFN11 functional ortholog in mice.

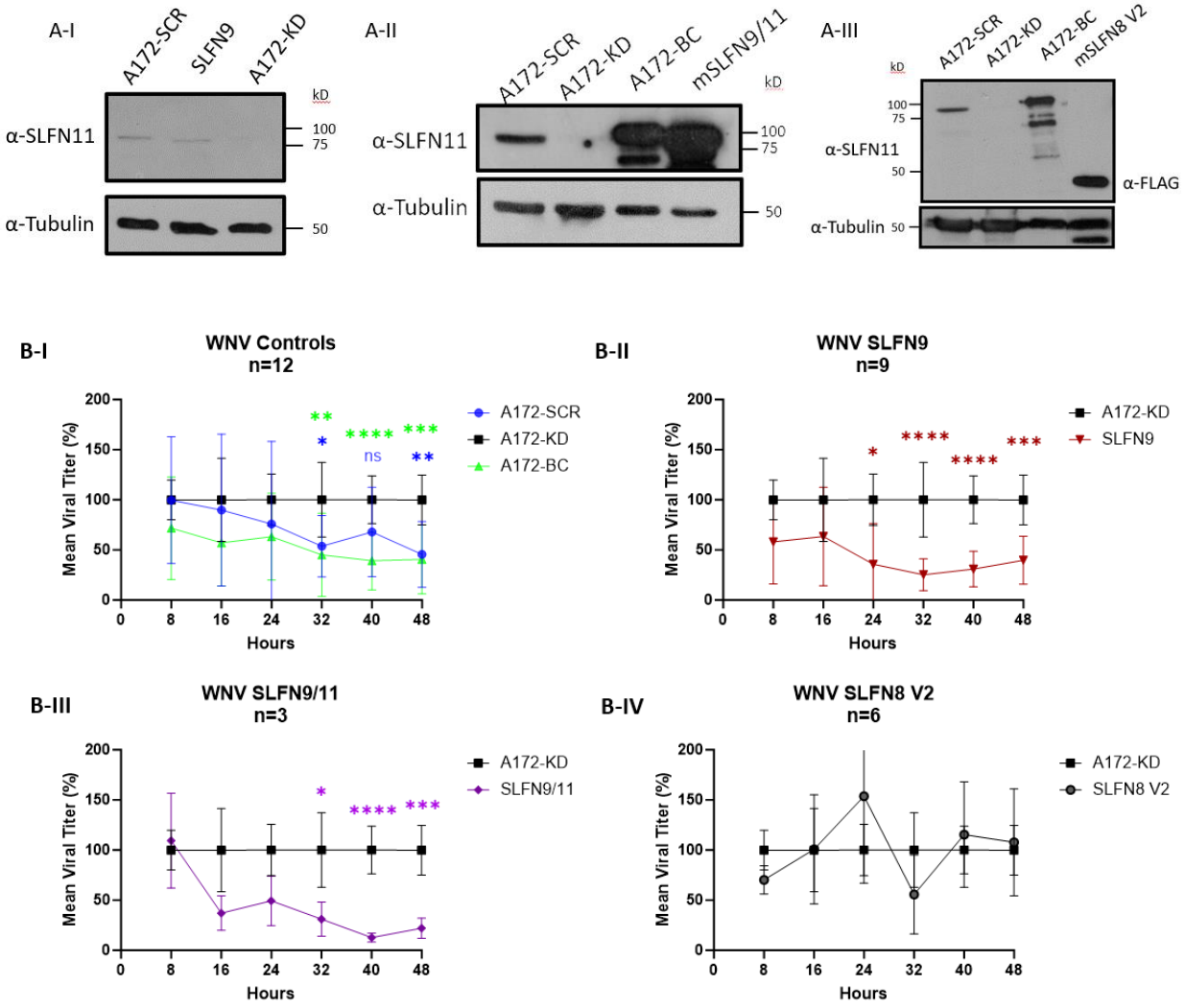

Fig. 3.2. Mouse SLFN8 and SLFN9 Anti-Viral Activity Against WNV. Immunoblot of stably expressed of mouse SLFN9 (**A-I**), chimeric SLFN9/11 (**A-II**), or SLFN8 V2 (**A-III**) in A172-KD cells. Replication of WNV (**B)** "n" indicates the number of experiments done with each cell line, A172-KD was used as base line in all graphs. (**B-I**) WNV replication in (control cell lines) A172-SCR (Blue), and A172-BC (Green). (**B-II**) SLFN9 (Red). (**B-III**) Chimeric SLFN9/11 (Purple). (**B-IV**) SLFN8 V2. Statistically significant differences were calculated

with repeated measures using two-way ANOVA Dunnett pos hoc test. **** $P \leq 0.0001$, *** $P \leq 0.001$, ** $P \leq 0.01$, * $P \leq 0.05$, and not significant was sometimes referred to as ns or not shown.

3.3.3 Effect of Type I IFN and WNV Infection on *SLFN8* and *SLFN9* mRNA Expression

We next evaluated the expression of SLFN8 and SLFN9 in mouse cells relevant to WNV infection. During WNV infection the initial infection occurs in the epidermis, where the virus infects keratinocytes and Langerhans cells. The virus then travels to the local lymph node, this triggers a primary viremia, then infects visceral organs mainly the spleen and the kidneys producing a secondary viremia and neuroinvasion.

The basal expression of β-actin-normalized SLFN8 was found in liver, spleen and kidneys, but not in lung and brain. SLFNs in organs including organs relevant during WNV infection (Brain, spleen, and kidneys) were evaluated. As seen in Fig. 3.5, the highest levels of SLFNs were observed on the liver. We failed to detect SLFN8 in the brain and lungs, while SLFN9 appears to be ubiquitously expressed.

We utilize NIH/3T3 mouse fibroblast, since these cells are susceptible to WNV infection and could represent the first stage of WNV infection *in vivo*.

Infection of NIH/3T3 cells with WNV (MOI 3) upregulated 10^5 folds β-actin-normalized SLFN8 mRNA levels and more modestly those of SLFN9 (~7 fold). A similar effect for SLFN8 was observed when cells were treated with IFN-α (2000 U/mL) but SLFN9 did not respond to the cytokine. The differential sensitivity to WNV could indicate a major role of SLFN8, but not

SLFN9, in WNV infection. Furthermore, WNV could induce SLFN9 expression in NIH/3T3 by a type I IFN-independent pathway.

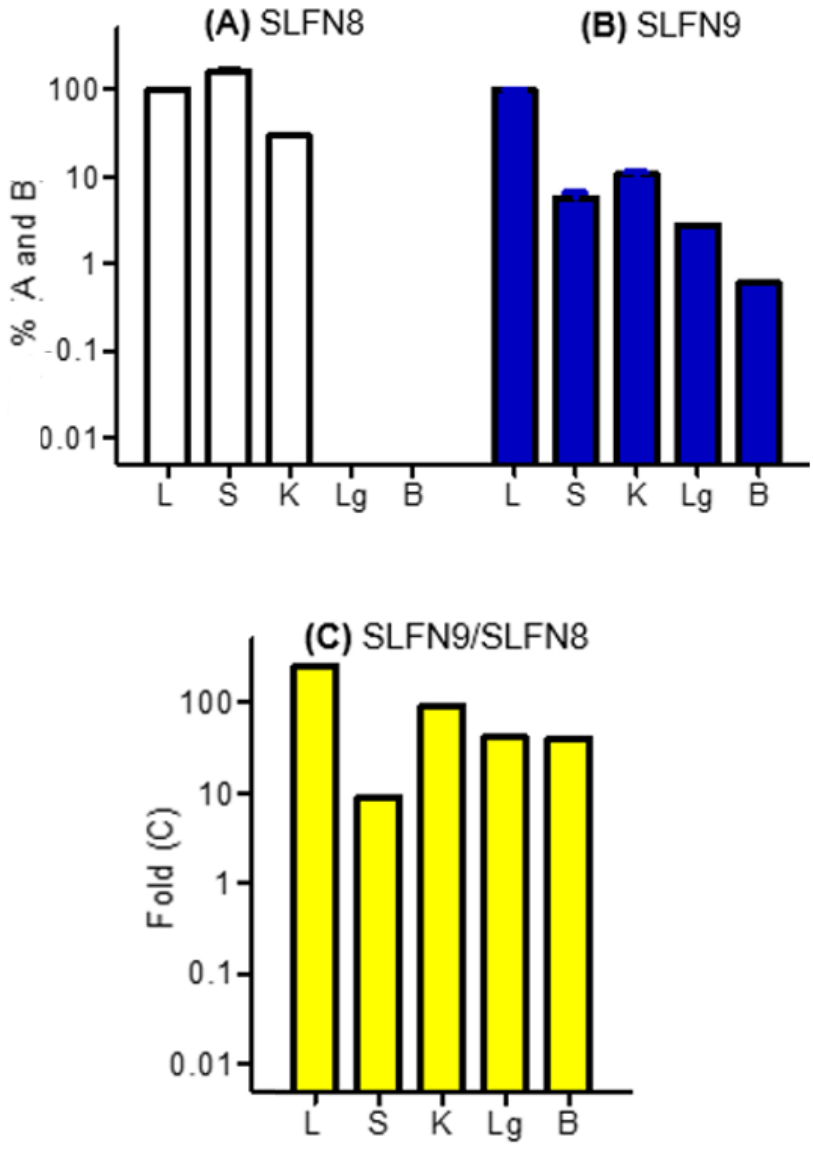

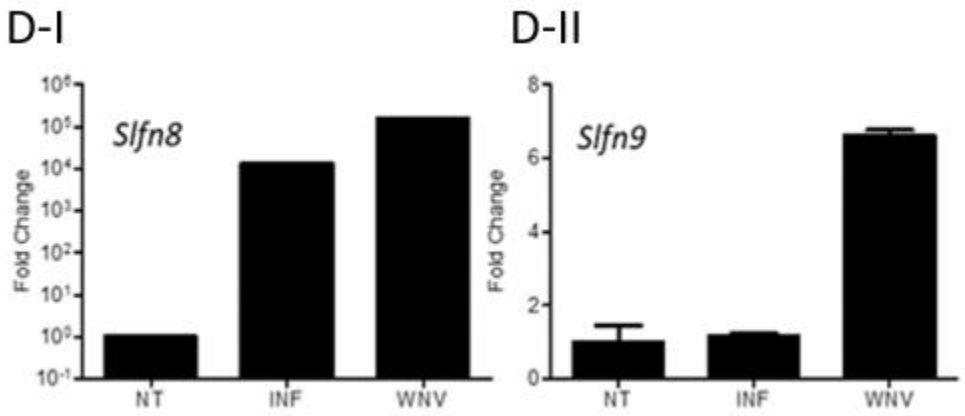

Figure 3.3. Differential Expression of *SLFN8* and *SLFN9* in Mouse Tissues. Levels of β-actin, SLFN8 and 9 mRNA were measured by RT-qPCR in liver (L), spleen (S), kidney (K), lung (Lg) and brain (B) of B6 background mice. β-actin-normalized SLFN mRNA values are represented. The values of SLFN8 (**A**) and SLFN9 (**B**) are expressed in %, relative to levels found in liver (100%). In **C**, SLFN9 levels normalized to SLFN8 levels are expressed in fold-change. Standard deviation (**A and B)** indicates the variability found in three different animals. Lg and B data correspond to only one animal. Each sample was evaluated in triplicate RT-qPCR reactions. (**D-I and D-II**) Effect of type I IFN and WNV infection on *SLFN8* and *SLFN9* expression in NIH/3T3**.** Cells were treated with αIFN (2000 U/ml) or infected with WNV (M.O.I 3) and 72 hrs later β-actin and SLFNs mRNA levels were determined by RT-qPCR. β-actin-normalized SLFNs mRNA levels were calculated and expressed relative to those found in non-treated, mock-infected control cells (NT). Standard deviation values (not visible in SLFN8 panel) represent the variability of triplicate RT-qPCR reactions. The experiment was done in singlicate. α-IFN failed to upregulate *SLFN9* expression.

Chapter 4: Sub-Cellular Localization of SLFN Proteins

4.1 Introduction

Nuclear localization signals (NLSs) are sequences of amino acids that direct proteins to the nucleus. For many proteins, sub-cellular localization is closely related to their function. Characterization of novel NLSs have many benefits such as understanding cellular trafficking, regulation of gene expression, and disease mechanisms. Aberrant NLSs, either by single nucleotide polymorphisms or somatic mutations, could lead to miss-localization of the protein which could lead to disease.

The sub-cellular distribution of SLFN proteins has not been carefully evaluated and for some of these proteins is debatable. To fully evaluate this, we performed confocal microscopy analysis of cells stably expressing SLFN group III proteins using anti-FLAG antibodies.

4.2 Materials and Methods

4.2.1 Cell Lines

HeLa cells and HEK293T transiently or A172 cells stably expressing SLFN proteins were used for immunofluorescence analysis. Cell were grown in Dulbecco's modified Eagle's medium (DMEM) supplemented with 10% heat-inactivated fetal calf serum (FBS), 2 mM L-glutamine, and 1% penicillin. Lipofectamine 3000 and calcium phosphate methods were used to transfect expression plasmid into HeLa cells and HEK293T cells, respectively. A172 cells expressing SLFN proteins were generated by transduction with lentivectors.

4.2.2 Expression Plasmids

Plasmids expressing SLFN group III proteins were obtained from commercial sources. SLFN11 was expressed as an N-terminal eGFP tagged protein. Primers listed in table 5 were used to make the SLFN11 mutants with Phusion Site-Directed Mutagenesis kit. Briefly, a segment of SLFN11 was subcloned into pUC19 for mutagenesis and then moved back to the SLFN11 expression plasmid. The entire sequence of the SLFN11 mutants was verified by overlapping DNA sequencing.

Table 5. Primer list used for the creation of hSLFN11-eGFP mutants.

Purpose	Primer	Sequence	Extension Time	Annealing
Δ594-748	CV58	5'-TCTGTTCTTGCGGAGGCTTCTGGAG-3'	2' 10''	62°C
	CV59	5'-AGTAATCCTTCATTTAACATCCCC-3'		
Δ750-901	CV60	5'-TCTAATTACTTGCATTTCTTTTTG-3'		60°C
	CV61	5'-CCTGCAGGTATGGTGAGCAAGGGCGAG-3'		
Δ750-800	CV60	5'-TCTAATTACTTGCATTTCTTTTTG-3'		60°C
	CV64	5'-GATAGGGGCTATTCTCCAAAG-3'		
R689Q, A691E, G693D, and G694C	CV62	5'-TTCTCTCTGAGTGATGCTTTTTGC-3'		60°C
	CV63	5'-AAGGATTGCCCAGGAATTCTCTGG-3'		
R834M	CV65	5'-ATGGTGGTGCAGCTCAGTGATG-3'		60°C
	CV66	5'-TTTCTTCCTCATTGCTTTCAAGAG-3'		
Δ735-761	CV69	5'-TGCATTGCGAACTATTCTGGTG-3'		62°C
	CV70	5'-GAGGTATTTCCTGAAGCCGAATG-3'		
Δ751-757	CV71	5'-ACTTCTAATTACTTGCATTTC-3'		60°C
	CV72	5'-ACTGGGTGCCTCGAGGTATTTCC-3'		

4.2.3 Fluorescence Microscopy

Cells were plated at $0.08x10^6$ cells/well in Lab-Tek® II Chamber Slide™ system (VWR, 15461), and the next day were transfected. 48 hrs post-transfection cells were fixed and permeabilized with Cytofix/Cytoperm buffer (BD Bioscience, Cat# 554714). SLFN5, SLFN8 and SLFN9 were detected with anti-FLAG ab (1/500) (M2, Sigma), whereas SLFN11 was identified with anti-SLFN11 ab (1/500) (sc-515071, Santa Cruz Biotech) as described in chapter 2. Antibody-stained cells or SLFN11-eGFP transfected cells were stained with 300uL of DAPI at 1ug/mL for 10 min at RT in the dark. DAPI was then removed and wash once with 1x PBS, after this last wash

the plastic was removed to mount the slide using Dakocytomation Fluorescent Mounting Medium (Agilent, S3023) and cover placing a 1oz microscope cover glass (24x60 mm) (VWR Vistavision^{TM} Cover Glass, 16004-096). Cell visualized by confocal microscopy in a Zeiss LSM 700 confocal microscope.

4.2.4 In silico Analysis

Prediction of NLS and protein post-translational modifications were conducted with cNLS Mapper [https://nls-mapper.iab.keio.ac.jp/cgi-bin/NLS_Mapper_form.cgi][125], and PhosphoSitePlus® [www.phosphosite.org[126]], respectively.

4.3 Results

4.3.1 Sub-Cellular Localization of SLFN Proteins

Using indirect immunofluorescent microscopy, we were able to detect the subcellular localization of the SLFN proteins. SLFN5 has been previously shown to be nuclear[49] our results collaborate these finding. However, the previously reported NLS located in the C-terminal is likely not the only NLS that SLFN5 contains since both N- and C- terminal fragments are cytoplasmic (Fig.4.2). Similarly, SLFN8 and SLFN9 are nuclear proteins. Interestingly, SLFN8 that we evaluated is the variant 2 which only codes for the N-terminal fragment of full-length SLFN8. This protein despite having a well conserved NLS located in the C-terminal, remains to be nuclear, which indicates that the N-terminal NLS of SLFN8 is strong enough for full nuclear localization, in contrast to SLFN5 and SLFN11, require the cooperation of additional NLS at least one of them located in the N-terminal region.

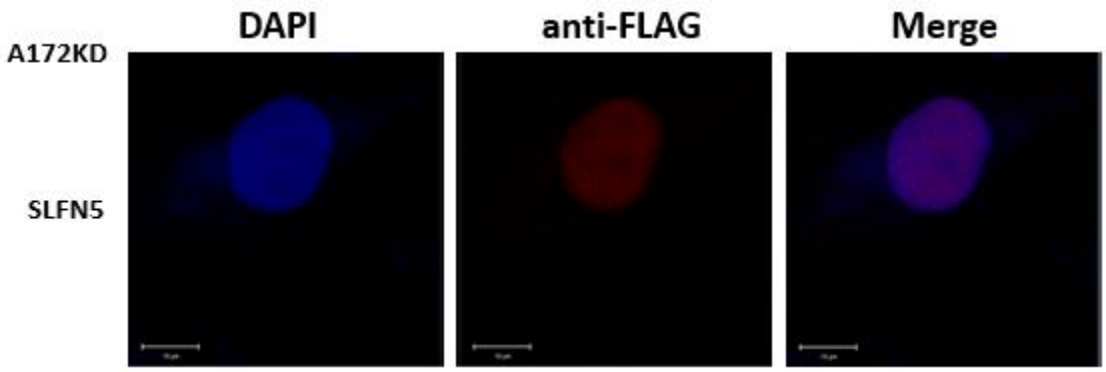

Figure 4.1. **Cellular Distribution of SLFN5**. Nuclear localization. A172-KD cells were fixed/permeabilized and stained with anti-FLAG antibody (red). Cell nuclei were identified with DAPI dye (blue).

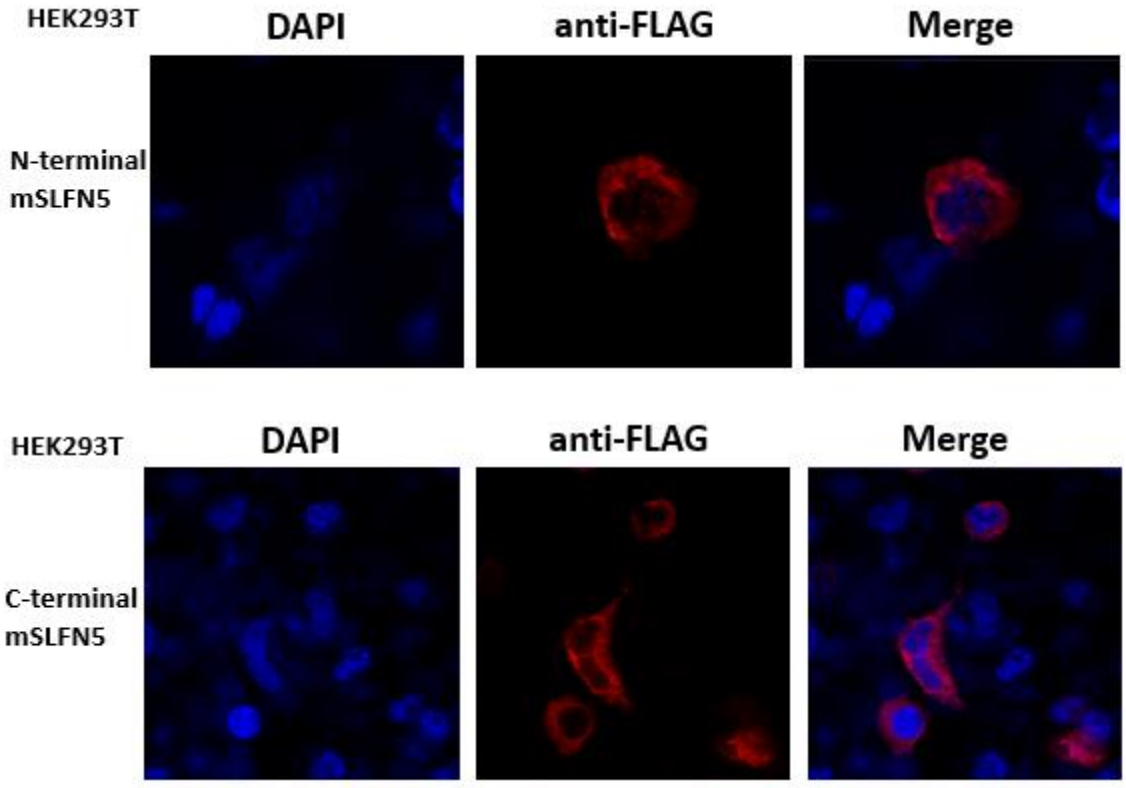

Figure 4.2. Cellular Distribution of N- and C-terminal SLFN5. Cytoplasmic localization. HEK293T cells were fixed/permeabilized and stained with anti-FLAG antibody (red). Cell nuclei were identified with DAPI dye (blue).

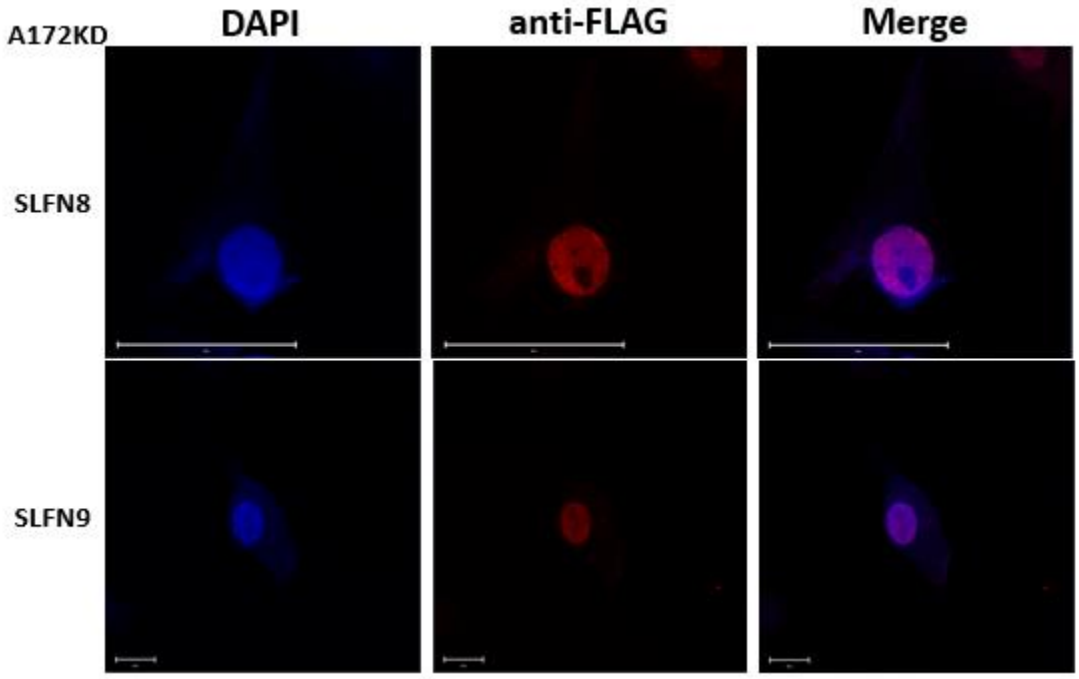

Figure 4.3. **Cellular distribution of SLFN8 and SLFN9**. Nuclear localization. A172-KD cells were fixed/permeabilized and stained with anti-FLAG antibody (red). Cell nuclei were identified with DAPI dye (blue).

4.3.2 Mapping the Nuclear Localization Signals of SLFN11

In correspondence with others, we have found SLFN11 in the nucleus of several cell types[16,28]. SLFN11 is not found to a particular compartment in the nucleus and is not tightly bound to the chromatin since can be extracted in Triton X-100 1%. Therefore, SLFN11 seems to be in the nucleoplasm. Unexpectedly, proteins containing the N- (aa 1-441) and C- (aa 442-902) terminus of SLFN11 are cytoplamic[28]. SLFN11 mutated in patch 1 (aa 39 and 43), but not in the patch 2 region (aa 228), lacks the nuclear localization indicating that these amino acids form the N-terminal NLS. To map the C-terminal NLS we generated a panel of deletion mutants in the SLFN11 full-length (FL) and determined their localization. Deletion of aa 594-748 localized the

protein to the cytoplasm, similarly to Δ750-901 and Δ750-800, suggesting that the region around aa 748 contains an NLS. This was confirmed by the Δ735-761 mutant that was also cytoplasmic; however, Δ751-757 was nuclear. These findings indicated that the region 735-750 contains an NLS. Analysis of SLFN11 with NLS prediction software did not identify an NLS in this region; but, indicated NLSs at aa 689-694 and 834 in SLFN11, although not in SLFN13. Then, mutation of aa 689-694 to residues present in SLFN13 demonstrated no effect on SLFN11 nuclear localization. In contrast, mutation of 834 to the corresponding SLFN13 residue abolished nuclear localization of SLFN11. In summary, SLFN11 nuclear localization requires the cooperative interaction of residues 39/43, 735-750, and 834. Interestingly, residues 739 and 743, and 750 are predicted to be ubiquitinylated, and phosphorylated, respectively (PhosphoSitePlus®). In particular, the phosphorylation of S750 was demonstrated by phosphoproteomic analysis of SLFN11, but its mutation to A/D did not affect the anti-HIV-1 activity of SLFN11[44].

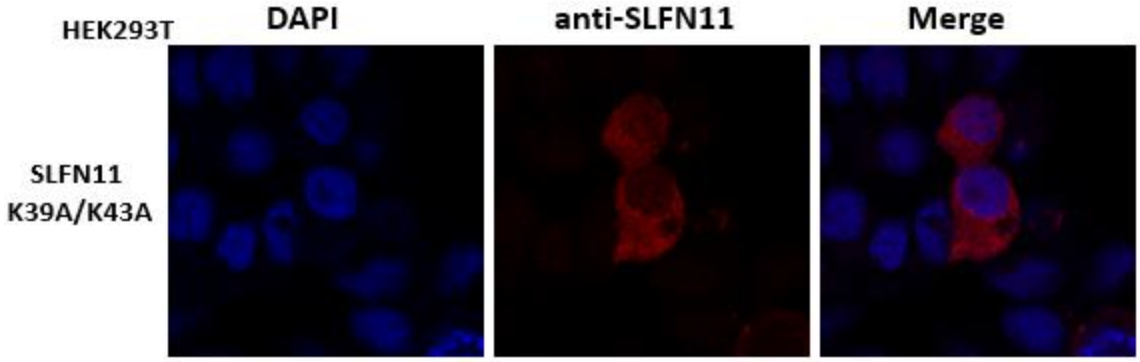

Figure 4.4. Cellular distribution of Slfn11 K39A/K43A (Patch 1). Cytoplasmic localization. HEK293T cells were fixed/permeabilized and stained with anti-SLFN11 E-4 antibody (red). Cell nuclei were identified with DAPI dye (blue).

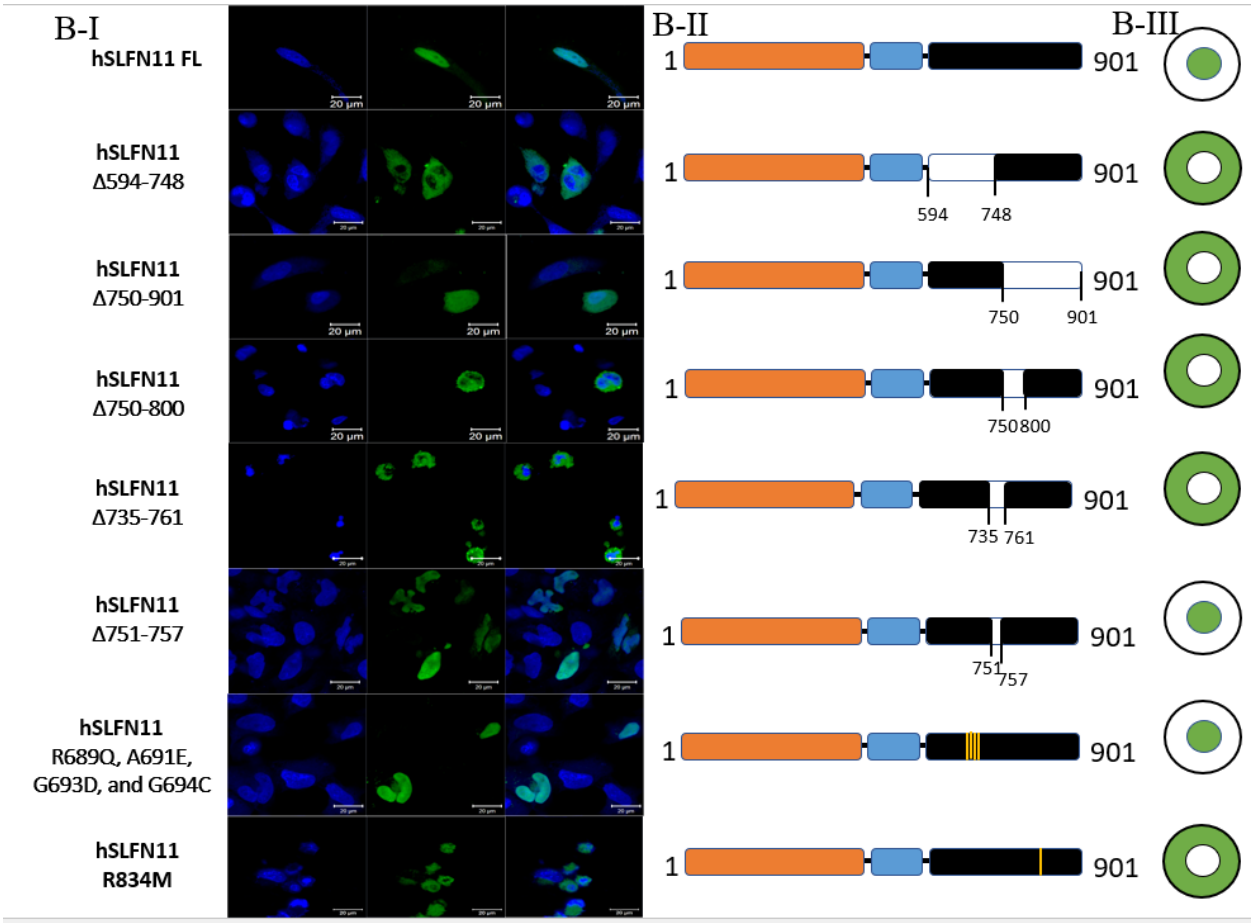

Figure 4.5. **Human SLFN11 Nuclear Localization Signals**. **(A)** Human SLFN11 full length (FL) protein defined by 3 domains N'-terminal domain (Orange), SWADL (Light blue), and C'-terminal domain (Black). **(B-I)** HeLa cells transfected with human (h) SLFN11 FL or respective mutant. **(B-II)** Diagram which depicts mutation within the C'-terminal domain of SLFN11. Deletion is shown as blank regions within the C-terminal domain. Mutations are shown as yellow lines within the C'-terminal domain. **(B-III)** Diagram depicts the localization of each respective hSLFN11 plasmid. Green filling indicates the localization of the given hSLFN11 plasmid, while blank filling indicates the absence of hSLFN11.

Chapter 5: Evaluation of the Antiviral Activity of SLFN13

5.1 Introduction

As with other members of the Schlafen family, SLFN13 has been poorly characterized. There is only 1 report describing the anti-HIV-1 SLFN13 activity and structure. SLFN13 degrades tRNAs and rRNA[30], affecting in this manner HIV-1 protein expression[30].

Perhaps one of the main limitations to study SLFN13 is its poor endogenous or exogenous protein expression. Our laboratory has demonstrated that this phenomenon is at a post-transcriptional level. We hypothesized that SLFN13 protein is unstable and we evaluated this hypothesis here. Importantly, we managed to increase SLFN13 protein stability and we were able to determine its subcellular localization and anti-HIV-1 activity.

5.2 Materials and Methods

5.2.1 Cell Culture

HEK293T and HeLa were grown in Dulbecco's modified Eagle's medium (DMEM) supplemented with 10% heat-inactivated fetal calf serum (FBS), 2 mM L-glutamine, and 1% penicillin.

5.2.2 Expression of Plasmids

pcDNA3.1+/C-(K)-DYK SLFN13 expression plasmid (OHu32094D, Genescript) was used to subclone SLFN13 into a pCMV-Myc[127] vector plasmid to improve expression levels. PCR with primers indicated in table 6 were used to generate SLFN13 deletion mutants.

Wild type Gag was expressed from pCMVΔR8.91 (a gift of D. Trono) and codon optimized Gag from pARP-8675 (NIH AIDS Reagent Program). This construct expresses a codon-optimized HIV-1 clone 96ZM651.8 Gag pre-protein[106]. Cyan fluorescent protein expression plasmid was pECFP-C1 (Clontech).

Table 6. List of primers used for the generation of SLFN13 truncated mutants.

Purpose	Primer	Sequence
SLFN13 FL	CV67	5'-TATAGCTAGCGTTTAAACTTAAGC-3'
	CV68	5'-TATAGGGCCCCAGAAAAATATATAGGTGC-3'
SLFN13 Δ353	CV67	5'-TATAGCTAGCGTTTAAACTTAAGC-3'
	CV69	5'-TATAGGGCCCTGCGTCCATCATTTTCTC-3'
SLFN13 Δ751	CV67	5'-TATAGCTAGCGTTTAAACTTAAGC-3'
	CV71	5'-TATAGGGCCCATTTTCTATAATTAGTTGC-3'

5.2.3 Generation of Viruses

Procedures previously described[108,109] were used for production of HIVeGFP. Briefly, HEK293T cells were co-transfected by calcium phosphate with 2 ug of pNLENG1-ES-IRES [Levy paper], 0.5 ug of pMD.G, a vesicular stomatitis virus glycoprotein G (VSV-G) expression plasmid, 0.5ug of CFP expressing plasmid and 2 ug of SLFN expressing plasmid or conrl. Seventy-two hours after transfection, the viral supernatants were harvested.

5.2.4 Analysis of the Anti-HIV-1 Activity of SLFN13

HEK293T plated at $1x10^5$ cell/well in a 12-wells plate were infected with HIVeGFP produced in the presence or absent of SLFN13, and three days later the cells were analyzed by flow cytometry to determine the percentage of infected cell, by immunoblot to verify SLFN13 protein expression, and by p24 ELISA.

The effect of SLFN13 on HIV-1 protein expression was determine in HEK293T cells. Cells were plated at $0.45 \times 10^{\mathbf{6}}$ cells/well in a six-well plate and transfected by calcium-phosphate with corresponding plasmids, and transfection medium was replaced with fresh culture medium 18 hrs later. In experiments evaluating the effect of SLFN13 on protein expression, cells were transfected in six-well plates. Each well was transfected with 2 ug of empty plasmid or 2ug of SLFN13 and 2ug of the target plasmid (pCMVΔR8.9, or pARP-8675), and cells were analyzed 72 hrs after transfection by measuring p24 in the supernatant with an HIV-1 p24 ELISA.

5.2.5 Flow Cytometry

HIV-1-driven eGFP was detected by flow cytometry as described in chapter 2.

5.2.6 HIV-1 p24 ELISA

HIV-1 p24 levels were determined by a sandwich ELISA according to the manufacturer's instructions (ZeptoMetrix, 22157319). Briefly, cell culture supernatants were diluted appropriately and incubated on the ELISA antibody pre-coated wells overnight at 37°C. Unbound proteins were removed by washing the wells 6 times with 200 µl of washing buffer, and bound HIV-1 p24 was detected by incubating each well with 100 µl of the anti-HIV-1 p24-HRP secondary antibody for 1 h. Unbound antibodies were removed by washing as described above, and bound antibodies were detected by incubating each well with 100 µl of substrate buffer for 30 min at room temperature until the reaction was stopped by adding 100 µl of stop solution into each well. The absorbance of each well was determined at 450 nm using a microplate reader (Versa max microplate reader; Molecular Devices).

5.2.7 Immunoblotting

HEK293T cells (~$3x10^6$) were lysed in 100 ul of Laemmli sample buffer (12 mM Tris-Cl, pH 6.8, 0.4% SDS, 2% glycerol, 1% β-mercaptoethanol, 0.002% bromophenol blue). Cell lysates were centrifuged at 22,000 × g for 3 min at 4°C, and the supernatant mixed with Laemmli sample buffer, boiled for 10 mins, and saved at -80ºC for further analysis. Cell lysates (15 ul) was resolved by SDS-PAGE and transferred overnight to polyvinylidene difluoride (PVDF) membranes at 100 mA at 4°C. Membranes were blocked with Tris-buffered saline (TBS) containing 10% milk for 1 h and then incubated with the corresponding primary antibody diluted

in TBS-5% milk-0.05% Tween 20 (antibody dilution buffer). FLAG-tagged mouse SLFN13 was detected with anti-FLAG MAb (1/500) (M2; Sigma). As a loading control, anti-α-tubulin MAb (clone B-5-1-2; Sigma) was used at a 1/4,000 dilution. Membranes were incubated overnight at 4°C with anti-FLAG, whereas anti-α-tubulin MAb was incubated for 30 mins at 25°C. Primary antibody-bound membranes were washed in TBS-0.1% Tween 20, and bound antibodies were detected with goat anti-mouse Ig-horseradish peroxidase (HRP) (Sigma, 1/2,000) or mouse anti-rabbit IgG-HRP (Santa Cruz Biotech, 1/4,000) diluted in antibody dilution buffer. These antibodies were incubated for 1 hr at 25°C. Unbound secondary antibodies were washed as described above and bound antibodies detected by chemiluminescence.

5.2.8 Fluorescence Microscopy

Cells were plated at $0.08x10^6$ cells/well in Lab-Tek® II Chamber Slide™ system (VWR, 15461), and the next day were transfected. 48 hrs post-transfection cells were fixed and permeabilized with Cytofix/Cytoperm buffer (BD Bioscience, Cat# 554714). SLFN13 FL and deletion mutants were detected with anti-FLAG ab (1/500) (M2, Sigma) as described in chapter 2. Antibody-stained cells were stained with 300uL of DAPI at 1ug/mL for 10 min at RT in the dark. DAPI was then removed and wash once with 1x PBS, after this last wash the plastic was removed to mount the slide using Dakocytomation Fluorescent Mounting Medium (Agilent, S3023) and cover placing a 1oz microscope cover glass (24x60 mm) (VWR Vistavision™ Cover Glass, 16004-096). Cell visualized in a Zeiss LSM 700 confocal microscope.

5.2.9 Statistical Analysis

GraphPad Prism version 9.4.1 was used for statistical analysis. One-way ANOVA was used to test the impact of SLFN13 on the expression of the proteins of interest, and the Dunnett's post hoc test was used to identify significant differences between cells expressing empty plasmid

(control group) and cells expressing SLFN13 proteins (experimental groups). Two-tailed t test was used to evaluate the statistically significant of experiments with only two groups (control and experimental). Experiments where the comparison was between a specific control and a specific experimental group two-way ANOVA and Bonferroni post hoc test was utilized. p-values were indicated as follow: no significant (ns) > 0.05, * ≤ 0.05, ** ≤ 0.01, *** ≤ 0.001, **** ≤ 0.0001.

5.3 Results

We have demonstrated that removal of the last 146 aa of SLFN13 (Δ751) dramatically stabilize the protein (Fig.5.1). These data support previous findings from our laboratory indicating that replacement of SLFN13 C-terminal with the C-terminal of SLFN11 stabilized the chimeric SLFN13/11 protein. SLFN13 N-terminus (aa 1-352, Δ353) is active against HIV-1 through a codon bias-based mechanism since inhibit expression of HIV-1 Gag WT but not Gag CO (Fig. 5.2). Interestingly, transfected SLFN13 FL, despite of the low global levels, can be detected exclusively in the nucleus of the cell, suggesting that degradation is mainly cytoplasmic. In contrast, SLFN13 Δ751 and Δ353 have a pancellular distribution.

5.3.1 SLFN13 FL Protein Expression is Post-Translationally Regulated

We notice that the expression of SLFN13 FL is low to almost undetectable levels. However, previous findings from our laboratory indicated that replacement of SLFN13 C-terminal with the C-terminal of SLFN11 stabilized the chimeric SLFN13/11 protein. Therefore, we hypothesize that there must be an area of instability within the C'-terminal region of SLFN13. To evaluate this hypothesis, we prepare two truncated mutants, one lacking the last (Δ751) 146 aa of the C'-terminal and another one only expressing the N'-domain (1-352, Δ353). We observed that expression of SLFN13 Δ751 and Δ353 was very robust (Fig.5.2). Next, we evaluated mRNA levels of SLFN13FL and Δ751, and showed that the low expression of SLFN13 FL is not due to low levels of mRNA (Fig. 5.1 B). In fact, mRNA SLFN13 FL levels are twice of those of SLFN13

Δ751, while proteins levels as measured by immunoblot are greatly diminished in SLFN13 FL (Fig. 5.1 A). These results suggest that the last 146 aa of the C'-domain of SLFN13 are responsible for SLFN13 post-translational regulation.

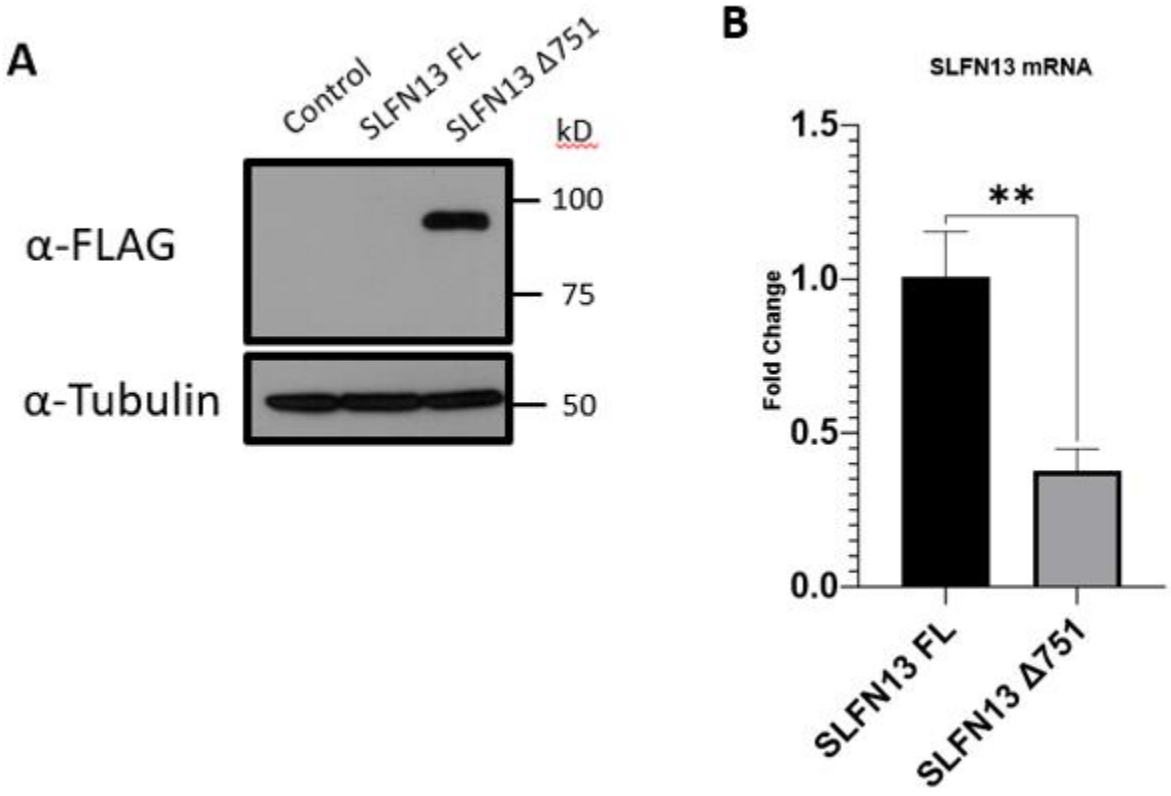

Fig. 5.1. Human SLFN13 Expression is Regulated Post-Translationally. **A)** Immunoblot of control, human SLFN13 Full length (FL) and Δ751 of HEK293T transiently transfected HEK293T cells using anti-FLAG. **B)** RT-PCR of Slfn13 FL and Δ751 mRNAs, GAPDH mRNA-normalized SLFN13 (FL, and Δ751) mRNA levels are expressed in relative values found in control cells (SLFN13 FL). Data corresponds to a triplicate experiment. Statistical significance in (B) was calculated with two-tailed t-test. ** $P \leq 0.01$.

5.3.2 Anti-HIV Activity of SLFN 13

We observed that HIVeGFP produced in the presence of SLFN13 Δ751 and Δ353 has very low viral titer (Fig. 5.2 A/B). These results indicated that SLFN13 N-terminal is required for HIV-1 inhibition. So far, all anti-HIV-1 SLFNs affect viral protein expression in a codon-biased manner. Then, we decided to evaluate if this was also the case for SLFN13 by analyzing the effect of SLFN13 Δ353 on the expression of Gag WT and CO (Fig. 5.2 C). SLFN13 Δ353 anti-HIV-1 activity diminished when Gag is CO (Fig. 5.2 C-II).

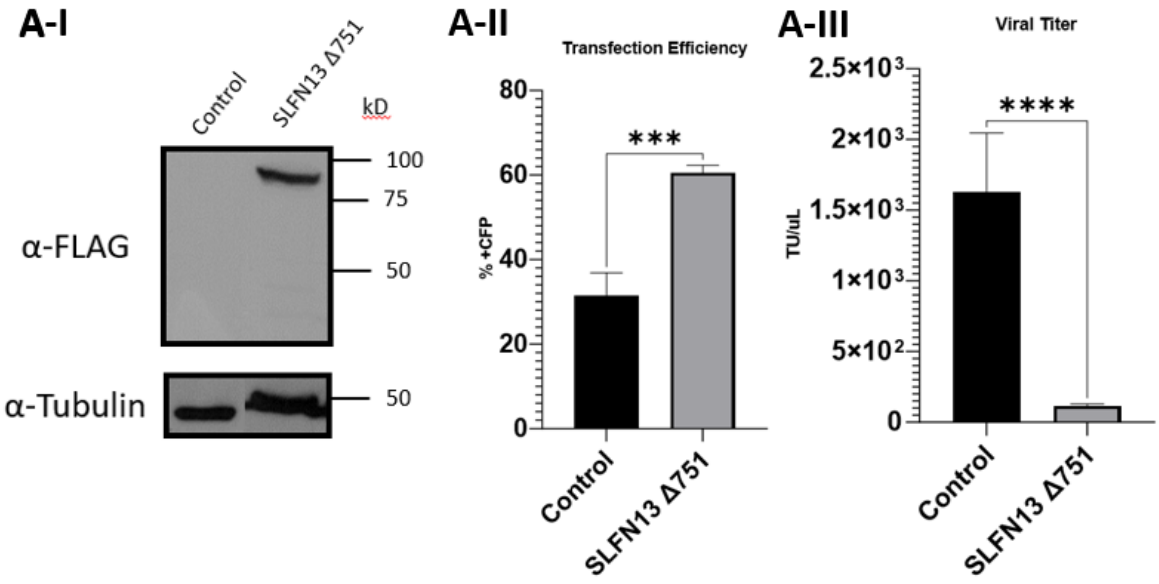

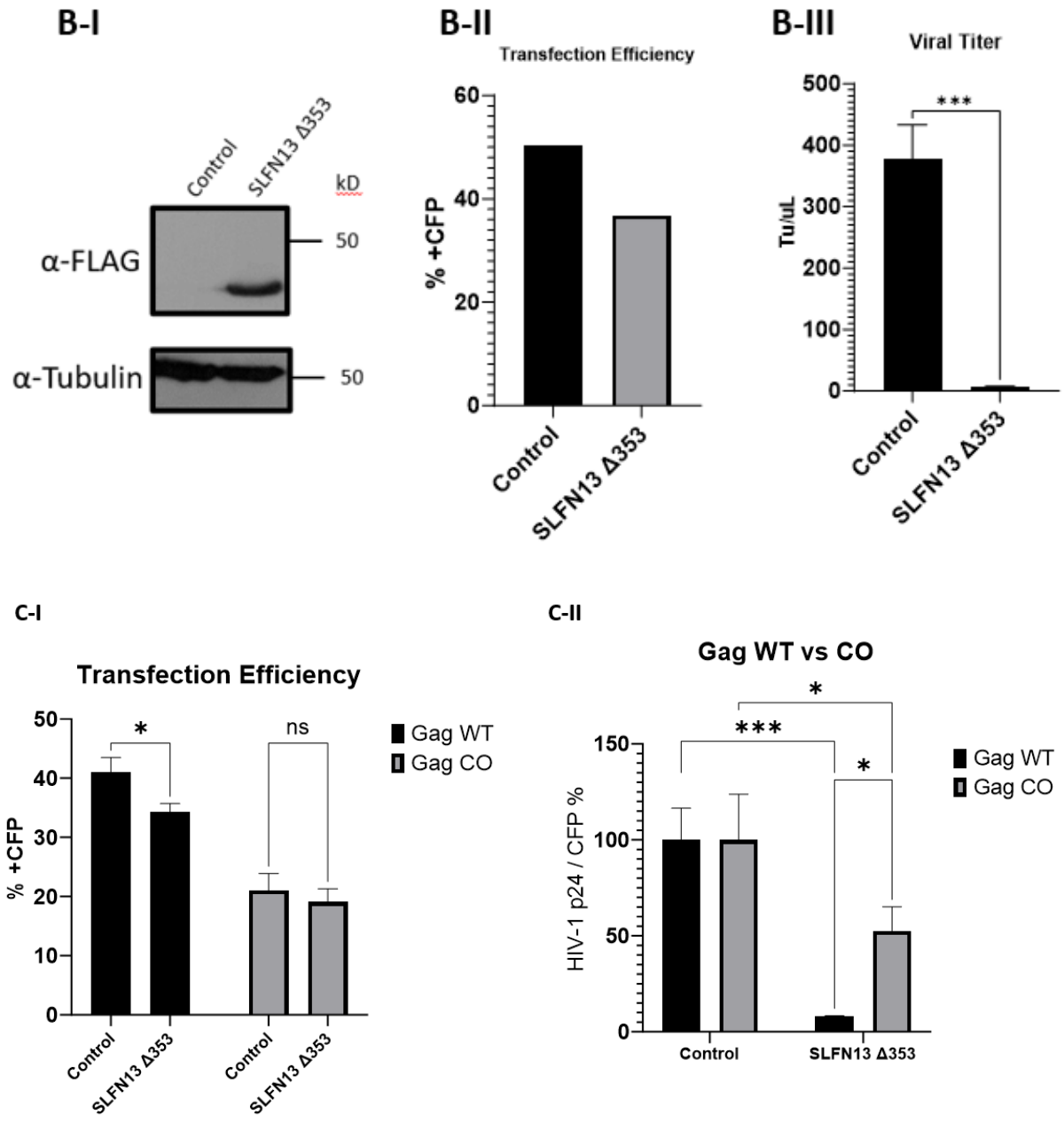

Fig. 5.2. Anti-HIV Activity of SLFN13. **A/B)** Anti-HIV activity of SLFN13 Δ751 and SLFN13 Δ353. **A-I/B-I)** Immunoblot of Δ751/Δ353 SLFN13 mutants transiently expressed in HEK293T using anti-FLAG antibody. **A-II/B-II)** Transfection efficiency calculated by flow cytometry by %CFP+ cells. **A-III/B-III)** Viral titer calculated as transduction units (TU) per microliter (uL) and normalized by transfection efficiency. **C-I)** Transfection efficiency as measured by %CFP+ by flow cytometry. **C-II)** Effect of SLFN13

Δ353 on WT or CO Gag expression of p24 in HEK293T cells. HIV-1 p24 was normalized for transfection efficiency (% of CFP+ cells) and expressed as % of control cells. Data corresponds to **A/C)** corresponds to a triplicate experiment, while **B)** corresponds to a single experiment. Statistical significance in **(A)** and **(B)** was calculated with two-tailed t-test. Statistical analysis of **C)** was calculated by two-way ANOVA Tukey post hoc test. **** $P \leq 0.0001$, *** $P \leq 0.001$, ** $P \leq 0.01$, * $P \leq 0.5$, and nonsignificant (ns) $P > 0.5$.

5.3.3 Sub-cellular Localization of SLFN13

Our results in HeLa and HEK293T cells indicated that SLFN13 FL is nuclear, whereas SLFN13 Δ751, and Δ353, are pancellular (Fig. 5.3 A). These results could indicate the existence of an NLS within the last 146 aa and that nuclear localization prevents SLFN13 degradation. In order to evaluate whether the protein is degraded preferentially in the cytoplasm we fused a strong NLS from simian virus 40 to SLFN13. This intervention modestly increased SLFN13 levels, suggesting that protein degradation occurred in the cytoplasm (Fig. 5.3 B).

The low levels of SLFN13 FL precludes the analysis of its anti-HIV-1 activity. SLFN13 Δ353 and Δ751 where active against HIV-1, but their subcellular distribution did not recapitulate the nuclear localization of the FL protein. This discrepancy in localization casts doubts on the relevance of SLFN13 Δ353 and Δ751 as functional surrogates of the FL protein. Thus, we fused SLFN13 Δ353 to the SV40 NLS to force this mutant into the nucleus and evaluate its anti-HIV-1 activity. Since SLFN13 Δ353-SV40 NLS was active against HIV-1, we believe that SLFN13 FL is also active against this virus.

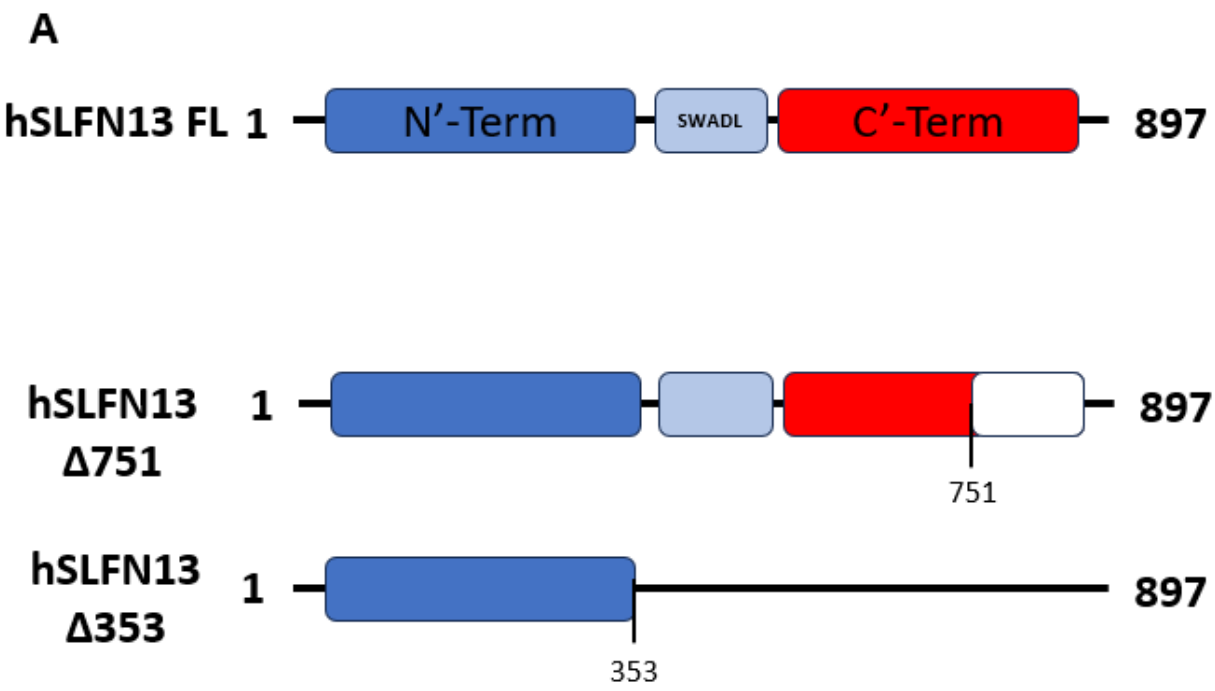
A
hSLFN13 FL
1
N'-Term
SWADL
C'-Term
897
hSLFN13
Δ751
1
897
751
hSLFN13
Δ353
1
897
353

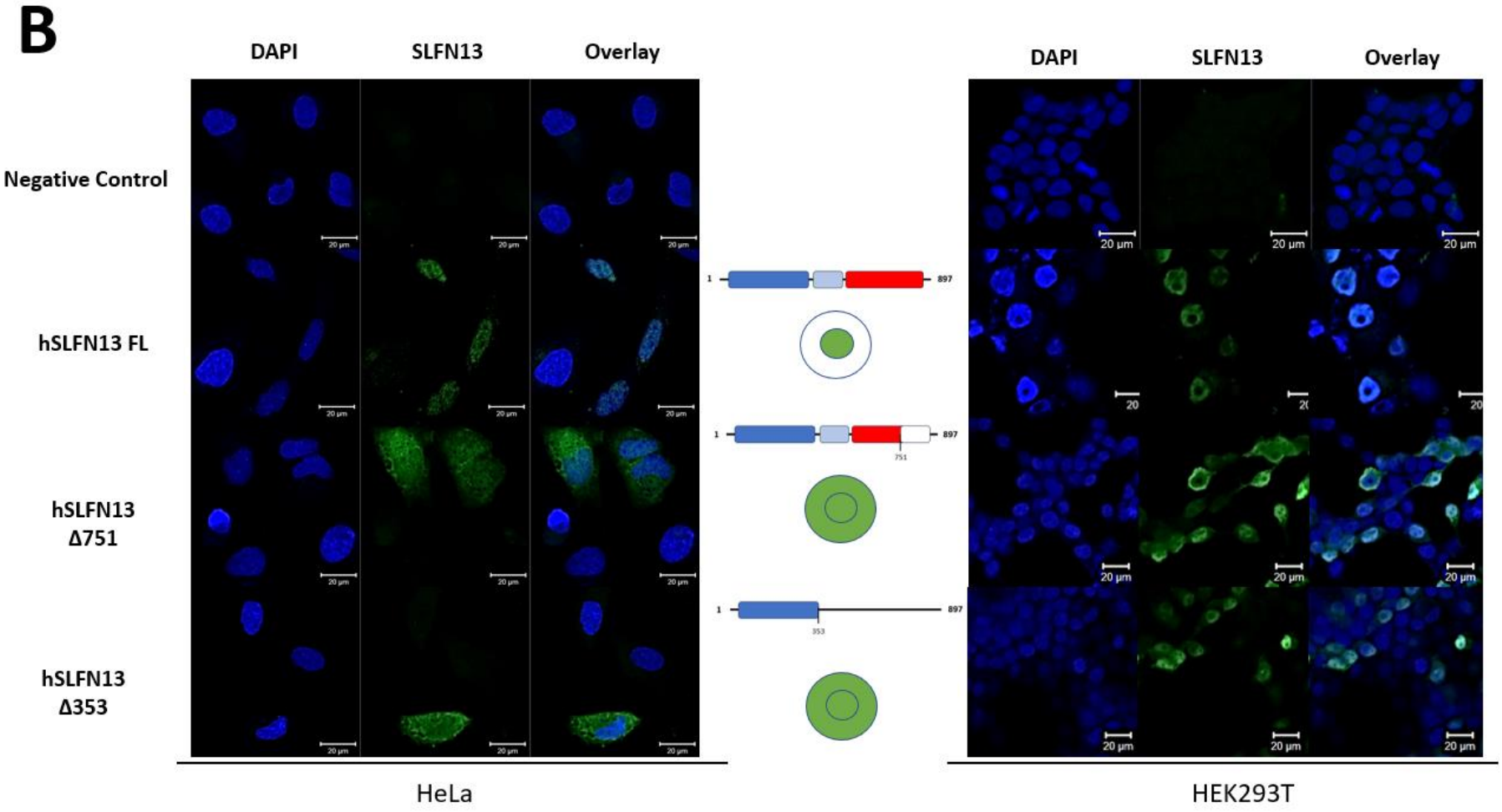
B
DAPI
SLFN13
Overlay
DAPI
SLFN13
Overlay
Negative Control
hSLFN13 FL
hSLFN13 Δ751
hSLFN13 Δ353
1
897
751
353
20 µm
HeLa
HEK293T

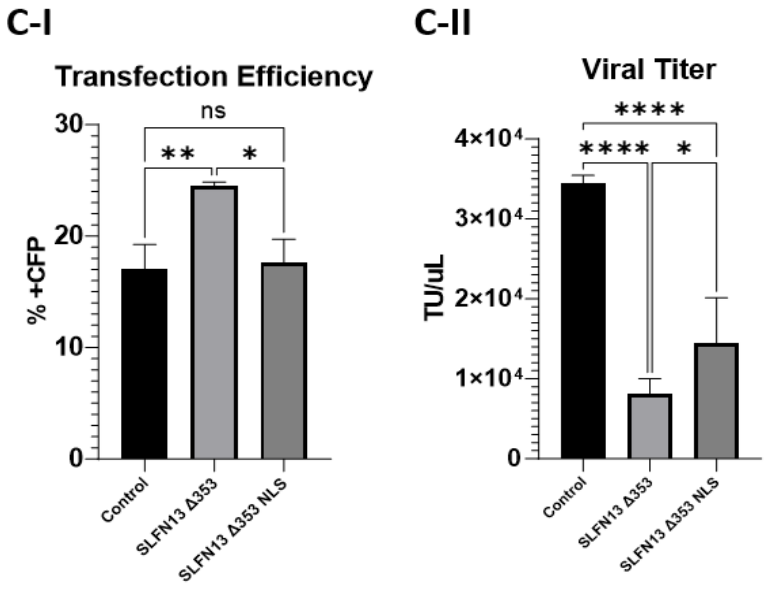
C-I
Transfection Efficiency
% +CFP
30
20
10
0
ns
**
*
Control
SLFN13 Δ353
SLFN13 Δ353 NLS
C-II
Viral Titer
TU/uL
4×10⁴
3×10⁴
2×10⁴
1×10⁴
0
****
****
*
Control
SLFN13 Δ353
SLFN13 Δ353 NLS

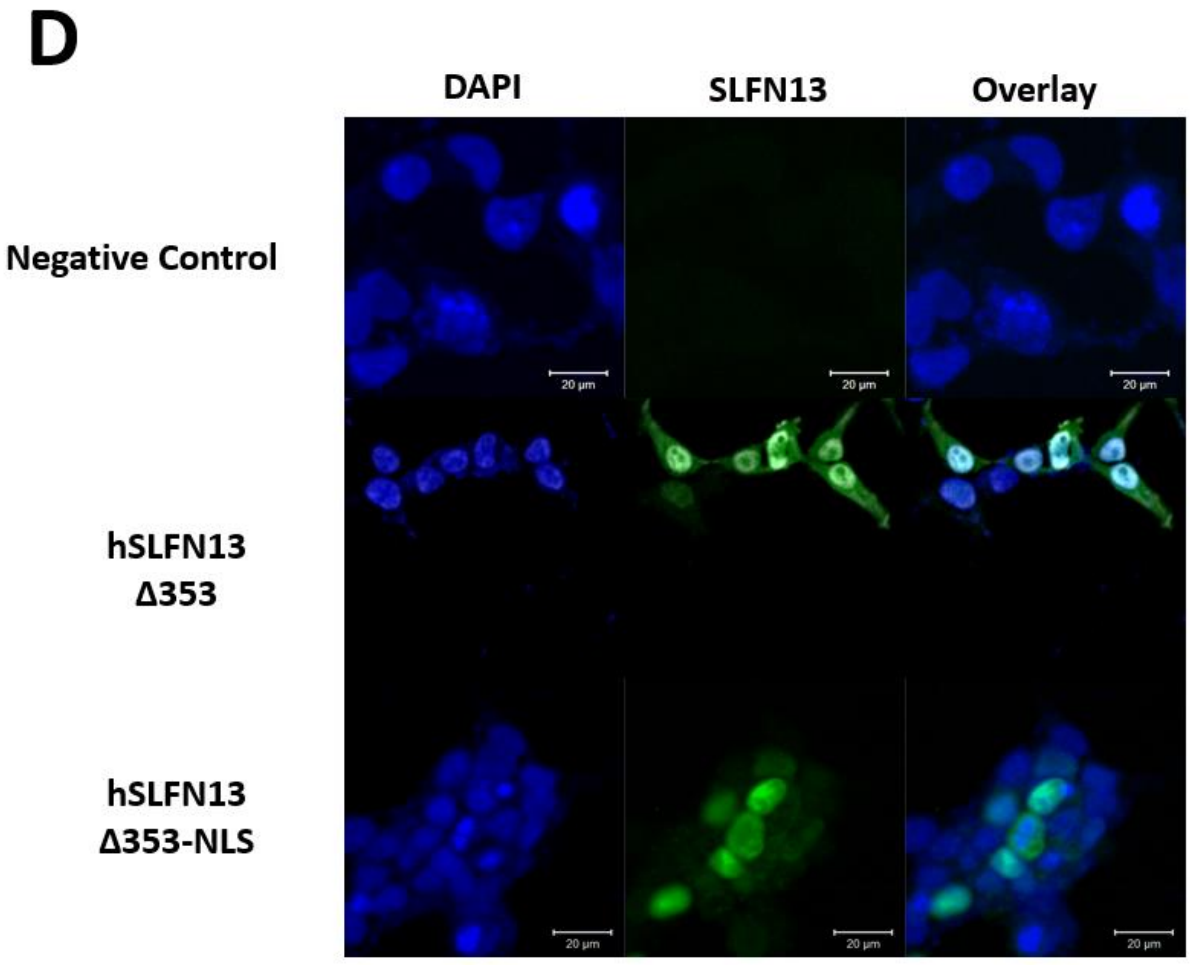
D
DAPI
SLFN13
Overlay
Negative Control
hSLFN13
Δ353
hSLFN13
Δ353-NLS
20 μm

Fig 5.3. Sub-cellular Localization of SLFN13. **A)** SLFN13 FL and truncated mutants, different domains are depicted with different colors N'-domain (blue), SWADL domain (light blue), and C'-domain (red), blank spaces depict truncation. **B)** Subcellular distribution of SLFN13 FL and truncated mutants. SLFN13 was detected with an anti-FLAG antibody (green fluorescence) in HEK293T transfected with plasmid expressing human SLFN13 FL or SLFN13 truncated mutants or an empty plasmid (control cells). Nuclei were stained with DAPI. Data in the figure corresponds to more than 100 cells in different fields of one experiment. **C-I)** Transfection efficiency of HEK293T transfected with SLFN13 Δ353 and SLFN13 Δ353-NLS and co-transfected with CFP and HIVeGFP. Transfection efficiency was measured by CFP positive cells. **C-II)** Viral titer of HEK293T cells transfected with SLFN13 Δ353 and SLFN13 Δ353-NLS as measured by transducing units per microliter (TU/uL) and normalized by transfection efficiency. **D)** Subcellular localization shown by immunohistochemistry using anti-FLAG antibody, couple with an anti-mouse FITC antibody on HEK293T cells transiently transfected with SLFN13 Δ353 and SLFN13 Δ353 NLS. Data corresponds to a triplicate experiment. Statistical significance in **(D)** and **(E)** was calculated using two-way ANOVA Tukey post hoc test. **** $P \leq 0.0001$, *** $P \leq 0.001$, ** $P \leq 0.01$, * $P \leq 0.5$, and nonsignificant (ns) $P > 0.5$.

Chapter 6: Discussion

6.1 Summary and Significance of Research Performed

Our data showed that all SLFN group III with nucleolytic activity have anti-HIV-1 activity, by a codon-usage-based inhibitory mechanism, affecting gene expression at the translational level. The mechanism is still not well understood, however we believe it to be dependent on the tRNase function, since the N-terminal region of these proteins is sufficient for the anti-HIV-1 activity.

Protein evolutionary conservation suggests that SLFN8 and SLFN9 could be the orthologs to SLFN11 and SLFN13. Our data indicate that SLFN9 seems to be the functional ortholog of SLFN11 since both share their anti-WNV activity. In contrast, SLFN8, similarly to SLFN13, did not inhibit flaviviruses[30].

We also determined the sub-cellular distribution of SLFN group III. Except SLFN14 that is located in cytoplasm all other SLFNs are nuclear proteins. We observed that the N- and C-terminal regions of SLFN5 and SLFN11 localized to the cytoplasm, suggesting that NLSs in the N- and C-terminus functionally cooperate in the FL protein. Our data confirmed that SLFN11 contains three NLSs, one of them in the N-terminus. Although, we didn't map the NLSs in SLFN13, we found that removing the last 146 aa of the protein impairs its nuclear distribution, suggesting this region contains an NLS. Importantly, this region contains one of the NLSs that we mapped in SLFN11 (R834), that corresponds to the NLS mapped in SLFN5 (R812)[49].

Previous findings from our laboratory indicated that SLFN13 is unstable at a post-transcriptional level. I found that the main contributor to the instability of this protein are the last 146 aa. Removal of this region greatly increases the expression of SLFN13 without affecting the anti-HIV-1 activity, although altering the subcellular localization.

In alignment with other's observations [41,101], our data support an important role of SLFN proteins in the translational control of codon-biased transcripts. This regulatory role suggests that SLFN proteins could shape the cell proteome with functional implications, encouraging further research in this area.

Human and mouse SLFN14, besides, to being characterized as to having tRNA activity, it also binds to the ribosome during translation, which could indicate a different mechanism reliant of this association, this mechanism however could also depend to some degree on the tRNA pool of the cell. They could all act together to stop translation or to tilt the balance of translation to favor specific genes, these being genes with optimized codon usage. The cell use of nucleotide composition to regulate expression levels of different genes is not a new concept, it has been known that nucleotide composition affects transcriptionally, translationally, and post-translationally the expression of genes[128].

We characterized SLFN11 mouse orthologs SLFN8 and SLFN9 subcellular localization and codon usage-based inhibition of HIV-1 Gag. We also determined SLFN11 NLS, and SLFN13 subcellular localization by fluorescent microscopy. Regulation of SLFN11 through phosphorylation/dephosphorylation of key amino acids, one of these located within the C-terminus suggested that C-terminus played a role in regulation of SLFN11[44]. We hypothesize that the C-terminal of SLFN13 may also play a role in its regulation. This opens the future research to uncover the mechanisms of degradation of SLFN13 and to uncover the function of SLFN13 in the cell.

6.2 Mechanisms Potentially Implicated in the Antiviral Activity of The SLFN Family

tRNA degradation is central in the known cellular functions of the SLFN group III family with nuclease activity. These proteins regulate the composition of the tRNA pool, all these SLFNs have been demonstrated *in vitro* or *in cellulo* to degrade tRNAs and the structural requirements for this function have been determined for SLFN13 and SLFN11 and predicted based on protein sequence homology for the others SLFNs. Furthermore, post-translational modifications of SLFN11 have been described to negatively regulate its tRNase activity [ref], suggesting an additional role of SLFN11 in protection of interacting tRNAs from degradation. Similarly, SLFN2, that lacks nucleolytic activity, protects tRNA from stress-induced degradation [ref]. Although it has not been demonstrated, SLFN5 could have a similar role. This places the SLFN family of

proteins as protectors of the tRNA pool. Therefore, it is possible that SLFNs could oppose changes in the tRNA pool by triggering or preventing their degradation. These potential functions of SLFNs are exploited in their anti-viral mechanisms, for example SLFN11 triggers degradation of tRNAs up regulated by HIV-1 infection and prevent changes in the tRNA pool induced by WNV, affecting their replication.

Viral-induced changes in the composition or the posttranscriptional modifications of the tRNA pool[2728100] could shift the balance of translation to favor viral replication. SLFN proteins could oppose to these changes, as for example, SLFN11 opposed HIV-1-increased tRNA abundance or WNV-induced tRNA decrease. SLFN11 by degradation of HIV-1-induced tRNA upregulation primarily affect translation of viral proteins encoded in codon biased transcripts impairing HIV-1 infection. In contrast, SLFN11 by impeding WNV-induced changes in the tRNA repertoire affect viral fitness[28]. During translation elongation the ribosome samples the local tRNA pool for the correct tRNA to be incorporated into the growing polypeptide. Lower levels of tRNAs would lead to longer pauses due to difficulty finding the right tRNA. The opposite would occur if the tRNA pool is large. tRNA levels are one of the contributors of the elongation rate of a protein. This is important because the pauses that the ribosome makes during elongation allow the protein to fold properly. This means that mRNA together with tRNA levels dictate to some degree the protein secondary structure. It has been observed that in *E. Coli* that α-helix used rapidly translated codons, while β-strands use slowly translated codons, changes to this codon to synonymous codons have a profound effect on protein folding[129]. These fine-tuning of mRNAs is also observed in viruses. A good example of the impact of codon bias is in Hepatitis A virus were optimization of the capsid lead to a decrease in viral fitness[63]. Similarly, a strategic decrease of a subset of tRNAs, as observed during WNV infection[28], could lead to an increase in viral fitness. Changes to viral fitness could modify the immune response against the virus.

These data suggest that changes to the tRNA may be a common strategy that viruses use to favor their own translation, while perhaps affecting the host innate immune response. In agreement with this hypothesis, CHIKV can reprogram the cell tRNA by inducting overexpression

of KIAA1456, a cellular tRNA methyltransferase, that modifies the decoding preferences of some tRNAs[100] favoring viral over host translation. The effect of tRNA modification on the SLFN tRNase activity is still unknown and should be investigated.

The effect on cellular physiology of the regulatory role of SLFN proteins on the tRNA pool is illustrated by the impact of SLFN11 on DNA repair. This protein affects the levels of the DNA repair proteins ATR and ATM during DNA damage response by degrading tRNAs decoding their messengers[41]. Therefore, it is possible that SLFN proteins shape the cellular proteome by regulating the tRNA pool. It is known that the composition of the tRNA pool vary in response to cellular stress and pathological conditions such as cancer, the implication of SLFN proteins in this phenomenon warrant investigation.

We should consider looking at the expression of the SLFN family in cellular events that require the reprogramming of the cell by change on translation profiles. The tRNA repertoire is very dynamic and has been demonstrated to change during different cell stages[130]. SLFNs with tRNase activity could have a role in reshaping tRNA pool in response to cellular requirements.

Heterozygous mutation on *SLFN14* gene have been identified in patients suffering from inherited thrombocytopenia, due to megakaryocyte maturation defects[42,67–69]. In addition, introduction of these mutations in mice cause the homozygotic animals to die during development due to defective hematopoiesis. These defects were also manifested in the heterozygotic animals[69]. Therefore, SLFN14 has a role in hematopoietic cell differentiation. Similarly, expression of group III SLFNs have been described to vary during thymocyte and myeloid differentiation in mice, whereas upregulation of all SLFN members with exception of SLFN3 and SLFN9 has been observed during myeloid linage differentiation[23]. Furthermore, ectopic expression of SLFN8 in T cells have a negative impact in proliferation and development in mice.

SLFN proteins have been described to be upregulated during bacterial infection-induced splenocyte activation and T cell receptor signaling[23]; however, the role of SLFNs in these processes have not been clarified. The potential implication of SLFNs in the generation of tRNA

fragments (tRF) could explain their role in cell differentiation and activation since the effect of tRF in cellular metabolism, cell death, and gene expression[131,132].

Importantly, SLFN11 has a role in chemosensitivity of cancer cells. SLFN11 tRNase activity is activated during DNA damage, affecting expression on DNA repair protein encoded by non-codon optimized messengers, leading to defective DNA repair and apoptosis. Furthermore, SLFN11 is recruited to the site of DNA-damage affecting repair[16].

The multiple consequences of the tRNase activity of SLFN proteins discussed above demand tight regulation. It has been observed that phosphorylation of key residues abolishes SLFN11 tRNase activity, and during DNA damage, SLFN11 is activated through dephosphorylation of these residues[44]. Furthermore, our data indicated that limited proteolysis of SLFN14 generates a fragment lacking the N-terminal region harboring the catalytic center. Whereas we discovered that the last 146 aa of SLFN13 trigger its degradation. Therefore, post-translational mechanisms seem to be central in the control of the tRNase activity of SLFNs.

Our data indicated that, except for the ribosomal protein SLFN14, all SLFN group III are nuclear proteins. However, nuclear localization is not functionally relevant for the antiviral activity of SLFN11. For example, nuclear and cytoplasmic forms of SLFN11 have a similar antiviral potency. Nevertheless, nuclear-specific functions of SLFNs, such as SLFN11-mediated transcriptional regulation, could require their controlled nuclear import. Our data indicates that SLFN11 has multiple NLSs that cooperate to drive the protein to the nucleus, none of them been sufficient. This seems to be also a characteristic of SLFN13 and SLFN5. The existence of multiple NLSs in a protein has been proposed as a mechanism to regulate graded nuclear localization of lipoxygenase-5[133]. Which will explain the apparent contradiction of our data with the reported cytoplasmic localization of SLFN13 in some cell types [The Human Protein Atlas]. Multiple NLSs have also been reported for Influenza A nucleoprotein (NP), where is believe to prevent unspecific association of NP to cellular or viral RNA over importing α and preventing nuclear import[134]. This explanation could also explain the existence of multiple NLSs in the case of nuclear SLFN proteins since they also bind RNA.

References

1. Gould, E., Pettersson, J., Higgs, S., Charrel, R. & Lamballerie, X. De. Emerging arboviruses : Why today ? **4**, 1–13 (2017).
2. Loo, Y. M. & Gale, M. Immune Signaling by RIG-I-like Receptors. *Immunity* **34**, 680–692 (2011).
3. Pichlmair, A. *et al.* Activation of MDA5 Requires Higher-Order RNA Structures Generated during Virus Infection. *J. Virol.* **83**, 10761–10769 (2009).
4. Kawasaki, T. & Kawai, T. Toll-like receptor signaling pathways. *Front. Immunol.* **5**, 1–8 (2014).
5. Kim, Y. K., Shin, J. S. & Nahm, M. H. NOD-like receptors in infection, immunity, and diseases. *Yonsei Med. J.* **57**, 5–14 (2016).
6. Iwasaki, A. Innate Immune Recognition of HIV-1. *Immunity* **37**, 389–398 (2012).
7. Manel, N. *et al.* A cryptic sensor for HIV-1 activates antiviral innate immunity in dendritic cells. *Nature* **467**, 214–217 (2010).
8. Murugaiah, V. *et al.* Innate Immune Response Against HIV-1. in 23–58 (2021). doi:10.1007/978-3-030-67452-6_3
9. Bourne, N. *et al.* Early Production of Type I Interferon during West Nile Virus Infection: Role for Lymphoid Tissues in IRF3-Independent Interferon Production. *J. Virol.* **81**, 9100–9108 (2007).
10. Samuel, M. A. & Diamond, M. S. Alpha/Beta Interferon Protects against Lethal West Nile Virus Infection by Restricting Cellular Tropism and Enhancing Neuronal Survival. *J. Virol.* **79**, 13350–13361 (2005).
11. Lazear, H. M., Pinto, A. K., Vogt, M. R., Gale, M. & Diamond, M. S. Beta Interferon Controls West Nile Virus Infection and Pathogenesis in Mice. *J. Virol.* **85**, 7186–7194 (2011).
12. Gómez-Lucía, E., Collado, V. M., Miró, G. & Doménech, A. Effect of type-I interferon on retroviruses. *Viruses* **1**, 545–573 (2009).
13. Suthar, M. S., Diamond, M. S. & Gale, M. West Nile virus infection and immunity. *Nat. Rev. Microbiol.* **11**, 115–128 (2013).
14. Diamond, M. S. *et al.* Modulation of Dengue Virus Infection in Human Cells by Alpha, Beta, and Gamma Interferons. *J. Virol.* **74**, 4957–4966 (2000).
15. Schneider, W. M., Chevillotte, M. D. & Rice, C. M. Interferon-Stimulated Genes: A Complex Web of Host Defenses. *Annu. Rev. Immunol.* **32**, 513–545 (2014).
16. Murai, J. *et al.* SLFN11 Blocks Stressed Replication Forks Independently of ATR. *Mol. Cell* **69**, 371-384.e6 (2018).
17. Mavrommatis, E. *et al.* Expression and Regulatory Effects of Murine Schlafen (Slfn) Genes in Malignant Melanoma and Renal Cell Carcinoma. *J. Biol. Chem.* **288**, 33006–33015 (2013).
18. Murai, J., Thomas, A., Miettinen, M. & Pommier, Y. Schlafen 11 (SLFN11), a restriction factor for replicative stress induced by DNA-targeting anti-cancer therapies. *Pharmacol. Ther.* **11**, 1–9 (2019).
19. Zoppoli, G. *et al.* Putative DNA/RNA helicase Schlafen-11 (SLFN11) sensitizes cancer cells to DNA-damaging agents. *Proc. Natl. Acad. Sci.* **109**, 15030–15035 (2012).
20. Atala, A. Re: Human Schlafen 5 (SLFN5) is a Regulator of Motility and Invasiveness of

Renal Cell Carcinoma Cells. *J. Urol.* **195**, 1169–1169 (2016).
21. Oh, P.-S. *et al.* Schlafen-3 decreases cancer stem cell marker expression and autocrine/juxtacrine signaling in FOLFOX-resistant colon cancer cells. *Am. J. Physiol. Liver Physiol.* **301**, G347–G355 (2011).
22. Li, D. *et al.* Estrogen-Related Hormones Induce Apoptosis by Stabilizing Schlafen-12 Protein Turnover. *Mol. Cell* **75**, 1–14 (2019).
23. Geserick, P., Kaiser, F., Klemm, U., Kaufmann, S. H. E. & Zerrahn, J. Modulation of T cell development and activation by novel members of the Schlafen (slfn) gene family harbouring an RNA helicase-like motif. *Int. Immunol.* **16**, 1535–1548 (2004).
24. Neumann, B., Zhao, L., Murphy, K. & Gonda, T. J. Subcellular localization of the Schlafen protein family. *Biochem. Biophys. Res. Commun.* **370**, 62–66 (2008).
25. van Zuylen, W. J. *et al.* Macrophage activation and differentiation signals regulate Schlafen-4 gene expression: Evidence for Schlafen-4 as a modulator of myelopoiesis. *PLoS One* **6**, (2011).
26. Bruno, L. *et al.* Molecular Signatures of Self-Renewal, Differentiation, and Lineage Choice in Multipotential Hemopoietic Progenitor Cells In Vitro. *Mol. Cell. Biol.* **24**, 741–756 (2004).
27. Li, M. *et al.* Codon-usage-based inhibition of HIV protein synthesis by human schlafen 11. *Nature* **491**, 125–128 (2012).
28. Valdez, F. *et al.* Schlafen 11 Restricts Flavivirus Replication. *J. Virol.* **93**, 1–45 (2019).
29. Seong, R.-K. *et al.* Schlafen 14 (SLFN14) is a novel antiviral factor involved in the control of viral replication. *Immunobiology* **222**, 979–988 (2017).
30. Yang, J. Y. *et al.* Structure of Schlafen13 reveals a new class of tRNA/rRNA- targeting RNase engaged in translational control. *Nat. Commun.* **9**, (2018).
31. Bustos, O. *et al.* Evolution of the Schlafen genes, a gene family associated with embryonic lethality, meiotic drive, immune processes and orthopoxvirus virulence. *Gene* **447**, 1–11 (2009).
32. Liu, F., Zhou, P., Wang, Q., Zhang, M. & Li, D. The Schlafen family: complex roles in different cell types and virus replication. *Cell Biol. Int.* **42**, 2–8 (2018).
33. Mavrommatis, E., Fish, E. N. & Platanias, L. C. The Schlafen Family of Proteins and Their Regulation by Interferons. *J. Interf. Cytokine Res.* **33**, 206–210 (2013).
34. Schwarz, D. A., Katayama, C. D. & Hedrick, S. M. Schlafen, a new family of growth regulatory genes that affect thymocyte development. *Immunity* **9**, 657–668 (1998).
35. Liu, X., Rao, L. & Gennerich, A. The regulatory function of the AAA4 ATPase domain of cytoplasmic dynein. *Nat. Commun.* **11**, 1–15 (2020).
36. Chaturvedi, L., Sun, K., Walsh, M. F., Kuhn, L. A. & Basson, M. D. The P-loop region of Schlafen 3 acts within the cytosol to induce differentiation of human Caco-2 intestinal epithelial cells. *Biochim. Biophys. Acta - Mol. Cell Res.* **1843**, 3029–3037 (2014).
37. Gilhooly, N. S., Gwynn, E. J. & Dillingham, M. S. Superfamily 1 helicases. *Front. Biosci. - Sch.* **5 S**, 206–216 (2013).
38. Tuteja, N. & Tuteja, R. Unraveling DNA helicases Motif, structure, mechanism and function. *Eur. J. Biochem.* **271**, 1849–1863 (2004).
39. Metzner, F. J. *et al.* Mechanistic understanding of human SLFN11. *Nat. Commun.* **13**, 5464 (2022).
40. Pisareva, V. P., Muslimov, I. A., Tcherepanov, A. & Pisarev, A. V. Characterization of novel ribosome-associated endoribonuclease SLFN14 from rabbit reticulocytes.

Biochemistry **54**, 3286–3301 (2015).
41. Li, M. *et al.* DNA damage-induced cell death relies on SLFN11-dependent cleavage of distinct type II tRNAs. *Nat. Struct. Mol. Biol.* **25**, 1047–1058 (2018).
42. Fletcher, S. J. *et al.* Role of the novel endoribonuclease SLFN14 and its disease-causing mutations in ribosomal degradation. *Rna* **24**, 939–949 (2018).
43. Metzner, F. J., Huber, E., Hopfner, K. P. & Lammens, K. Structural and biochemical characterization of human Schlafen 5. *Nucleic Acids Res.* **50**, 1147–1161 (2022).
44. Malone, D., Lardelli, R. M., Li, M. & David, M. Dephosphorylation activates the interferon-stimulated Schlafen family member 11 in the DNA damage response. *J. Biol. Chem.* **294**, 14674–14685 (2019).
45. Hughes, J. M., Wilson, M. E. & Sejvar, J. J. The Long-Term Outcomes of Human West Nile Virus Infection. *Clin. Infect. Dis.* **44**, 1617–1624 (2007).
46. De Filette, M., Ulbert, S., Diamond, M. S. & Sanders, N. N. Recent progress in West Nile virus diagnosis and vaccination. *Vet. Res.* **43**, 1–15 (2012).
47. Brinton, M. A. The Molecular Biology of West Nile Virus: A New Invader of the Western Hemisphere. *Annu. Rev. Microbiol.* **56**, 371–402 (2002).
48. Roosendaal, J., Westaway, E. G., Khromykh, A. & Mackenzie, J. M. Regulated Cleavages at the West Nile Virus NS4A-2K-NS4B Junctions Play a Major Role in Rearranging Cytoplasmic Membranes and Golgi Trafficking of the NS4A Protein. *J. Virol.* **80**, 4623–4632 (2006).
49. Ding, J. *et al.* Schlafen 5 suppresses human immunodeficiency virus type 1 transcription by commandeering cellular epigenetic machinery. *Nucleic Acids Res.* **50**, 6137–6153 (2022).
50. Kim, E. T. *et al.* Comparative proteomics identifies Schlafen 5 (SLFN5) as a herpes simplex virus restriction factor that suppresses viral transcription. *Nat. Microbiol.* **6**, 234–245 (2021).
51. Gu, X. *et al.* Human Schlafen 5 inhibits proliferation and promotes apoptosis in lung adenocarcinoma via the PTEN/PI3K/AKT/mTOR pathway. *Biomed Res. Int.* **2021**, (2021).
52. Gu, X. *et al.* SLFN5 influences proliferation and apoptosis by upregulating PTEN transcription via ZEB1 and inhibits the purine metabolic pathway in breast cancer. *Am. J. Cancer Res.* **10**, 2832–2850 (2020).
53. Wan, G. *et al.* Human Schlafen 5 regulates reversible epithelial and mesenchymal transitions in breast cancer by suppression of ZEB1 transcription. *Br. J. Cancer* **123**, 633–643 (2020).
54. Murai, J. *et al.* Resistance to PARP inhibitors by SLFN11 inactivation can be overcome by ATR inhibition. *Oncotarget* **7**, (2016).
55. Shin, Y. C., Bischof, G. F., Lauer, W. A. & Desrosiers, R. C. Importance of codon usage for the temporal regulation of viral gene expression. *Proc. Natl. Acad. Sci.* **112**, 14030–14035 (2015).
56. Van Weringh, A. *et al.* HIV-1 modulates the tRNA pool to improve translation efficiency. *Mol. Biol. Evol.* **28**, 1827–1834 (2011).
57. Lin, Y. Z. *et al.* Equine schlafen 11 restricts the production of equine infectious anemia virus via a codon usage-dependent mechanism. *Virology* **495**, 112–121 (2016).
58. Van Hecke, C. *et al.* Early treated HIV-1 positive individuals demonstrate similar restriction factor expression profile as long-term non-progressors. *EBioMedicine* **41**, 443–

454 (2019).
59. Abdel-Mohsen, M. *et al.* Expression profile of host restriction factors in HIV-1 elite controllers. *Retrovirology* **10**, 1–13 (2013).
60. Pechmann, S. & Frydman, J. Evolutionary conservation of codon optimality reveals hidden signatures of cotranslational folding. *Nat. Struct. Mol. Biol.* **20**, 237–243 (2013).
61. Ma, X. *et al.* The effects of the codon usage and translation speed on protein folding of 3Dpol of foot-and-mouth disease virus. *Vet. Res. Commun.* **37**, 243–250 (2013).
62. Zhou, M., Wang, T., Fu, J., Xiao, G. & Liu, Y. Nonoptimal codon usage influences protein structure in intrinsically disordered regions. *Mol. Microbiol.* **97**, 974–987 (2015).
63. Aragonès, L., Guix, S., Ribes, E., Bosch, A. & Pintó, R. M. Fine-Tuning Translation Kinetics Selection as the Driving Force of Codon Usage Bias in the Hepatitis A Virus Capsid. *PLoS Pathog.* **6**, e1000797 (2010).
64. Burns, C. C. *et al.* Modulation of Poliovirus Replicative Fitness in HeLa Cells by Deoptimization of Synonymous Codon Usage in the Capsid Region. *J. Virol.* **80**, 3259–3272 (2006).
65. Callaghan, A. J. *et al.* Structure of Escherichia coli RNase E catalytic domain and implications for RNA turnover. *Nature* **437**, 1187–1191 (2005).
66. Gan, J. *et al.* Structural insight into the mechanism of double-stranded RNA processing by ribonuclease III. *Cell* **124**, 355–366 (2006).
67. Stapley, R. J., Pisareva, V. P., Pisarev, A. V. & Morgan, N. V. SLFN14 gene mutations associated with bleeding. *Platelets* **31**, 407–410 (2020).
68. Simpson, M. A. *et al.* SLFN14 mutations underlie thrombocytopenia with excessive bleeding and platelet secretion defects. *J. Clin. Invest.* **125**, 3600–3605 (2015).
69. Stapley, R. J. *et al.* Heterozygous mutation SLFN14 K208N in mice mediates species-specific differences in platelet and erythroid lineage commitment. *Blood Adv.* **5**, 377–390 (2021).
70. Mao, Y., Ding, J. W., Chen, M. S., Cen, S. & Li, X. Y. SLFN14 inhibits LINE-1 transposition activity. *Yi chuan = Hered.* **42**, 669–679 (2020).
71. Zhang, Z. *et al.* Global analysis of tRNA and translation factor expression reveals a dynamic landscape of translational regulation in human cancers. *Commun. Biol.* **1**, 1–11 (2018).
72. Brockmann, R., Beyer, A., Heinisch, J. J. & Wilhelm, T. Posttranscriptional expression regulation: What determines translation rates? *PLoS Comput. Biol.* **3**, 0531–0539 (2007).
73. Tuller, T., Kupiec, M. & Ruppin, E. Determinants of protein abundance and translation efficiency in S. cerevisiae. *PLoS Comput. Biol.* **3**, 2510–2519 (2007).
74. Ishihama, Y. *et al.* Protein abundance profiling of the Escherichia coli cytosol. *BMC Genomics* **9**, 1–17 (2008).
75. Hanson, G. & Coller, J. Codon optimality, bias and usage in translation and mRNA decay. *Nat. Rev. Mol. Cell Biol.* **19**, 20–30 (2018).
76. Carlini, D. B. & Stephan, W. In vivo introduction of unpreferred synonymous codons into the drosophila Adh gene results in reduced levels of ADH protein. *Genetics* **163**, 239–243 (2003).
77. Pershing, N. L. K. *et al.* Rare codons capacitate Kras-driven de novo tumorigenesis. *J. Clin. Invest.* **125**, 222–233 (2015).
78. Kotsopoulou, E., Kim, V. N., Kingsman, A. J., Kingsman, S. M. & Mitrophanous, K. A. A Rev-Independent Human Immunodeficiency Virus Type 1 (HIV-1)-Based Vector That

Exploits a Codon-Optimized HIV-1 gag-pol Gene . *J. Virol.* **74**, 4839–4852 (2000).
79. Peterson, J., Li, S., Kaltenbrun, E., Erdogan, O. & Counter, C. M. Expression of transgenes enriched in rare codons is enhanced by the MAPK pathway. *Sci. Rep.* **10**, 1–12 (2020).
80. Wu, C. C. C., Zinshteyn, B., Wehner, K. A. & Green, R. High-Resolution Ribosome Profiling Defines Discrete Ribosome Elongation States and Translational Regulation during Cellular Stress. *Mol. Cell* **73**, 959-970.e5 (2019).
81. Douka, K., Agapiou, M., Birds, I. & Aspden, J. L. Optimization of Ribosome Footprinting Conditions for Ribo-Seq in Human and Drosophila melanogaster Tissue Culture Cells. *Front. Mol. Biosci.* **8**, 1–12 (2022).
82. Hussmann, J. A., Patchett, S., Johnson, A., Sawyer, S. & Press, W. H. Understanding Biases in Ribosome Profiling Experiments Reveals Signatures of Translation Dynamics in Yeast. *PLoS Genet.* **11**, 1–25 (2015).
83. Yan, X., Hoek, T. A., Vale, R. D. & Tanenbaum, M. E. Dynamics of Translation of Single mRNA Molecules in Vivo. *Cell* **165**, 976–989 (2016).
84. Darnell, A. M., Subramaniam, A. R. & O'Shea, E. K. Translational Control through Differential Ribosome Pausing during Amino Acid Limitation in Mammalian Cells. *Mol. Cell* **71**, 229-243.e11 (2018).
85. Joazeiro, C. A. P. Mechanisms and functions of ribosome-associated protein quality control. *Nat. Rev. Mol. Cell Biol.* **20**, 368–383 (2019).
86. Presnyak, V. *et al.* Codon optimality is a major determinant of mRNA stability. *Cell* **160**, 1111–1124 (2015).
87. Shoemaker, C. J. & Green, R. Translation drives mRNA quality control. *Nat. Struct. Mol. Biol.* **19**, 594–601 (2012).
88. Letzring, D. P., Dean, K. M. & Grayhack, E. J. Control of translation efficiency in yeast by codon-anticodon interactions. *Rna* **16**, 2516–2528 (2010).
89. De, S. & Mühlemann, O. A comprehensive coverage insurance for cells: revealing links between ribosome collisions, stress responses and mRNA surveillance. *RNA Biol.* **19**, 609–621 (2022).
90. Chu, D. *et al.* Translation elongation can control translation initiation on eukaryotic mRNAs. *EMBO J.* **33**, 21–34 (2014).
91. Torrent, M., Chalancon, G., De Groot, N. S., Wuster, A. & Madan Babu, M. Cells alter their tRNA abundance to selectively regulate protein synthesis during stress conditions. *Sci. Signal.* **11**, 1–10 (2018).
92. Pang, Y. L. J., Abo, R., Levine, S. S. & Dedon, P. C. Diverse cell stresses induce unique patterns of tRNA up- and down-regulation: tRNA-seq for quantifying changes in tRNA copy number. *Nucleic Acids Res.* **42**, (2014).
93. Smith, B. L., Chen, G., Wilke, C. O. & Krug, R. M. Avian influenza virus PB1 gene in H3N2 viruses evolved in humans to reduce interferon inhibition by skewing codon usage toward interferon-altered tRNA pools. *MBio* **9**, (2018).
94. Saikia, M. *et al.* Codon optimality controls differential mRNA translation during amino acid starvation. *Rna* **22**, 1719–1727 (2016).
95. Yue, T. *et al.* SLFN2 protection of tRNAs from stress-induced cleavage is essential for T cell-mediated immunity. *Science* **372**, (2021).
96. Chan, C. T. Y. *et al.* A quantitative systems approach reveals dynamic control of tRNA modifications during cellular stress. *PLoS Genet.* **6**, 1–9 (2010).

97. Chionh, Y. H. *et al.* TRNA-mediated codon-biased translation in mycobacterial hypoxic persistence. *Nat. Commun.* **7**, 1–12 (2016).
98. Patil, A. *et al.* Increased tRNA modification and gene-specific codon usage regulate cell cycle progression during the DNA damage response. *Cell Cycle* **11**, 3656–3665 (2012).
99. Pavon-Eternod, M., Wei, M., Pan, T. & Kleiman, L. Profiling non-lysyl tRNAs in HIV-1. *Rna* **16**, 267–273 (2010).
100. Jungfleisch, J. *et al.* CHIKV infection reprograms codon optimality to favor viral RNA translation by altering the tRNA epitranscriptome. *Nat. Commun.* **13**, 1–12 (2022).
101. Stabell, A. C. *et al.* Non-human Primate Schlafen11 Inhibits Production of Both Host and Viral Proteins. *PLoS Pathog.* **12**, 1–19 (2016).
102. Sharp, P. M. & Li, W.-H. The codon adaptation index-a measure of directional synonymous codon usage bias, and its potential applications. *Nucleic Acids Res.* **15**, 1281–1295 (1987).
103. Pandit, A. & Sinha, S. Differential trends in the codon usage patterns in HIV-1 genes. *PLoS One* **6**, 1–10 (2011).
104. Martrus, G., Nevot, M., Andres, C., Clotet, B. & Martinez, M. A. Changes in codon-pair bias of human immunodeficiency virus type 1 have profound effects on virus replication in cell culture. *Retrovirology* **10**, 1–12 (2013).
105. Llano, M. *et al.* An Essential Role for LEDGF/p75 in HIV Integration. *Science (80-.).* **314**, 461–464 (2006).
106. Haas, J., Park, E. C. & Seed, B. Codon usage limitation in the expression of HIV-1 envelope glycoprotein. *Curr. Biol.* **6**, 315–324 (1996).
107. Levy, D. N., Aldrovandi, G. M., Kutsch, O. & Shaw, G. M. Dynamics of HIV-1 recombination in its natural target cells. *Proc. Natl. Acad. Sci. U. S. A.* **101**, 4204–4209 (2004).
108. Bueno, M. T. D., Reyes, D. & Llano, M. LEDGF/p75 deficiency increases deletions at the HIV-1 cDNA ends. *Viruses* **9**, 1–13 (2017).
109. Garcia-Rivera, J. A. *et al.* Implication of Serine Residues 271, 273, and 275 in the Human Immunodeficiency Virus Type 1 Cofactor Activity of Lens Epithelium-Derived Growth Factor/p75. *J. Virol.* **84**, 740–752 (2010).
110. Stojdl, D. F. *et al.* VSV strains with defects in their ability to shutdown innate immunity are potent systemic anti-cancer agents. *Cancer Cell* **4**, 263–275 (2003).
111. Llano, M. *et al.* Identification and Characterization of the Chromatin-binding Domains of the HIV-1 Integrase Interactor LEDGF/p75. *J. Mol. Biol.* **360**, 760–773 (2006).
112. Lee, S., Trivedi, U., Johnson, C., Farquharson, C. & Bergkvist, G. T. Optimised isolation method for RNA extraction suitable for RNA sequencing from feline teeth collected in a clinical setting and at post mortem. *Vet. Res. Commun.* **43**, 17–27 (2019).
113. Puigbò, P., Bravo, I. G. & Garcia-Vallve, S. CAIcal: A combined set of tools to assess codon usage adaptation. *Biol. Direct* **3**, 1–8 (2008).
114. Jeon, J. S. *et al.* Analysis of single nucleotide polymorphism among Varicella-Zoster Virus and identification of vaccine-specific sites. *Virology* **496**, 277–286 (2016).
115. Yamasoba, D. *et al.* N4BP1 restricts HIV-1 and its inactivation by MALT1 promotes viral reactivation. *Nat. Microbiol.* **4**, 1532–1544 (2019).
116. Gelderblom, H. C. *et al.* Viral complementation allows HIV-1 replication without integration. *Retrovirology* **5**, 1–18 (2008).
117. Altschul, S. F. *et al.* Gapped BLAST and PSI-BLAST: A new generation of protein

database search programs. *Nucleic Acids Res.* **25**, 3389–3402 (1997).
118. Chiu, Y. H., MacMillan, J. B. & Chen, Z. J. RNA Polymerase III Detects Cytosolic DNA and Induces Type I Interferons through the RIG-I Pathway. *Cell* **138**, 576–591 (2009).
119. Ran, Y. *et al.* African swine fever virus I267L acts as an important virulence factor by inhibiting RNA polymerase III-RIG-I-mediated innate immunity. *PLoS Pathog.* **18**, 1–21 (2022).
120. van der Kuyl, A. C. & Berkhout, B. The biased nucleotide composition of the HIV genome: a constant factor in a highly variable virus. *Retrovirology* **9**, 1–14 (2012).
121. Jarrous, N. & Rouvinski, A. RNA polymerase III and antiviral innate immune response. *Transcription* **12**, 1–11 (2021).
122. Chesebro, B., Wehrly, K., Metcalf, J. & Griffin, D. E. Use of a new CD4-positive HeLa cell clone for direct quantitation of infectious human immunodeficiency virus from blood cells of AIDS patients. *J. Infect. Dis.* **163**, 64–70 (1991).
123. Levitz, R. *et al.* The optional E. coli prr locus encodes a latent form of phage T4-induced anticodon nuclease. *EMBO J.* **9**, 1383–1389 (1990).
124. Sarkar, S. & Heise, M. T. Mouse Models as Resources for Studying Infectious Diseases. *Clin. Ther.* **41**, 1912–1922 (2019).
125. Kosugi, S., Hasebe, M., Tomita, M. & Yanagawa, H. Systematic identification of cell cycle-dependent yeast nucleocytoplasmic shuttling proteins by prediction of composite motifs. *Proc. Natl. Acad. Sci. U. S. A.* **106**, 10171–10176 (2009).
126. Hornbeck, P. V. *et al.* PhosphoSitePlus, 2014: Mutations, PTMs and recalibrations. *Nucleic Acids Res.* **43**, D512–D520 (2015).
127. Llano, M. *et al.* Blockade of Human Immunodeficiency Virus Type 1 Expression by Caveolin-1. *J. Virol.* **76**, 9152–9164 (2002).
128. Parvathy, S. T., Udayasuriyan, V. & Bhadana, V. Codon usage bias. *Mol. Biol. Rep.* **49**, 539–565 (2022).
129. Adzhubei, A. A., Adzhubei, I. A., Krasheninnikov, I. A. & Neidle, S. Non-random usage of 'degenerate' codons is related to protein three-dimensional structure. *FEBS Lett.* **399**, 78–82 (1996).
130. Aharon-Hefetz, N. *et al.* Manipulation of the human trna pool reveals distinct trna sets that act in cellular proliferation or cell cycle arrest. *Elife* **9**, 1–28 (2020).
131. Zeng, T. *et al.* Relationship between tRNA-derived fragments and human cancers. *Int. J. Cancer* **147**, 3007–3018 (2020).
132. Thompson, D. M. & Parker, R. Stressing Out over tRNA Cleavage. *Cell* **138**, 215–219 (2009).
133. Lou, M., Pang, C. W. M., Gerken, A. E. & Brock, T. G. Multiple nuclear localization sequences allow modulation of 5-lipoxygenase nuclear import. *Traffic* **5**, 847–854 (2004).
134. Wu, W. *et al.* Synergy of two low-affinity NLSs determines the high avidity of influenza A virus nucleoprotein NP for human importin α isoforms. *Sci. Rep.* **7**, 1–16 (2017).

Vita

Carlos Valenzuela was born in Mexico where he live his early years before immigrating into the United States with his family. After graduating High School he attended community college and later enrolled to the University of Texas at El Paso.

He earned his Bachelor of Science degree in Cellular and Molecular Biochemistry from the University of Texas at El Paso in the Spring of 2017. Later that year was accepted to join the doctoral program in Pathobiology at the University of Texas at El Paso.

While pursuing his degree, Carlos was awarded the Graduate Research Initiative for Scientific Enhancement (RISE) scholarship to fund his studies from 2017 to 2021. He was later a teaching assistant from 2021 to 2023. Later he was awarded the Keelung Hong Graduate Research Fellowship in 2023 to fund two years of his doctoral studies.

Carlos has co-authored 5 publications, 3 while pursuing his bachelor's degree, and 2 while pursuing his Ph.D degree. Before graduating, Carlos had a first author manuscript submitted to bioRxiv title: “Schlafen14 Regulates Gene Expression Depending on Codon Usage”. This manuscript will be later submitted to a peer-reviewed journal.